Heterogeneous *Salmonella*-host encounters determine disease progression in a typhoid fever model

Inauguraldissertation

zur

Erlangung der Würde eines Doktors der Philosophie

vorgelegt der

Philosophisch-Naturwissenschaftlichen Fakultät

der Universität Basel

von

Nura Schürmann

aus Schwetzingen, Deutschland

Basel, 2016

Genehmigt von der Philosophisch-Naturwissenschaftlichen Fakultät

auf Antrag von

Prof. Dr. Dirk Bumann

Prof. Dr. Petr Broz

Basel, den 23.02.2016

Prof. Dr. Jörg Schibler

(Dekan der Philosophisch-

Naturwissenschatlichen Fakultät)

STATEMENT TO MY THESIS

This work was carried out in the group of Prof. Dr. Dirk Bumann in the Focal Area Infection Biology at the Biozentrum Basel, Switzerland.

My PhD thesis committee consisted of:

Prof. Dr. Dirk Bumann

Prof. Dr. Petr Broz

Prof. Dr. Markus Heim

My thesis is written as a cumulative dissertation. It consists of an abstract, a general introduction covering aspects for this work followed by the result sections composed of three published articles, one submitted article and one manuscript in preparation. Finally the different aspects of my thesis are discussed and future directions are suggested.

Table of contents

Abstract

An infectious disease is an illness that is caused by invasion and multiplication of pathogenic microorganisms in body tissues of a host. The complex and heterogeneous tissue microenvironments provide different growth opportunities for pathogens with implications for disease outcome. However, the heterogeneous host environment has been largely neglected, because suitable methods to analyze single-cell host-pathogen encounters *in vivo* were largely lacking.

In this work, we addressed the implications of heterogeneous host-*Salmonella* encounters on disease progression in the well characterized mouse typhoid fever model. Specifically, we combined *Salmonella* biosensors with high resolution microscopy, flow cytometry and proteomics to reveal the fate of *Salmonella* in the diverse host microenvironments of spleen.

We showed that neutrophils and inflammatory monocytes are recruited to *Salmonella* infectious foci in spleen where they produce large amounts of reactive oxygen species (ROS), reactive nitrogen species (RNS) and lipids. We revealed that neutrophils and monocytes kill *Salmonella* with ROS generated through NADPH oxidase and myeloperoxidase (MPO), whereas RNS play a negligible role for infection control. However, ROS can also cause substantial collateral damage in host tissue. We showed that MPO protects the host against self-damage by converting diffusible long-lived ROS into highly reactive ROS with short reach that remain confined to the pathogen microenvironment. Some *Salmonella* escape to resident red pulp macrophages, which impose only sublethal oxidative bursts on *Salmonella*. Although macrophages are a primary niche for *Salmonella* survival, a specific subset of IFNγ activated macrophages can kill *Salmonella* with guanylate binding protein associated mechanisms. In addition, we showed that *Salmonella* growth in spleen is heterogeneous, independently of regional factors or host cell types. Overall, our analysis revealed numerous different *Salmonella*-host cell encounters in spleen with divergent outcomes. Local failures to control bacterial replication appear next to regions where the host successfully eradicates the pathogen.

Together, these data show that disease progression does not necessarily reflect an overall weak host immune response, but rather result from disparate host-pathogen encounters.

The following word cloud is a word summary of my thesis. The cloud gives greater prominence to words which appear more frequent in the text. The word cloud was created at www.wordle.net.

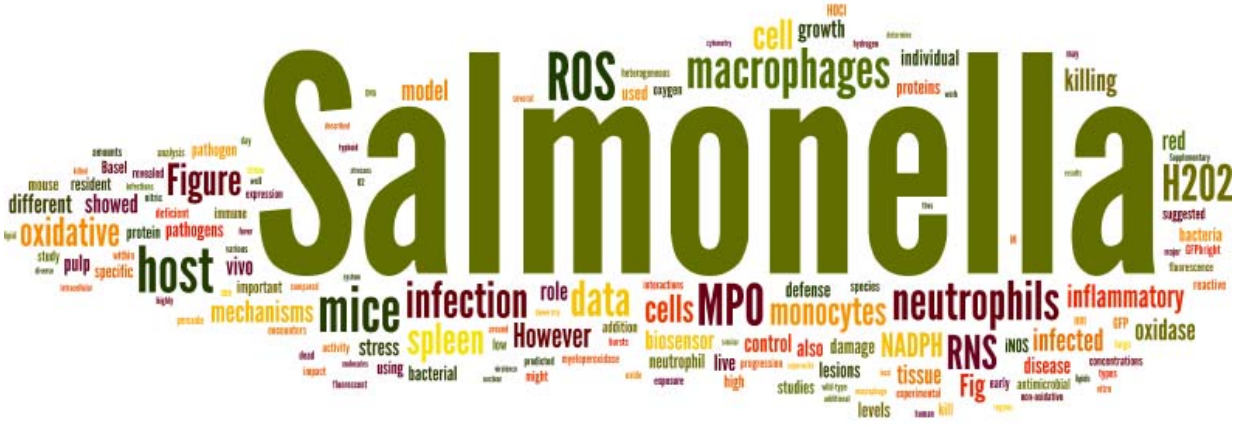

Figure 1 Summary of this thesis by frequency of words

1 Introduction

Infectious diseases are the second most important cause of death worldwide [1]. The rising resistance of pathogens to antimicrobial therapy has increased the need for novel antimicrobials and vaccines. However, approval of new antibacterial agents have decreased over the past twenty years [2, 3] and efficacious vaccines are lacking for major pathogens [4, 5]. The emerging crisis in infectious diseases poses a major threat to the human population in both developing and industrialized countries. A more detailed understanding of host-pathogen interactions will help to improve treatment options.

Infections usually start with just a few pathogen cells penetrating body surfaces. Disease signs appear only later when pathogens consume host nutrients for growth to high tissue loads [6]. The host immune system detects and attacks infectious foci with an arsenal of immune weapons in order to eradicate the pathogen. Pathogens in turn use stealth, defense and counter attack to evade the host's immune response, survive and grow. However, it remains unclear which interactions determine disease progression or disease control.

Past research has uncovered many virulence factors in major pathogens and microbial effector mechanisms, as well as host molecules involved in pathogen recognition and signal transduction. However, one critical aspect of host-pathogen interactions has been largely ignored. Pathogens encounter heterogeneous host environments with distinct structures and functions. Hence, pathogens likely respond according to their individual host environment. These encounters could generate heterogeneous pathogen subpopulations which might influence disease progression.

Experimental evidence for host-induced pathogen heterogeneity is rare. Most current approaches are based on cell culture experiments or bulk analyses of tissue homogenates which cannot capture the spatial complexity of host environments. A few recent studies, however, describe heterogeneous host-pathogen encounters and support a crucial role for disease progression and control. *Salmonella* Typhimurium net growth in mouse liver depends on continuous spreading and formation of new infection foci [7]. *Mycobacterium tuberculosis* reside in diverse microenvironments in infected lung [8]. Some of these regions express high levels of inducible nitric oxide synthase (iNOS), which imposes diverse stresses on *M. tuberculosis* [9]. High or low local iNOS activites also correlates with metabolic activity of the parasite *Leishmania major* [10]. RNA-RNA in situ hybridization demonstrated differential *M. tuberculosis* gene expression in necrotic lesions [11] and immunofluorescent imaging of *M. tuberculosis* in mouse and guinea pig lung revealed multiple

M. tuberculosis phenotypes [12]. These studies support a crucial role of heterogeneous host-pathogen interactions for disease progression, however several issues remain unanswered.

The major unresolved questions are:

1) What are the relevant host molecular antimicrobial mechanisms in different tissue areas?
2) How do pathogens adapt to these stresses?
3) Which interactions determine the fates of local pathogens in various regions?
4) How can some pathogens escape from hostile regions?
5) What determines overall pathogen tissue loads and disease progression?

Suitable methods to answer these questions are still largely lacking. One of the major technical challenges is to find, quantify and analyze small pathogens in large organs with various compartments (e.g. mouse spleen is about 10,000 fold larger than *Salmonella* with a volume of about 2 μm^3). This requires single-cell methods that are sensitive enough to yield sufficient signal-to background ratios. To address these questions a well characterized model system should be applied to minimize additional technical challenges.

1.1 Murine typhoid fever as a model to study host-pathogen interactions

Murine typhoid fever belongs to the best studied disease models for host-pathogen interactions. *Salmonella enterica* (*S. enterica*) is a gram negative, facultative intracellular bacterium with more than 2500 different serovars. *S. enterica* serovar Typhi and Paratyphi causes in humans typhoid fever, a disease that leads to approximately 20 million cases and 200,000 deaths annually [13].

The mouse infection model *S. enterica* serovar Typhimurium mimics important aspects of typhoid fever. Susceptible mouse lineages are widely used to study the pathogenesis of *Salmonella* Typhimurium infections. For example, natural resistance associated macrophage protein (NRAMP)1 , also called Slc11a1, deficient mouse strains are highly susceptible to *Salmonella* infection and are therefore a suitable tool to study early systemic infection [14, 15].

In the mouse model, *Salmonella* Typhimurium is either applied orally, intraperitoneally (IP) or intravenously (IV). Depending on the route of infection, *Salmonella* is confronted with different host cell types.

If *Salmonella* are ingested orally, the majority is killed by the low pH of the stomach. However, some *Salmonella* survive gastric acidity and evade multiple defenses of the small intestine to get access to the epithelium. *Salmonella* invades the epithelium by expression of specific gene sets which are

encoded on the *Salmonella* pathogenicity island 1 (SPI-1). These genes encode for a type 3 secretion system (T3SS), which is active on contact with the host cell and transports effector proteins required for invasion [16].

Salmonella preferentially enter phagocytic epithelial M-cells that transport them to lymphoid cells in the underlying Peyer's patches. From the Peyer's patches most bacteria reach the mesenteric lymph node (MLN) in dendritic cells or macrophages via the lymphatic system. Few bacteria escape the MLN and disseminate via the blood stream to liver and spleen. However, Pabst and coworkers showed data that contradicts this hypothesis. The characterization of genome tagged *Salmonella* strains in different organs led them conclude that *Salmonella* from spleen and liver are not derived through gut lymphoid tissues [17]. Alternatively, upon extraintestinal infection (IV or IP), the bacterium reaches liver and spleen by carriage within CD18 expressing phagocytes [18-20] (see Figure 1).

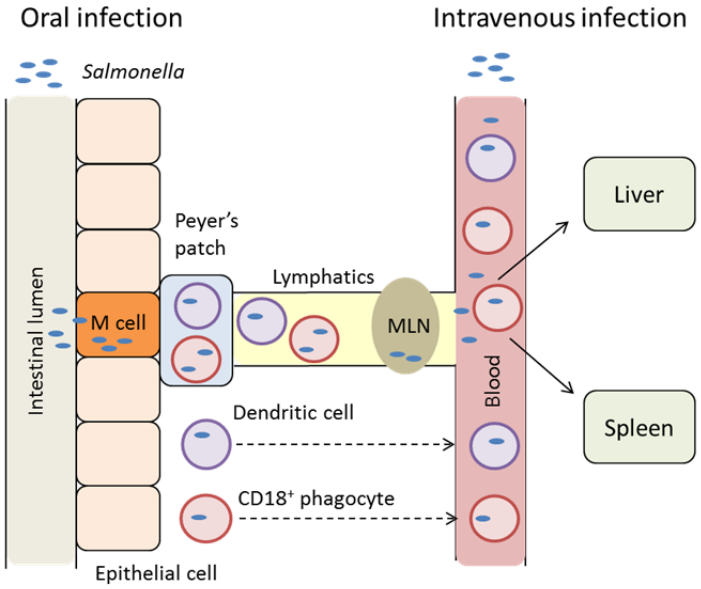

Figure 2 Routes of dissemination of *Salmonella* in the mouse

Independent of the infection route, susceptible mice develop a systemic disease characterized by rapid bacterial replication in liver and spleen with a net growth of 0.5-1.5 log/day [21]. Growth of bacteria leads to acute abscesses which become enlarged and transformed to granulomatous lesions with central necrosis and peripheral mononuclear leukocytes. The lesions in internal organs of mice and the distribution of *Salmonella* Typhimurium in tissue are similar to these in typhoid fever patients. Generally, symptoms in human patients closely resemble signs of disease in murine typhoid fever [15].

Overall, murine typhoid fever is a prime disease model to study host-pathogen interactions, not only because of similarity to systemic enteric fever, but also because of extensive literature, facile *Salmonella* microbiology and defined mouse mutants.

1.2 Heterogeneous host-*Salmonella* encounters

Systemic typhoid fever is characterized by rapid bacterial replication in liver and spleen. The complex anatomy of spleen and liver with different tissue compartments and host cells likely provides different growth opportunities for *Salmonella*. To get a deeper understanding which interactions determine disease progression, it is essential to focus on individual host-*Salmonella* encounters. Infected spleen and liver have similar pathogen loads, but liver is around 6-8 times bigger and about 10 times heavier than spleen, which makes single-cell analysis even more challenging. Moreover, infected livers accumulate large amounts of lipids, leading to additional challenges in FACS. Due to these additional technical challenges this thesis focuses on host-pathogen interaction in spleen.

1.2.1 Structure and function of the spleen

The spleen is the body's largest filter of blood and the most important organ for antibacterial immune reactivity. It is divided in three main compartments, the red pulp, the white pulp and the marginal zone, which are different in architecture, vascular organization and cellular composition.

The red pulp is composed of a tree-like meshwork of splenic cords and venous sinuses. The major cell types in the cords are macrophages. In the spaces between the cords are mainly erythrocytes, granulocytes, and circulating mononuclear cells. The main functions of the red pulp include filtering blood to remove old or damaged erythrocytes, and recycling of iron [22, 23].

The white pulp is divided into the T-cell zone, also known as the periarteriolar lymphoid sheath (PALS), and B-cell follicles. It is organized as lymphoid sheets around branching arterial vessels and plays a major role in the adaptive immunity. In the PALS T-cells interact with dendritic cells and passing B-cells. After contact with antigen-presenting cells T-cells become activated and migrate to B-cell follicles. The contact between B-cells and activated T-cells leads to clonal expansion of B-cells, isotype switching and somatic hypermutation [22].

The marginal zone is a unique region which is situated at the interface of the red pulp and the white pulp. It is a transit area for cells leaving the blood stream and entering the white pulp. The marginal zone screens the circulation for antigens and pathogens and plays an important role in antigen processing. The marginal zone contains two specific macrophage subsets, marginal zone macrophages and marginal zone metallophilic macrophages, in addition to marginal zone B-cells.

These specific macrophage subsets are apparently important in clearance of microorganisms and viruses [24, 25]. With the bloodstream flow many lymphocytes, dendritic cells and granulocytes can be found in transit from or to the red pulp. With its specific macrophage populations and B-cells the marginal zone is involved in both innate and adaptive immunity [22, 23].

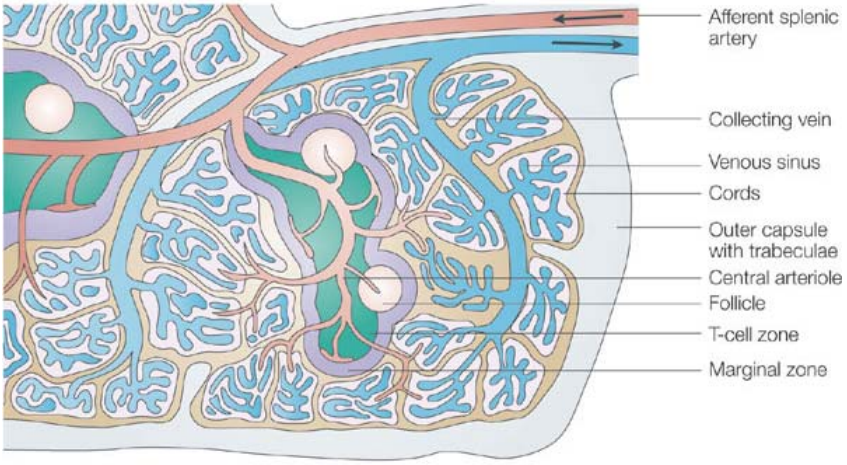

Figure 3 Structure of the spleen. The afferent splenic artery branches into central arterioles, which are sheathed by white pulp areas. Arterioles end in cords in the red pulp, from where the blood runs into venous sinuses which collect into the efferent splenic vein. The larger arteries and veins run together in connective tissue trabeculae, which are continuous with the capsule that surrounds the spleen [22].

1.2.2 Dynamics of growth and dissemination of *Salmonella*

Salmonella growth in spleen leads to drastic changes of the host environment arising from the influx of immune cells and the development of pathological lesions. Bacteria spread and distribute in the tissue in parallel to the onset and escalation of the host immune response [7]. Lesion formation is a dynamic process. It usually begins with recruitment of polymorphonuclear cells (PMNs) to individual infection foci. Lesions continuously grow and develop into multicellular lesions with mononuclear cells and PMNs. Mononuclear cells are recruited from bone marrow and possibly from spleen [26] to form an outer core around an inner core of PMNs [27, 28]. The recruitment of mononuclear cells is mediated by adhesion molecules and cytokines. This leads to a formation of tight clusters, in which neutrophils and monocytes cooperate and stimulate each other, enhancing their antimicrobial activity [29]. Most bacteria are contained in these well-defined lesions and failure of lesion development results in abnormal growth of *Salmonella* [30]. Sheppard and coworkers [7] showed that lesions increase in number rather than in size with an increase in microbial burden. Moreover, bacterial foci are independent of each other i.e. each focus evolves from clonal growth of an

individual founder bacterium. This indicates that bacteria grow within distinct infection foci and escape from these sites to disseminate to new foci. Importantly, disease progression is driven mainly through establishment of new infection foci, whereas old infection foci remain unproductive. Further work showed that the numerical distribution of intracellular bacteria is dependent on intrinsic bacterial growth rate and immune control mechanisms, such as interferon gamma (IFNγ) and NADPH oxidase [31]. How intracellular *Salmonella* access new cells is still unclear. Several studies showed that this may occur through a process of cell death and subsequent phagocytosis (reviewed by Watson et al. [20]).

To get a more defined understanding of *Salmonella* growth dynamics the factors underlying the net growth rate need to be dissected. The net growth rate depends on bacterial replication, bacterial killing and heterogeneity of growth within the bacterial population.

To distinguish between bacterial replication and killing early studies used non-replicating elements, including super-infecting phages [32], temperature sensitive mutants [33] and temperature sensitive plasmids [34] within the growing bacterial population. Grant and coworkers [35] provided a more comprehensive analysis of global population dynamics. They used a technique to tag individual subpopulations of bacteria, called wild-type isogenic tagged strains (WITS). This allowed estimating bacterial expansion, killing and spreading. Their data indicated that death and rapid bacterial replication occur early in infection and lead to establishment of independent bacterial subpopulation in different organs. An elegant tool to measure intracellular bacterial growth kinetics at the single cell level was developed by Helaine and coworkers [36]. Their reporter system is based on fluorescence intensity which correlates with growth rates of individual bacteria. Here, the decrease in fluorescence intensity within a bacterial cell is used as an alternate marker for cell division. This technique can provide information about replication diversity within a bacterial population. Overall, their work showed that replication of *Salmonella* within macrophages is heterogeneous.

To understand detailed dynamics of population growth, it is crucial to investigate what occurs at the single cell level *in vivo*. Some studies already indicated that *Salmonella*-host interactions *in vitro* and *in vivo* are heterogeneous [7, 35, 36]. Nonetheless, it is unclear which heterogeneous interactions drive *Salmonella* disease progression. Several important questions which remain unanswered include: What is the distribution of *Salmonella* in different cell types? Which cell types and which host molecules are important for *Salmonella* growth, survival or killing? To answer these questions it is essential to know which host cells and molecules are pivotal in infection. The following paragraphs review the roles of host cells and molecules, which are central for innate immune defense in an early infection.

1.2.3 Host response to *Salmonella*

Neutrophils

Neutrophils, also named PMNs, are the most abundant leukocytes in circulation. Deriving from myeloid progenitor cells in bone marrow, they are the first cells to be recruited to a site of infection. In humans and mice, a total absence or low numbers of neutrophils leads to severe immunodeficiency [37]. In their role as efficient phagocytes, they engulf and degrade microorganisms in phagolysosomes using oxidative and non-oxidative mechanisms. The oxidative pathway generates large quantities of reactive oxygen species (ROS). ROS are responsible for oxidative stress; they can damage DNA, proteins and lipids. In the non-oxidative pathway antimicrobial peptides (AMPs) and hydrolases are released from neutrophil granules. These enzymes can induce membrane permeabilization, hydrolysis of lipids, hydrolysis of carbohydrates or hydrolysis of proteins. However, how oxidative and non-oxidative pathways kill bacteria is still under debate [38, 39].

Phagosomal killing by oxidative pathways

Phagocytosis of microorganisms is followed by a burst of oxygen consumption, also known as oxidative or respiratory burst. The enzyme responsible for oxygen consumption is the NADPH oxidase, which upon activation is assembled at the plasma or phagosomal membrane [40]. The NADPH oxidase transfers electrons from cytoplasmic NADPH to extracellular or phagosomal molecular oxygen (O_2) to generate superoxide (O_2^{*-}). Superoxide spontaneously dismutates to hydrogen peroxide (H_2O_2), a reaction that maintains intraphagosomal pH near neutrality [41]. Myeloperoxidase (MPO), a key enzyme in neutrophils, is released from azurophilic granules and converts almost all O_2^{*-} or H_2O_2 into highly toxic hypohalous acids (e.g OCl^- OBr^-, OI^-). Hypochlorite (HOCl) is one of the most abundant species in phagosomes if chloride supply is not limited [42, 43]. HOCl (bleach) has strong microbicidal properties and is considered as the major oxidative weapon of the neutrophil [44-46]. It can react with a wide range of amino acids, proteins and peptides yielding oxidized and/or chlorinated peptides and proteins. Reaction with tyrosine residues leads to formation of 3-chlorotyrosine, 5-chlorotyrosine and 3,5-chlorotyrosine, which are implicated in impaired protein function. Oxidation of methionine residues can correlate with loss of bacterial viability [47]. MPO also oxidizes thiocyanate and H_2O_2 to the product HOSCN, a weaker oxidant than HOCl, but which can penetrate cell membranes and oxidize intracellular sulfhydryl groups [48]. Overall, MPO provides neutrophils with their most effective mechanisms for killing [45] (see Figure 4).

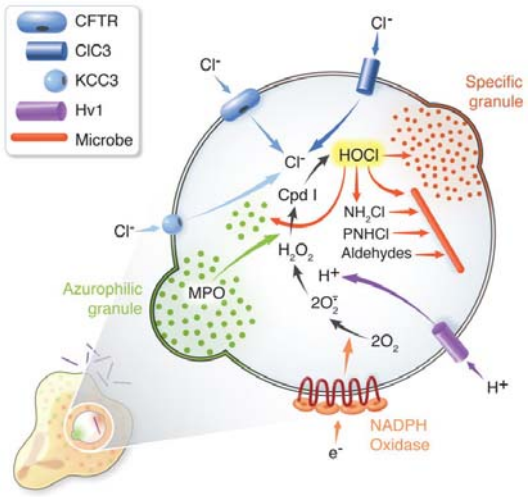

Figure 4 NADPH oxidase and MPO dependent events in human neutrophil phagosomes [49].

The clinical consequences of NADPH oxidase and MPO deficiency highlight their differential relevance in host defense. Individuals with defects of NADPH oxidase components develop a rare immunodeficiency called chronic granulomatous disease (CGD). CGD is the most common inherited disorder of neutrophil function with an estimated incidence of around 1 in 200,000. CGD patients often suffer recurrent, life-threatening bacterial and fungal infections [50, 51]. Neutrophils of CGD patients show normal antimicrobial activity if hydrogen peroxide is introduced exogenously. This indicates that except for superoxide production CGD neutrophils function normally [52]. In comparison to NADPH oxidase deficiency, MPO deficiency is relatively common with a prevalence of around 1 in 2000-4000 individuals in Europe and the US [53-55]. Early studies suggested a correlation between MPO deficiency and cancer or bacterial and fungal infections [56, 57]. Screening of several thousand individuals, however, led to the conclusion that MPO plays only a minor role in infection, because most MPO deficient individuals' showed no clinical phenotype. However, there may be different reasons for this discrepancy. Several clinically MPO deficient people still have residual MPO activity, and partial MPO deficiency does not correlate with pathology [53]. It is possible that residual MPO activity might be sufficient for antimicrobial activity, as it is the case for NADPH oxidase.

In vitro studies with MPO deficient neutrophils supplement the *in vivo* observations described above. Neutrophils deficient in MPO are still able to kill microbes with oxidative stress, although less efficiently [45]. In the absence of MPO, superoxide and H_2O_2 are still produced and can potentially lead to damage to microbes [44]. Hydrogen peroxide and superoxide can oxidize solvent exposed iron- sulfur clusters. The released ferrous iron can generate highly reactive hydroxyl radicals ($^{*}OH$) via the Fenton reaction leading to further damage of biomolecules, including DNA [58]. Superoxide could also react with nitric oxide (NO), generated by inducible nitric oxide synthase (iNOS), to form peroxynitrite. Peroxynitrite is a strong oxidant producing reactive radical species, such as NO_2, $^{*}OH$

and carbonate radicals [59]. These reactive oxygen and nitrogen species (RNS) can oxidize non-protein and protein sulfhydryl groups. Computational modeling of neutrophil phagosomes proposed superoxide concentration of >100 µM and hydrogen peroxide concentrations of about 30 µM in the absence of MPO [44]. If these concentrations are sufficient to kill pathogens with oxidative defense mechanisms needs to be elucidated. Most of the data presented here were derived from enzymatic *in vitro* assays, cell culture studies or computational modeling. However, reliable *in vivo* data confirming these results are missing due to technical challenges in detecting short-lived ROS and RNS. Overall, the roles of ROS, RNS and myeloperoxidase in infection still remain controversial.

Phagosomal killing by non-oxidative pathways

Phagosomal killing by non-oxidative pathways is induced by fusion of neutrophil granules with the phagolysosome. There are four different types of neutrophil granules: azurophilic or primary, specific or secondary, gelatinase or tertiary and secretory granules. The granules are classified according to protein content and ability to exocytose after neutrophil activation by inflammatory stimuli or phagocytosis of microorganisms [60]. In general, they contain a broad spectrum of bactericidal and degradative proteins. In addition, they can prevent growth by limiting availability of essential nutrients inside the phagosome. Nutrient deprivation can for example be exerted by lactoferrin and NRAMP1 (Slc11a1). Lactoferrin is a glycoprotein that sequesters iron, an essential growth factor for bacteria, whereas Slc11a1 is a membrane protein, which extrudes from the phagosomal lumen important divalent cations, such as Zn^{2+}, Fe^{2+} and Mn^{2+}. Proteins using bactericidal mechanisms react directly with proteins, membranes, or carbohydrates of the ingested microorganism. Cationic antimicrobial proteins (CAMPs), such as defensins and cathelicidins, bind to negatively charged molecules on the microbial surface. This leads subsequently to membrane permeabilization induced by formation of ion-permeable channels [61, 62]. Another CAMP that binds specifically surfaces of gram-negative bacteria is the bactericidal permeability increasing protein (BPI). A few studies showed that BPI might be important in the degradation of bacterial membranes [63, 64], whereas another study reported that recombinant mouse BPI inhibits endotoxic capacity of LPS but failed to inhibit bacterial growth [65]. Perforin-2, a specific pore forming protein expressed by all mammalian cells, was recently described to have bactericidal specificity for pathogenic and non-pathogenic bacteria [66]. *In vitro*, Perforin-2 prevents intracellular replication and proliferation of pathogens. *In vivo*, Perforin-2 deficient mice were unable to control systemic dissemination of *Staphylococcus aureus* or *Salmonella* Typhimurium [67].

Hydrolysis of proteins is mainly exerted by the cathepsin family consisting of serine proteases (cathepsins A and G), aspartate proteases (cathepsins D and E) and cysteine proteases (cathepsins B,

C, F, H, K, L, O, S, V, X, and W). In addition to the cathepsin family, neutrophil elastase and proteinase 3 have a high degree of homology and functional similarity to serine protease cathepsin G. Neutrophil elastase, for example, cleaves virulence factors of enterobacteria such as *Shigella flexneri* and *Salmonella enterica* [68]. Elastase and cathepsin G require activity of cathepsin C, also known as dipeptidyl peptidase I (DPPI), to become active. DPPI is an important regulator for bacterial control and clearance in a mouse model for sepsis [69], in a lung infection model [70] and in mice deficient in olfactomedin 4 (a glycoprotein with diverse functions) [71]. Humans lacking DPPI suffer from Papillon-Lefevre syndrome, a rare immunodeficiency disease. However, only a small number of patients succumb to severe systemic infections and only some neutrophils from patients are defective in killing bacteria [72]. Other proteolytic proteins which might be involved in non-oxidative killing include calprotectin, which sequesters manganese and zinc to alter bacterial growth and tartrate resistant acid phosphatase, which degrades phosphoproteins.

Hydrolases that target carbohydrates include lysozyme, beta-hexosaminidase and beta-glucuronidase. Lysozyme degrades bacterial cell walls by hydrolysis of peptidoglycan. Most Gram negative bacteria, however, are not susceptible to the action of lysozyme alone because their outer membrane prevents access of the enzyme to the peptidoglycan layer. Hydrolysis of lipids is induced by the phospholipase A2 family and phospholipase D [60-62].

Overall, the importance of non-oxidative mechanisms for killing microbes remains unclear. The significance of individual antimicrobial factors for bacterial killing is pathogen-specific and differs according to experimental settings. Moreover, a vast number of proteins are known for non-oxidative killing, but only DPPI shows clinical significance. This indicates that non-oxidative killing mechanisms might act synergistically or redundantly and/or are a back-up mechanism if oxidative killing fails.

Synergism between oxidative and non-oxidative pathways

Synergism between oxidative and non-oxidative pathways exists, but the relative contributions of each mechanism remain unclear and vary among microorganisms [38]. In mice infected with *Klebsiella pneumonia*, animals succumbed if either MPO or elastase was missing [73]. In contrast to this, another study showed that double knockout neutrophil elastase and cathepsin G mice cleared infection of *Burkholderia cepacia*, whereas NADPH oxidase was indispensable [74]. However, neutrophil elastase activity is apparently promoted by the presence of the MPO/H_2O_2/Cl^- chlorinating system [75]. Another example of synergism was demonstrated between NADPH oxidase and phospholipase gIIa-PLA2 in degrading *Staphylococcus aureus* phospholipids [76]. Very recently, the

pore forming protein perforin-2 was described to potentiate antibacterial activity of ROS and RNS [67]. A different view of synergism has been proposed by Segal and coworkers, where the central role of NADPH oxidase is not to produce ROS, but to polarize the phagosomal membrane to drive the influx of K^+ ions. In this model, osmolarity causes granule derived microbicidal proteinases, including elastase and cathepsin G, to be activated by release from proteoglycan complexes. These proteases lead to bacterial killing, whereas MPO has a major function as catalase to protect the neutrophil from H_2O_2 damage [77]. However, experimental evidence of other researchers could not confirm this hypothesis [78].

In addition to phagosomal killing neutrophils can kill microbes extracellular with so called neutrophil extracellular traps (NETs). NETs contain histones, antimicrobial granules and cytoplasmic proteins. NADPH oxidase and MPO are required for NET formation; however the mechanism and relevance is not completely understood. NETs may be especially important under certain conditions, such as during infections with large pathogens that are not readily phagocytosed [79].

Overall, neutrophil recruitment to the site of infection is crucial for clearance of infection. Neutrophils possess multiple mechanisms with a vast number of toxic molecules to eliminate pathogens. Which mechanisms and molecules are used to clear specific pathogens remains, however, controversial.

Macrophage

Macrophages (from greek makros “large” + phagein “eat”) are the “big eaters” of the immune system. They are located throughout the body tissues, ingesting and processing foreign material, dead cells and debris and recruiting additional macrophages in response to inflammatory stimuli [80]. Macrophages encounter and engulf invading microbes at infection sites and utilize specialized effector functions to kill or damage pathogens. Nonetheless, several pathogens exploit macrophages as a niche for survival. To resolve this macrophage paradox it is necessary to acknowledge the diversity and complexity of macrophages [81].

Macrophage is a global term for a whole subpopulation of different cell types in different locations and with different functions. Macrophages generally consist of two classes: tissue resident macrophages and infiltrating macrophages. Tissue resident macrophages originate early in embryogenesis, primarily from cells in the yolk sac or fetal liver, expressing characteristically the F4/80 antigen [82]. They reside in specific microenvironments and perform homeostatic functions in their respective tissues in the steady state. In spleen, the main function of resident red pulp macrophages is erythrophagocytosis (removal of old erythrocytes) and recycling of iron [83].

On the other hand, infiltrating macrophages are recruited from bone marrow or spleen from a common myeloid progenitor shared with neutrophils. Infiltrating macrophages are traditionally divided into two main subsets in mice and human. The first type is designated classical monocyte, also known as inflammatory monocyte, which differentiate into inflammatory macrophages, also known as M1 macrophage. The second type is designated non-classical monocyte, which differentiates into a wound-healing macrophage also known as M2 macrophage [80, 84].

Classical monocytes are characterized by expressing specific receptor antigens on their surface, for example the characteristic Ly6C antigen. Once they are released into peripheral blood, they circulate for several days before entering tissue, differentiating into macrophages and replenishing the tissue macrophage population [85]. Undifferentiated monocytes also reside in spleen and apparently outnumber their equivalents in circulation [26]. Classical monocytes are important in innate immune protection against infectious pathogens. They become activated by various cytokines (e.g. IFNγ) that are released from neighboring inflammatory cells, including neutrophils, natural killer cells, resident tissue macrophages and T cells. IFNγ strongly induces several antimicrobial defenses, particularly autophagy, RNS and antimicrobial GTPases such as guanylate binding protein (GBP) family members [86]. Once activated, monocytes secrete pro-inflammatory mediators such as tumor necrosis factor (TNF) and IL-1, which participate in the activation of various antimicrobial mechanisms.

Similar to neutrophils, M1 macrophages produce reactive oxygen and nitrogen intermediates, as well as antimicrobial peptides. Nonetheless, they are not as efficient in killing as neutrophils, because neutrophils exhibit more rapid rates of phagocytosis and higher intensities of oxidative bursts. M1 macrophages digest microbes in mature acidified phagosomes, whereas neutrophil phagosomes remain neutral [87] or get alkaline [88]. Although the acidic pH should help to eliminate pathogens, in some cases it benefits bacteria to survive intracellularly [89, 90]. Microbes that escape the phagosome can be targeted for elimination by autophagy [91].

In contrast to neutrophils, classical monocytes contribute to the development of adaptive immune responses by presenting bacterial antigens to lymphocytes. In addition they can give rise to the main antigen presenting cells, TNF and iNOS producing dendritic cells [92, 93].

Non-classical Ly6C^{lo} monocytes patrol the blood circulation and clear damaged epithelial cells. However, they do not enter the tissue to differentiate into M2 macrophages. Instead, classical Ly6C^{hi} monocytes are recruited into tissue and differentiate into Ly6C^{lo} M2 macrophages, when stimulated by interleukin-4 (IL-4) or IL-13 [94]. M2 macrophages have important roles in wound-healing and fibrosis and are strongly anti-inflammatory. They also counteract the classical M1 macrophage

response, which may be critical for the activation of the wound healing response and for restoration of tissue homeostasis [80]. In addition to the described macrophage subsets, several other macrophage subpopulations and definitions are emerging in the literature, but will not be discussed here [95, 96].

Immune cell response to *Salmonella* infection in spleen

In spleen *Salmonella* resides in diverse cell types, including red pulp and marginal zone macrophages [97], neutrophils, monocytes, DC cells [98, 99] and B lymphocytes [100]. However, there is contradictory evidence which cell types or host molecules are important for *Salmonella* replication or killing. One recent study showed that infection of *S. typhimurium* leads to increased proportion of red pulp macrophages and decreased proportions of B- cells, T-cells and marginal zone macrophages, limiting the impact of lymphocytes in infection [101]. Some studies have suggested that *Salmonella* mainly resides and replicates in red pulp macrophages [97, 102]. Other data showed that *Salmonella* may establish a chronic infection via replication in M2 macrophages [103]. One study even suggested that *Salmonella* replicates in neutrophils [104]. Dendritic cells also harbor *Salmonella* during infection; however specific subsets only become important 5 days post infection [105].

Although the relative role of the various cell types is still unclear, *Salmonella* seem to reside in neutrophils, monocytes and macrophages *in vivo*. These cells are equipped to destroy pathogens with oxidative and non-oxidative mechanisms. Cell culture studies showed that neutrophils, monocytes and macrophages can kill *Salmonella* effectively, mainly with NADPH oxidase dependent mechanisms [36, 106, 107]. NADPH oxidase is also crucial for infection control in mice [108], but it is unclear if this is due to a direct bactericidal effect of ROS [39]. INOS has substantial bacteriostatic effect in cell culture models, however it is dispensable for *Salmonella* control during the first 7 days of infection [108]. The role of MPO in a typhoid fever model has not been studied yet. A few non-oxidative mechanism might also play a role in *Salmonella* killing *in vivo* (see above), but conclusive evidence is lacking.

The role of macrophages in *Salmonella* infection remains unclear. On the one hand, murine macrophage cell lines, such as RAW 264.7 cells or J774.1 cells, are a niche of *Salmonella* survival. On the other hand, primary macrophages, such as peritoneal elicited macrophages or bone marrow derived macrophages kill *Salmonella* efficiently. Primary macrophages mimic more closely the natural interaction between *Salmonella* and monocytes/macrophages than macrophage cell lines. However, the *in vitro* differentiated macrophage may still respond and behave differently compared

to a macrophage *in vivo*, which receive stimuli and interact with other immune cells. In addition, *Salmonella* may respond differently in cell culture compared to *in vivo* environments.

1.2.4 *Salmonella* response to host environments

Salmonella response to oxidative stress

Salmonella Typhimurium is equipped with a vast array of detoxification systems and virulence genes to survive and grow inside host cells. To counteract microbicidal ROS *Salmonella* uses several enzymes, including catalases (KatE, KatG, KatN), peroxiredoxins (AhpC, TsaA, TpX) and superoxide dismutases (SodA, SodB, SodCI, SodCII). Catalases and peroxiredoxins are scavengers of H_2O_2. SODs are scavengers of O_2^{*-} and may thereby prevent cytotoxic reactions with other species. A protein called Dps sequesters iron to prevent its interaction with H_2O_2, limiting the possibility of DNA damage by the Fenton reaction. In addition, a variety of repair enzymes can reverse oxidative DNA damage. [78]. The contribution of these defense enzymes for ROS detoxification is controversial. Several studies suggested that only periplasmic SodC plays a specific role in virulence [109, 110]. However, Aussel and coworkers showed that *Salmonella* HpxF(-) mutant, deficient in all three catalases and the two alkyl hydroperoxide reductases (AhpC and TsaA) exhibited a severe survival defect in macrophages and attenuated virulence in a mouse model [111]. Interestingly, individual catalase or peroxiredoxin defects were dispensable for *Salmonella* virulence, illustrating its redundant defense mechanisms. A study by Craig and Slauch [112] suggested that SodCI acts independently of other SODs, and RuvAB, which is involved in DNA repair. They concluded that ROS primarily damages extracytoplasmic targets, rather than DNA, to inhibit or kill *Salmonella*. However, additional studies suggested that DNA is an important target for phagocyte derived ROS, and DNA repair enzymes are important for *Salmonella* virulence [113, 114]. Another study highlights the importance of ferritins for *Salmonella* virulence. Ferritins store intracellular free iron, which would be otherwise accessible for Fenton mediated damage. In addition, the specific ferritin B appears to be important for repair of damaged iron-sulfur clusters [115].

Another potential mechanism of ROS evasion and intracellular survival is derived by the Type 3 Secretion system (T3SS) encoded by *Salmonella* pathogenicity island 2 (SPI-2). The SPI-2 T3SS injects specific effector proteins across the vacuolar membrane into the host cytosol. Effectors interact with the host machinery to affect vesicular trafficking and maturation of the phagolysosome, which allow *Salmonella* to grow in the *Salmonella* containing vacuole (SCV) [19]. The SPI-2 T3SS was reported to interfere with the localization of a functional NADPH oxidase complex in SCVs and to reduce the colocalization of *Salmonella* and H_2O_2 [116, 117]. SPI-2 was also reported to protect *Salmonella* from

nitrotyrosine, which is indicative for peroxynitrite formation [118]. In addition Finlay and coworkers found that SPI-2 is required for ROS evasion by directly measuring redox stress of *Salmonella* Typhimurium in human and murine macrophages [119]. Whether the SPI-2 T3SS is really important for protecting *Salmonella* from oxidative stress is controversial. Aussel and coworkers utilized a *Salmonella* biosensor to monitor oxidative stress experienced by *Salmonella* in infection. Host ROS production was independent of SPI-2, suggesting that SPI-2 is unrelated to interaction with NADPH oxidase [120]. Helaine and coworkers suggested that SPI-2 promotes bacterial replication rather than resistance to killing [36]. However, Suvarnapunya and Stein demonstrated that macrophages cause increased oxidative DNA damage in *Salmonella* mutants that lack SPI-2 T3SS [121]. A different role for SPI-2 was suggested by Mastroeni and colleagues, who showed that SPI-2 mutants grow to high intracellular numbers in host cells *in vivo* but cannot spread. Interestingly, SPI-2 mutant *Salmonella* could spread in mice deficient in NADPH oxidase, suggesting that SPI-2 T3SS becomes dispensable in the absence of an active NADPH oxidase [122]. In addition to ROS defense mechanisms *Salmonella* is also equipped with genes responding to non-oxidative stress.

Salmonella response to non-oxidative stress

In order to cope with non-oxidative stress *Salmonella* induces various regulatory systems including OmpR/EnvZ, PhoP/PhoQ, RpoS/RpoE, PmrA/PmrB, Cya/Cyp and cyclic diGMP. In macrophages *Salmonella* sense the acidic environment of the SCV which promotes upregulation of specific proteins leading for example to remodeling of the protein, carbohydrate and membrane components of the bacterial envelope [123]. It is probable that several regulatory systems work together to fulfill these tasks and promote intracellular survival. The best characterized system is the PhoQ sensor, which promotes resistance to antimicrobial peptides [124, 125]. Further studies on *Salmonella* regulatory systems have been reviewed by Haraga and LaRock [19, 126], and will not be discussed here. A large body of research has been dedicated to revealing functions and mechanisms of *Salmonella* virulence genes, which are important for intracellular survival. Most of these data, however, were derived by *in vitro* cell culture studies, which are not ideal to mimic the complexity of host environments *in vivo*. A very recent study, however, demonstrates that variable PhoPQ activity drives variable host responses, which has implications for host-pathogen dynamics *in vivo* [127].

Overall, *Salmonella* is equipped with several defense systems to counteract a variety of host defense mechanisms, including ROS and RNS. However, it remains controversial which mechanisms are used and different results may appear from various experimental conditions (as described above). Hence, a detailed analysis of single *Salmonella*-host encounters *in vivo* will clarify which *Salmonella* defense mechanisms are used in which host microenvironment.

1.3 Goal of the thesis

Infectious diseases are caused by the immune system's failure to eradicate pathogens. Past research has unraveled a large number of important host defense mechanisms, as well as pathogen counterattack systems. However, one central aspect of host-pathogen interactions has been largely neglected. Host-pathogen interaction takes place in tissues with complex anatomy, (e.g. white pulp vs. red pulp in spleen), diverse cell types (e.g. neutrophils, monocytes, macrophages) and different host molecules (e.g. ROS, RNS, cytokines, AMPs), which likely impose different stresses on pathogens. However, commonly used bulk average measurements and cell culture experiments do not cover the spatial complexity and cannot reveal individual host-pathogen encounters, which might be central for disease progression. My aim was to investigate the diversity of host-pathogen interactions in the well characterized mouse typhoid fever model. To achieve this aim, I combined fluorescent *Salmonella* biosensors with high-resolution confocal imaging to reveal the unique fate of *Salmonella* in specific host environments.

My main questions were:

1) How does the host environment change upon *Salmonella* infection?

2) Which host antimicrobial mechanisms are operative in the various environments?

3) What is the fate of *Salmonella* in these host environments e.g. growth, survival, or death?

4) Which interactions determine the overall pathogen tissue loads and disease progression?

Answering these questions was crucial to determine the importance of host-pathogen interactions for disease control.

2 Publications

2.1 Disparate Impact of Oxidative Host Defenses Determines the Fate of *Salmonella* during Systemic Infection in Mice

Neil A. Burton[1]‡, **Nura Schürmann[1]‡,** Olivier Casse[1], Anne K. Steeb[1], Beatrice Claudi[1], Janine Zankl[2], Alexander Schmidt[3], Dirk Bumann[1]*

[1] Focal Area Infection Biology, University of Basel, 4056 Basel, Switzerland

[2] FACS Core Facility, University of Basel, 4056 Basel, Switzerland

[3] Proteomics Core Facility, Biozentrum, University of Basel, 4056 Basel, Switzerland

‡ These authors contributed equally to the work.

*Corresponding Author

The manuscript was published in Cell Host & Microbe Volume 15, Issue 1, 15 January 2014, 72–83

doi:10.1016/j.chom.2013.12.006

Statement of my work:

Design of experiments

Immunohistochemistry (Fig. 1C-G, Fig. 2D, Fig S1B)

Analysis of immunohistochemistry (Fig 1 H-J, Fig. 2B, C, E, F)

Flow Cytometry + Analysis (Fig.4D)

Manuscript writing and revision with N.B. and D.B.

Disparate Impact of Oxidative Host Defenses Determines the Fate of *Salmonella* during Systemic Infection in Mice

Neil A. Burton[1]‡, Nura Schürmann[1]‡, Olivier Casse[1], Anne K. Steeb[1], Beatrice Claudi[1], Janine Zankl[2], Alexander Schmidt[3], Dirk Bumann[1*]

[1]Focal Area Infection Biology, [2]FACS Core Facility, [3]Proteomics Core Facility, Biozentrum, University of Basel, CH-4056 Basel, Switzerland

*Correspondence to: dirk.bumann@unibas.ch

‡ contributed equally

Summary:

Reactive oxygen and nitrogen species are fundamental for host defense against infections, but underlying mechanisms remain controversial. Here, we used single-cell approaches to show that *Salmonella* are exposed and respond to both species in a mouse typhoid fever model, but levels and impact vary widely during early infection. Neutrophils and inflammatory monocytes kill *Salmonella* by generating overwhelming oxidative stress through NADPH oxidase and myeloperoxidase. This controls *Salmonella* within inflammatory lesions, but does not prevent spreading to more permissive resident red pulp macrophages, which generate only sub-lethal oxidative bursts. Regional host expression of inducible nitric oxide synthase exposes some *Salmonella* to nitrosative stress triggering effective local *Salmonella* detoxification through nitric oxide denitrosylase. These data show how reactive oxygen and nitrogen species influence the dramatically different outcomes of many disparate *Salmonella*-host cell encounters, which together determine overall disease progression.

Introduction:

Infectious diseases remain an important health problem. Host defense against pathogens depends on generation of reactive oxygen species (ROS) using NADPH oxidase, and reactive nitrogen species (RNS) using inducible nitric oxide synthase (iNOS) [128, 129]. ROS and RNS can inhibit microbial growth or even kill microbes, and this is often assumed to represent their main mechanisms in infection control. However, this hypothesis remains highly controversial [130-134]. Various pathogens are highly resistant to ROS/RNS stress due to protective mechanisms that directly interfere with NADPH oxidase or iNOS activities, detoxify ROS and RNS before these compounds can damage the pathogen, and/or repair or replace damaged pathogen components. Moreover, ROS and RNS have additional important functions as host signaling molecules that regulate a wide variety of innate immune mechanisms including chemotaxis, signaling, cell activation, vasculature tension, etc., which all could contribute to infection control. Unfortunately, available data and interpretations are conflicting and as a result, these fundamental aspects in infection biology remain largely unclear.

This confusion could in part reflect that pathogens colonize remarkably diverse host cell types and tissue microenvironments during infection. In these microenvironments, pathogens might encounter varying levels of oxidative and/or nitrosative stress with different impact on pathogen survival and growth. Commonly used experimental approaches rely on bulk average measurements such as pathogen net growth or number of infiltrating host cells. Such average measurements fail to capture any heterogeneity of host/pathogen interactions and might thus yield confusing data that are difficult to interpret.

Here, we developed single-cell approaches to determine the impact of ROS and RNS on individual *Salmonella* in an extensively characterized mouse typhoid fever model. We

focused on early stages of acute infection in genetically susceptible mice, which have been investigated in many, apparently conflicting studies. Our goal was to clarify several controversial issues including the extent of *Salmonella* killing by host defenses, the impact of ROS and RNS on *Salmonella* properties and fates, and the potential role of diverse *Salmonella*/host encounters on overall disease progression.

Results:

Oxidative killing of *Salmonella* by neutrophils and monocytes in inflammatory lesions

In infected mouse spleen at day 4 post infection, *Salmonella* almost exclusively colonized the red pulp (Figure 1A,B), consistent with previous observations [97]. Neutrophils and inflammatory monocytes accumulated in inflammatory lesions in infected regions, as expected [135, 136]. *Salmonella* resided in neutrophils and monocytes within lesions, and primarily in resident red pulp macrophages outside of these lesions (Figure 1C-H).

An antibody to *Salmonella* lipopolysaccharide (LPS) stains both live and dead *Salmonella*, but intracellular retention of fluorescent proteins can be used to discriminate live from dead *Salmonella* [137]. Using *Salmonella* expressing the red fluorescent protein mCherry (RFP), we determined that most *Salmonella* within neutrophils and inflammatory monocytes in inflammatory lesions were dead (LPS^+ RFP^-; Figure 1D,E,I). Large lesions contained little detectable LPS suggesting successful *Salmonella* clearance. In comparison, red pulp macrophages outside of inflammatory lesions contained lower proportions of dead *Salmonella* (LPS^+ RFP^+; Figure 1F,G,I). *Salmonella* killing in macrophages was almost abolished in mice treated with a neutralizing antibody to IFNγ (Figure 1J), consistent with the crucial role of IFNγ in early *Salmonella* control [138-140] and activation of macrophage killing capabilities [141].

Cybb$^{-/-}$ mice deficient for cytochrome b-245 heavy chain, an essential subunit of NADPH oxidase, are hyper-susceptible for *Salmonella* infection [142]. The high spleen loads in such mice (Figure 2A) correlated with less *Salmonella* killing within neutrophils and inflammatory monocytes, whereas *Salmonella* live/dead ratios remained unaltered in resident macrophages (Figure 2B). As a consequence, higher proportions of live *Salmonella* resided in neutrophils and inflammatory monocytes in *Cybb*$^{-/-}$ mice (Figure 2C). These data indicated

that neutrophils and inflammatory monocytes effectively killed *Salmonella* using NADPH oxidase, while resident macrophages used less effective, largely NADPH oxidase-independent *Salmonella* killing mechanisms in this infection model.

NADPH oxidase generates superoxide $O_2^{\cdot -}$, which spontaneously dismutates to hydrogen peroxide H_2O_2 and molecular oxygen. Neutrophils and inflammatory monocytes, but not resident macrophages, express myeloperoxidase (MPO) that converts $O_2^{\cdot -}$ or H_2O_2 almost quantitatively into highly bactericidal hypohalites hypochlorite OCl^- (bleach), hypobromite, and/or hypoiodite [143, 144]. In infected spleen, myeloperoxidase preferentially co-localized with dead *Salmonella* (Figure 2D,E), and *MPO*$^{-/-}$ mice deficient for myeloperoxidase had slightly elevated *Salmonella* loads (Figure 2F). Together, these data suggest a contribution of hypochlorite (and/or related species) in *Salmonella* killing.

Nevertheless, myeloperoxidase was largely dispensable for *Salmonella* control indicating alternative NADPH oxidase-mediated killing mechanisms. In the absence of myeloperoxidase, neutrophils accumulate increased levels of $O_2^{\cdot -}$ and H_2O_2 [145]. To explore the potential impact on *Salmonella*, we combined a published computational model for oxidative bursts in neutrophil phagosomes [145] with *in vivo* expression data for *Salmonella* ROS defense enzymes [146]. This in silico model predicted that in absence of myeloperoxidase, superoxide and hydrogen peroxide accumulate in the phagosomal lumen (Figure 3), as expected [145]. According to the model, superoxide was largely present in the deprotonated form $O_2^{\cdot -}$ that poorly penetrated into bacteria [147], whereas H_2O_2 reached levels around 15 μM within *Salmonella*, far above the lethality threshold for *Salmonella* of approximately 2 μM [148]. This predicted lethal internal H_2O_2 concentration was the consequence of phagosomal H_2O_2 (17 μM) readily diffusing through the *Salmonella* envelope [148] at rates matching the *Salmonella* detoxification rate (0.15×10^6 molecules s^{-1}).

Salmonella killing by moderate but stable levels of luminal H_2O_2 would be consistent with previous data for high lethality of continuous H_2O_2 exposure [149].

Interestingly, increasing *Salmonella* detoxification by 0.15 x 10^6 molecules s^{-1} (thus doubling its rate) would marginally affect predicted phagosomal H_2O_2 (16.3 μM vs. 17 μM), due to buffering by the much larger H_2O_2 diffusion out of the phagosome to the host cell cytosol (3.8 x 10^6 molecules s^{-1}; Figure 3). This diffusion is by definition proportional to the concentration gradient between phagosome and cytosol, and a slight decrease of phagosomal H_2O_2 from 17 μM to 16.3 μM would lower its rate already by 0.15 x 10^6 s^{-1}. As *Salmonella* detoxification increased, less H_2O_2 would thus be lost to the host cell cytosol, and this compensated for the increase in *Salmonella* detoxification resulting in almost unaltered phagosomal steady state concentrations.

Together, these data suggested NADPH oxidase-dependent oxidative killing of *Salmonella* in neutrophils (and inflammatory monocytes) either by hypohalites, or by overwhelming hydrogen peroxide if myeloperoxidase was absent. In addition to such direct bactericidal ROS effects, synergism with other bactericidal mechanisms including antimicrobial peptides and hydrolases might contribute to *Salmonella* killing but further studies are required to clarify this issue.

Moderate oxidative bursts fail to kill *Salmonella*

While *Salmonella* in neutrophils and monocytes were largely killed through NADPH oxidase-dependent mechanisms, most live *Salmonella* resided in macrophages with apparently little impact of NADPH oxidase (Figure 2B). To determine if such live *Salmonella* experienced any oxidative stress, we used *Salmonella* carrying an episomal *katGp-gfpOVA* fusion as a

ROS biosensor (Figure 4A). The *katGp* promoter is activated when the transcription factor OxyR reacts with H_2O_2 [150]. This promoter has low baseline activity and a large dynamic range compared to previously used *ahpCp* [151] (Figure 4B). We used the unstable GFP variant GFP_OVA [152] to measure current promoter activities instead of integrating over many hours with stable GFP. We co-expressed RFP from the *sifBp* promoter with constitutive *in vivo* expression [152] to distinguish autofluorescent host cell fragments and dead RFP^- *Salmonella* from live RFP^+ *Salmonella* regardless of their GFP content (Figure 4C). Biosensor *Salmonella* showed normal virulence in infected mice and stably maintained the episomal *katGp-gfpOVA* fusion (>99% plasmid maintenance at day 5 p.i.). Proteome analysis of ex vivo purified biosensor *Salmonella* revealed unaltered expression of OxyR-regulon members compared to *Salmonella* without the episomal fusion (Figure S2A), indicating negligible OxyR titration by multicopy *katGp*.

Live RFP^+ biosensors had heterogeneous green fluorescence distributions with large GFP^{dim} and small but highly reproducible GFP^{bright} subpopulations (Figure 4D). This heterogeneity reflected *katGp* activities since episomal *gfpOVA*-fusions to unrelated promoters had unimodal GFP distributions (Figure S2B). GFP^{bright} *Salmonella* resided in various host cell types (Figure S2C), but were absent in *Cybb*$^{-/-}$ mice indicating specific responses to ROS generated by host NADPH oxidase (Figure 4D). In contrast, myeloperoxidase-deficient *MPO*$^{-/-}$ mice contained a larger fraction of GFP^{bright} *Salmonella*, consistent with enhanced H_2O_2 levels/leakage in these mice (see above). GFP^{dim} biosensors had green fluorescence levels close to those of control *Salmonella* without any GFP expression but maintained active *katGp-gfpOVA* fusions as demonstrated by ex vivo sorting followed by *in vitro* stimulation or re-injection into mice (Figure 4E). This suggested that their low *in vivo* GFP content reflected limited ROS exposure instead of plasmid loss or

mutation. Together, these data indicated heterogeneous oxidative stress levels in live *Salmonella* in infected spleen.

Heterogeneous ROS exposure could reflect temporal dynamics of host cell oxidative bursts with peak ROS generation early after bacterial contact followed by extended periods with little ROS generation [153]. To test this hypothesis, we injected ex vivo sorted RFP^{+} GFP^{dim} biosensor *Salmonella* into mice pre-infected with non-fluorescent *Salmonella* (to ensure ongoing tissue inflammation). A large majority of biosensor *Salmonella* activated *katGp* within 1 h but became less active at 3 h post injection (Figure 4E). At 20 h post injection, we again observed the typical distribution with a small tail of GFP^{bright} *Salmonella*. We also constructed a modified *katGp-gfp* biosensor expressing stable GFP instead of unstable GFP_OVA. This modified biosensor showed larger proportions of NADPH oxidase-dependent GFP^{bright} *Salmonella* (Figure 4F) compared to the unstable GFP-biosensor, as expected for differential GFP retention after transient expression. Together, these data suggested temporal variations in *katGp* activities of live *Salmonella* consistent with transient ROS exposure due to host cell oxidative bursts. The small steady state number of ROS biosensor with high *katGp* activities at later time points might reflect ongoing exposure of some *Salmonella* after spreading to new host cells.

How do live *Salmonella* respond to this transient oxidative stress? To address this question we purified GFP^{dim} and GFP^{bright} subpopulations of *katGp-gfpOVA* biosensor *Salmonella* ex vivo (Figure 4G), and compared their proteomes. Abundance data for 966 different proteins revealed upregulation of several proteins involved in *Salmonella* oxidative stress defense including catalase G and YaaA in GFP^{bright} biosensor *Salmonella* (Figure 4H, Table S1), supporting enhanced oxidative stress in this subpopulation. The protein profiles were otherwise highly similar suggesting no major physiological differences between the two

subpopulations. Interestingly, several *Salmonella* ROS defense proteins had very high abundance even in GFP^{dim} *Salmonella* (e.g., SodCI, 52'000 ± 2'000 copies per *Salmonella* cell; TsaA, 22'000 ± 2'000 copies; AhpC, 16'000 ± 2'000 copies). This could reflect residual low-level ROS exposure in this subset. Alternatively, *Salmonella* might stay prepared to cope with rapid onsets and short durations of host oxidative bursts (both within a few minutes), which cannot be efficiently countered by comparatively slow de novo protein synthesis.

Why were these oxidative bursts sub-lethal in resident red pulp macrophages? In part, this could reflect generally low NADPH oxidase activities in resident red pulp macrophages [154, 155]. To explore this issue, we build a computational model of *Salmonella* oxidative stress in macrophage phagosomes based on our model for neutrophils (see above), but incorporating lower oxidative burst activities and acidic phagosomal pH (Figure 3). This in silico model predicted effective *Salmonella* ROS detoxification to sub-lethal concentrations in macrophages in agreement with previous semi-quantitative estimates [132, 154]. Interestingly, periplasmic SodCI was the only individual *Salmonella* defense enzyme with predicted critical impact on any ROS level. In absence of SodCI, predicted $HO_2^{\bullet}$ concentration in the periplasm increased some 12'000fold from 0.38 nM to 4.7 µM (Figure 3). Such high levels are likely to damage periplasmic biomolecules [156], although experimental data are lacking due to technical difficulties. SodCI deficiency was also predicted to increase cytosolic $HO_2^{\bullet}$ but the resulting level (0.3 nM) was likely sub-lethal, given that external amino acids are available *in vivo* [146, 156]. These results are fully consistent with previous experimental data on the role of various *Salmonella* defense proteins [110, 112, 157].

Together, these data supported the hypothesis that NADPH oxidase activities in macrophages during early infection might be insufficient to overwhelm the potent, redundant *Salmonella* anti-oxidative defense. Our simplified computational model ignores potential

synergism of ROS with RNS [158], antimicrobial peptides, hydrolases, and acidic conditions that might contribute to *Salmonella* killing. However, our data for *Cybb*$^{-/-}$ mice suggested that NADPH oxidase-mediated mechanisms were dispensable for *Salmonella* killing in resident macrophages (Figure 2B) arguing against a major role of directly bactericidal ROS, or synergism of ROS with other killing mechanisms, in these cells during early infection.

Local nitrosative stress triggers effective *Salmonella* defense

In addition to ROS generation, *Salmonella*-infected tissues express inducible nitric oxide synthase (iNOS) [159, 160]. iNOS was predominantly expressed by inflammatory monocytes in peripheral regions around an inner core of neutrophils in inflammatory lesions (Figure 5), as expected [136, 159, 160]. Live *Salmonella* resided both inside and outside of these regions in microenvironments with widely different iNOS concentration (Figure 5 insets; Figure 6A).

To determine the impact of iNOS-generated reactive nitrogen species (RNS) on local *Salmonella* populations, we used RFP^{+} *Salmonella* carrying an episomal *hmpAp-gfpOVA* fusion as an RNS biosensor (Figure 6B). *hmpAp* is repressed by active NsrR, but de-repressed when NO inactivates NsrR [161, 162]. As expected, this strain responded to stimulation with acidified nitrite. In infected mouse spleen, it stably maintained the episomal fusion (>99% plasmid maintenance at day 5 p.i.) and showed normal virulence.

Live RFP^{+} biosensor *Salmonella* had bimodal green fluorescence distributions (Figure 6C) with large GFP^{bright} subpopulations in proportions that varied between individual mice (45 ±15%). GFP^{bright} *Salmonella* were absent in iNOS-deficient mice indicating specific biosensor responses to RNS generated by host iNOS, but not host eNOS or endogenously produced *Salmonella* NO [163]. Ex vivo purified GFP^{dim} biosensors maintained active

hmpAp-gfpOVA fusions as demonstrated by *in vitro* stimulation (Figure S3A) and re-injection into mice (Figure S3B), suggesting that their initial low *in vivo* GFP content reflected limited RNS exposure instead of plasmid loss or mutation.

GFP^{bright} *Salmonella* resided in various phagocytes including cells with low iNOS content such as resident red pulp macrophages (Figure S2C). Many such GFP^{bright} *Salmonella* had, however, highly iNOS-positive cells in their close vicinity, likely reflecting the fact that NO can diffuse freely through cellular membranes [164]. Indeed, analysis of regional iNOS concentration within a radius of 15 μm [165] around individual *Salmonella* revealed a strong correlation between *Salmonella* GFP expression and local iNOS levels (Figure 6E).

RFP^{+} GFP^{bright} RNS biosensor *Salmonella* specifically upregulated three prototypical RNS defense proteins (Figure 6F; Table S2); HmpA, YtfE, and Hcp, which function as an NO denitrosylase [166], an iron sulphur cluster repair protein [167], and a hydroxylamine reductase [168], respectively. Hcp had low abundance around the detection threshold (100 ± 40 copies per *Salmonella* cell; detected in only 2 of 4 samples) resulting in poor statistical significance. All three proteins are subject to NsrR repression, and are upregulated upon NO exposure *in vitro* and in cell culture infections [161, 169-171], consistent with RNS stress specifically in GFP^{bright} *Salmonella*. Comparison of protein levels to *Salmonella* without episomal *hmpA-gfpOVA* fusion demonstrated normal NsrR activity without detectable NsrR titration by multi-copy *hmpAp* (Figure S3C). Apart from HmpA, YtfE, and Hcp, GFP^{bright} and GFP^{dim} RNS biosensor *Salmonella* had highly similar protein profiles suggesting no major physiological differences. This specific *Salmonella* response to RNS in our model differed markedly from observations for *Mycobacterium tuberculosis* that appears to encounter multiple different stresses predominantly in tissue areas with high iNOS expression [172].

A *Salmonella hmpA ytfE hcp* triple mutant lacking all three upregulated proteins showed enhanced GFP fluorescence (Figure 6D) suggesting exacerbated RNS stress, as expected in absence of the major NO detoxifying enzyme HmpA [170]. This exacerbated stress induced upregulation of alternative RNS defense enzymes including NorVW [173, 174] in GFP^{bright} *Salmonella hmpA ytfE hcp* (Figure 6F). However, this exacerbated stress did not result in growth attenuation (Figure S3D). *Salmonella hmpA ytfE hcp hcr norVW yoaG yeaR SL1344_1208 SL1344_1736 nrfABCDEFG nfnB cadABC metQ* lacking a total of 22 genes involved in RNS defense/repair [162, 167, 168, 171, 175, 176] had a slight virulence defect, which could be rescued by a functional *hmpA* allele (Figure S3D) suggesting toxic effects of physiological RNS levels only when diverse *Salmonella* defense systems were all dysfunctional.

RNS have a minor impact on early salmonellosis in genetically susceptible BALB/c and C57BL/6 mice, but may have more profound effects in resistant mice carrying functional *Slc11a1* (*NRAMP1*) alleles [177]. To investigate this further, we infected genetically resistant 129/Sv mice that controlled *Salmonella* much better compared to BALB/c mice (Figure S4A), as expected. We observed patchy iNOS expression (Figure S4B) and heterogeneous *Salmonella hmpAp-gfpOVA* biosensor activities (Figure S4C) at day 5, and minor virulence defects of RNS defense mutants at day 8 (Figure S4D) in infected 129/Sv spleen, consistent with previous data for *Salmonella hmpA* at day 5 in a similar infection model [162], and an at most minor role of iNOS for early *Salmonella* control in resistant mice [178]. Together these data suggested similar heterogeneous but sub-lethal RNS stress for *Salmonella* during early infection in both susceptible and resistant mice. Future studies might investigate what mechanisms enable host RNS to effectively control *Salmonella* at later stages of infection [142, 162, 178].

Lack of coordination between oxidative and nitrosative stresses

Salmonella biosensor data suggested ROS and RNS exposure of live *Salmonella* in similar host cell types (Figure S2C), raising the question if these stresses co-occurred in the same cells. However, comparison of proteome data revealed that ROS-induced proteins SitA, KatG, and YaaA were similarly abundant in *Salmonella* with high or low RNS exposure, whereas RNS-induced HmpA and YtfE were equally abundant in *Salmonella* regardless of ROS exposure (Figure S3E), suggesting independently acting ROS and RNS stresses.

To further explore this issue, we constructed a dual ROS/RNS biosensor carrying ROS-responsive *katGp-rfp* and RNS-responsive *hmpAp-gfp* on compatible plasmids (and chromosomal *sifBp::cfp* as a constitutive marker for all live *Salmonella* cells). As expected, this biosensor responded *in vitro* to individual ROS or RNS stresses, as well as to a ROS/RNS combination. In infected spleen, the dual biosensor stably maintained both plasmids and retained full virulence. Analysis of GFP and RFP expression in live CFP^+ biosensors revealed four distinct reproducible subpopulations (Fig. 7): (i) 54 ± 3% GFP^{dim} RFP^{dim} *Salmonella* with low stress, (ii) 19 ± 1% GFP^{dim} RFP^{bright} *Salmonella* with substantial ROS but low RNS stress, (iii) 19 ± 1% GFP^{bright} RFP^{dim} *Salmonella* with substantial RNS but low ROS stress, and (iv) 9 ± 1% GFP^{bright} RFP^{bright}*Salmonella* exposed to both stresses (the proportion of ROS stressed *Salmonella* appeared larger compared to *katGp-gfpOVA* data because we used stable RFP instead of unstable GFP as a reporter; the proportions of RNS stressed *Salmonella* appeared lower compared to the single biosensor data because of differential plasmid copy numbers, see Supplemental Experimental Procedures). *katGp-rfp* activities were similar among *Salmonella* with high or low RNS stress and *hmpAp-gfp* activities were similar among *Salmonella* with high or low ROS stress (Fig. 7). Together, these data confirmed largely independent action of ROS and RNS on *Salmonella*.

It is important to note that both approaches reported exclusively on live *Salmonella*, thus underestimating the proportion of *Salmonella* that were exposed to highly toxic ROS-RNS reaction products such as peroxynitrite. ROS/RNS synergy likely played a minor role in our conditions since iNOS has no detectable impact on early *Salmonella* control in susceptible mice [177], but it might become important at later stages when iNOS is involved in effective *Salmonella* control.

Discussion

In this study, we used single-cell approaches to investigate key host defense mechanisms against *Salmonella* in a typhoid fever model. Our results show that many *Salmonella* experience and respond to ROS and RNS, but exposure levels and impact vary widely.

All three major infected host cell types (macrophages, neutrophils, inflammatory monocytes) can effectively kill *Salmonella in vitro* [36, 107, 141], but *in vivo* evidence has been inconclusive [21, 35, 140, 179-182]. Our results showed continuous *Salmonella* net growth and disease progression in spite of extensive *Salmonella* killing. Specifically, neutrophils and inflammatory monocytes accumulated in inflammatory lesions around growing infection foci and efficiently killed *Salmonella*, while resident red pulp macrophages outside of inflammatory lesions were more permissive for *Salmonella* survival. Our data were consistent with the strong yet incomplete control of salmonellosis by neutrophils and inflammatory monocytes [183-186]; and *Salmonella* tissue loads that increase primarily as a result of continuously forming new infection foci, while *Salmonella* growth inside existing infection foci is limited [186]. The efficient control of local *Salmonella* growth within inflammatory lesions markedly differed from the role of early granulomas in promoting mycobacterial proliferation during zebrafish tuberculosis [187].

NADPH oxidase is essential for *Salmonella* control [142], but the relevance of directly bactericidal ROS vs. indirect effects was unclear [130-132]. Our data suggested that neutrophils and inflammatory monocytes used NADPH oxidase and myeloperoxidase to kill *Salmonella* with bactericidal ROS. In contrast, resident macrophages outside of inflammatory lesions imposed only sub-lethal, transient oxidative bursts on *Salmonella* during early infection, and killed *Salmonella* through NADPH oxidase-independent mechanisms. Our data confirmed previously proposed non-lethal ROS levels [151] specifically for macrophages but

not for neutrophils and monocytes. This partial agreement might reflect that previous studies compared live mutant and wild-type *Salmonella* (which mostly reside in macrophages) and did not account for lethal hypohalite action in neutrophils and monocytes, thus focusing on read-outs that were biased towards *Salmonella*-macrophage interactions.

Infected tissues expressed inducible nitric oxide synthase in specific regions, which exposed local *Salmonella* to substantial RNS. However, affected *Salmonella* upregulated defense proteins that provided full RNS protection in both susceptible and resistant mice during early infection. It is unclear how host RNS can more effectively control *Salmonella* at later stages of infection.

Taken together, these data show surprisingly diverse temporal and spatial ROS and RNS levels that generate at least 6 different *Salmonella* subpopulations with distinct properties and fates that have escaped previous bulk analyses (live with low-level stress, live ROS-stressed, live-RNS stressed, live ROS/RNS-stressed, killed by NADPH oxidase-dependent mechanisms, killed by unrelated mechanisms). Defects in host defense (as in *Cybb*$^{-/-}$, *MPO*$^{-/-}$, or *iNOS*$^{-/-}$ mice; IFNγ neutralization) or *Salmonella* stress protection (such as inactivation of *hmpA ytfE hcp*) selectively affected only specific *Salmonella* subpopulations. Further studies might investigate why some *Salmonella* survive even in neutrophils and monocytes, and how macrophages kill *Salmonella* through NADPH oxidase-independent mechanisms. Moreover, *Salmonella* experiences additional stresses, and both host and *Salmonella* activities show substantial cell-to-cell variation [188-192] suggesting that *Salmonella*/host interactions may be even more complex.

Overall, our findings revealed mouse typhoid fever as a race between infiltrating host cells that accumulate around infection foci and kill local *Salmonella*, and *Salmonella* escaping to more permissive sites. The net balance of disparate *Salmonella* / host encounters with

dramatically different individual outcomes thus determines overall disease progression. Similarly complex host/pathogen interactions might govern many other infectious diseases such as tuberculosis [172, 187, 193]. Single-cell *in vivo* approaches as developed in this study might help to better understand this complexity and its impact on disease progression and control.

Experimental procedures:

Bacterial genetics.

Salmonella strains used in this study were derived from *Salmonella enterica* serovar Typhimurium SL1344. Promoter regions of interest were cloned upstream of *gfp_ova*, *gfp*, or *mCherry* on pBR322- or pSC101-based plasmids. *Salmonella* mutants were generated using red recombinase-mediated allelic replacement followed by P22 phage transduction. For additional information see extended experimental procedures.

Mice infections.

All animal experiments were approved (license 2239, Kantonales Veterinäramt Basel-Stadt) and performed according to local guidelines (Tierschutz-Verordnung, Basel-Stadt) and the Swiss animal protection law (Tierschutz-Gesetz). Female 10-14 weeks old mice were infected i.v. with 400-2000 CFU *Salmonella* and euthanized 4-5 days later. Competitive indices of *Salmonella* mutants were determined by plating on selective media. Some mice received injections with a neutralizing antibody to IFNγ or an appropriate isotype control antibody. For additional information see extended experimental procedures.

Immunohistochemistry.

Spleen portions were fixed with 4% paraformaldehyde, soaked in 40% sucrose, and frozen in OCT. Cryosections were stained with primary and secondary antibodies diluted in TBS-Tween containing 2% mouse serum, and examined by confocal microscopy (Leica SP5, Zeiss LSM 700). Image stacks were analyzed with FIJI and Imaris. For additional information see extended experimental procedures.

Flow cytometry and proteomics.

Spleen was homogenized in ice-cold PBS containing 0.2% Triton X-100. All samples were kept on ice until analysis. Large host cell fragments were removed by centrifugation at 500xg for 5 min. *Salmonella* were sedimented at 10'000xg for 10 min and resuspended in PBS-Triton. Samples were analyzed in a Fortessa II flow cytometer, or sorted using an Aria III sorter equipped with an BSL2 aerosol management system. Instruments were calibrated daily with fluorescent beads.

For proteome analysis, samples were prepared and sorted in PBS-Triton containing 170 μg chloramphenicol ml^{-1} to block de novo protein biosynthesis. Samples were digested with LysC and trypsin and analyzed by nLC-MS/MS. Peptides and proteins were identified by searching databases containing all predicted tryptic peptides for *Salmonella* SL1344 and mouse, as well as the corresponding decoy databases for adjusting peptide and protein false-discovery rates at <1%. For additional information see extended experimental procedures.

Computational modeling of *Salmonella* oxidative stress protection.

We build a diffusion-reaction model based on a previous neutrophil phagosome model [145]. We combined *Salmonella* dimensions and surface area with reported membrane permeabilities for various ROS. We derived *Salmonella* detoxification kinetics from experimental data on *Salmonella* protective enzyme expression as obtained by ex vivo proteomics [146] and reported enzyme kinetic parameters. Modeling was done using the Simulink feature of MATLAB. For additional information see extended experimental procedures.

Acknowledgments:

We thank Mauricio Rosas Ballina for help with preparing Figures, and Swiss National Foundation (31003A-121834) and Deutsche Forschungsgemeinschaft (SPP1316 Bu971/6) for funding.

Author Contributions:

D.B. conceived the study. D.B., N.B., N.S., O.C. designed the experiments. All authors performed experiments and analyzed the data. O.C. wrote code and ran the models. D.B., N.B., and N.S. wrote the paper.

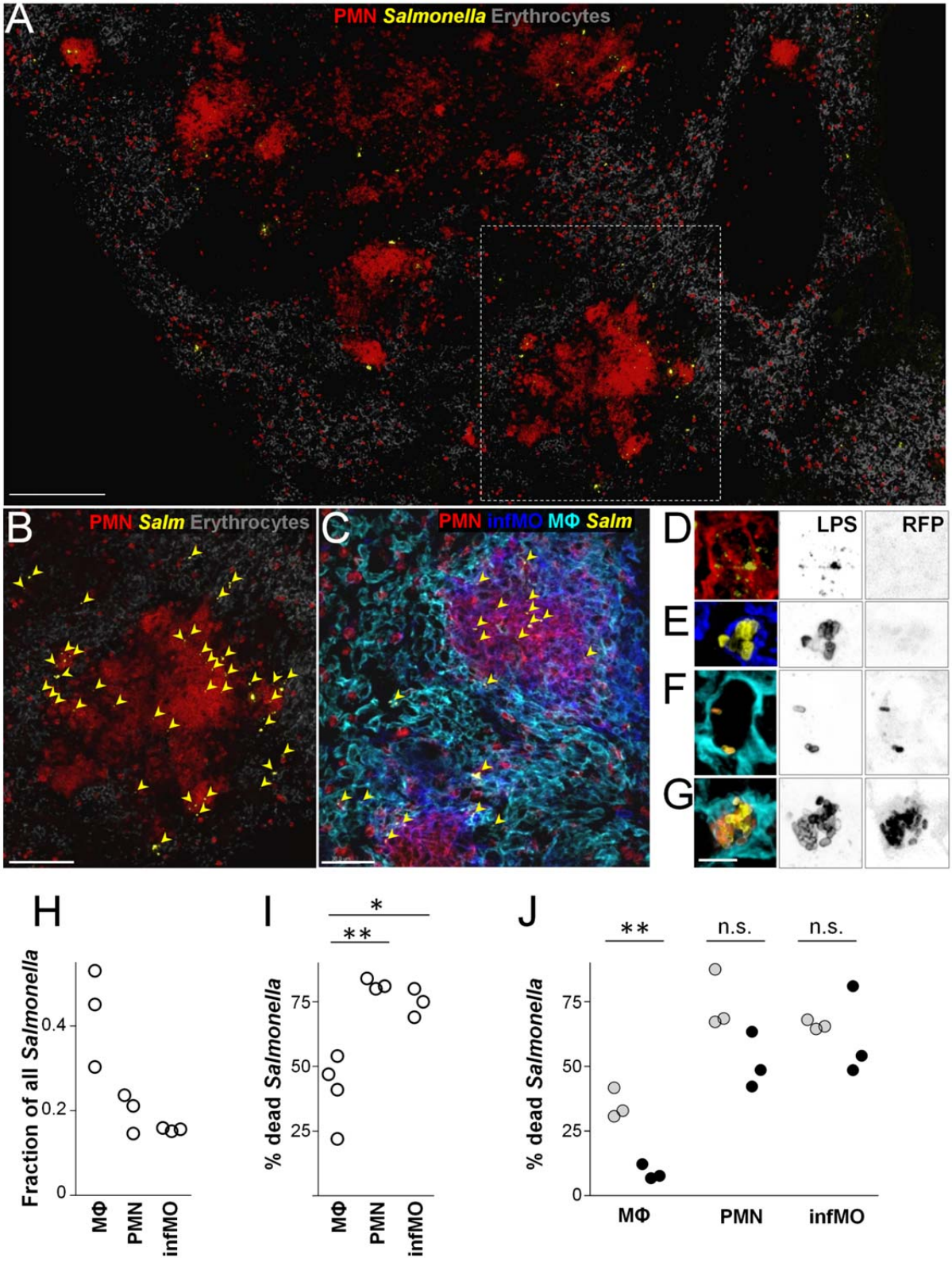
A
PMN Salmonella Erythrocytes
B
PMN Salm Erythrocytes
C
PMN infMO MΦ Salm
D
E
F
G
LPS
RFP
H
Fraction of all Salmonella
0
0.2
0.4
MΦ
PMN
infMO
I
*
**
% dead Salmonella
25
50
75
MΦ
PMN
infMO
J
**
n.s.
n.s.
% dead Salmonella
25
50
75
MΦ
PMN
infMO

Figure 1: Disparate *Salmonella* fates in spleen microenvironments (see also Figure S1).

A, Infected mouse spleen immunohistochemistry with markers for erythrocytes (Ter-119), polymorphonuclear neutrophils (PMN; Ly-6G), and *Salmonella* (anti-lipopolysaccharide, LPS). The area labeled with a dashed line is shown at higher magnification in B. The scale bar represents 200 μm. Similar observations were made for 10 BALB/c mice and 10 C57BL/6 mice. **B**, Higher magnification of labeled area in A. Yellow arrowheads indicate *Salmonella*. The scale bar represents 100 μm. **C**, Identification of infected neutrophils (PMN), inflammatory monocytes (infMO), resident red pulp macrophages (MΦ), and *Salmonella* (Salm) (Gr-1 red; anti-CD11b, blue; F4/80, cyan; anti-LPS, yellow; for use of infiltrate markers see Figure S1). The scale bar represents 30 μm. **D-G**, Live and dead *Salmonella* (yellow, anti-LPS; orange, RFP) in a neutrophil (**D**), an inflammatory monocyte (**E**), and two resident macrophages (**F**,**G**). LPS and RFP channels are also shown as grayscale-inverted images for better visibility of weak signals. **H**, Distribution of intracellular *Salmonella* among various host cell types. The data represent results from three BALB/c mice (total N of all *Salmonella*, 1363). **I**, Proportions of dead *Salmonella* in various host cell types. The data represent results from three BALB/c mice (total N of all *Salmonella*, 619; **, $P = 0.0042$; *, $P = 0.011$; two-tailed t-test). **J**, Proportions of dead *Salmonella* at day 4 p.i. in mice that had received an isotype control antibody (grey) or anti-IFNγ (black) at day 3. Data from three BALB/c mice in each group are shown ($N_{control}$, 624; $N_{IFN\gamma}$, 436; **, $P = 0.0022$).

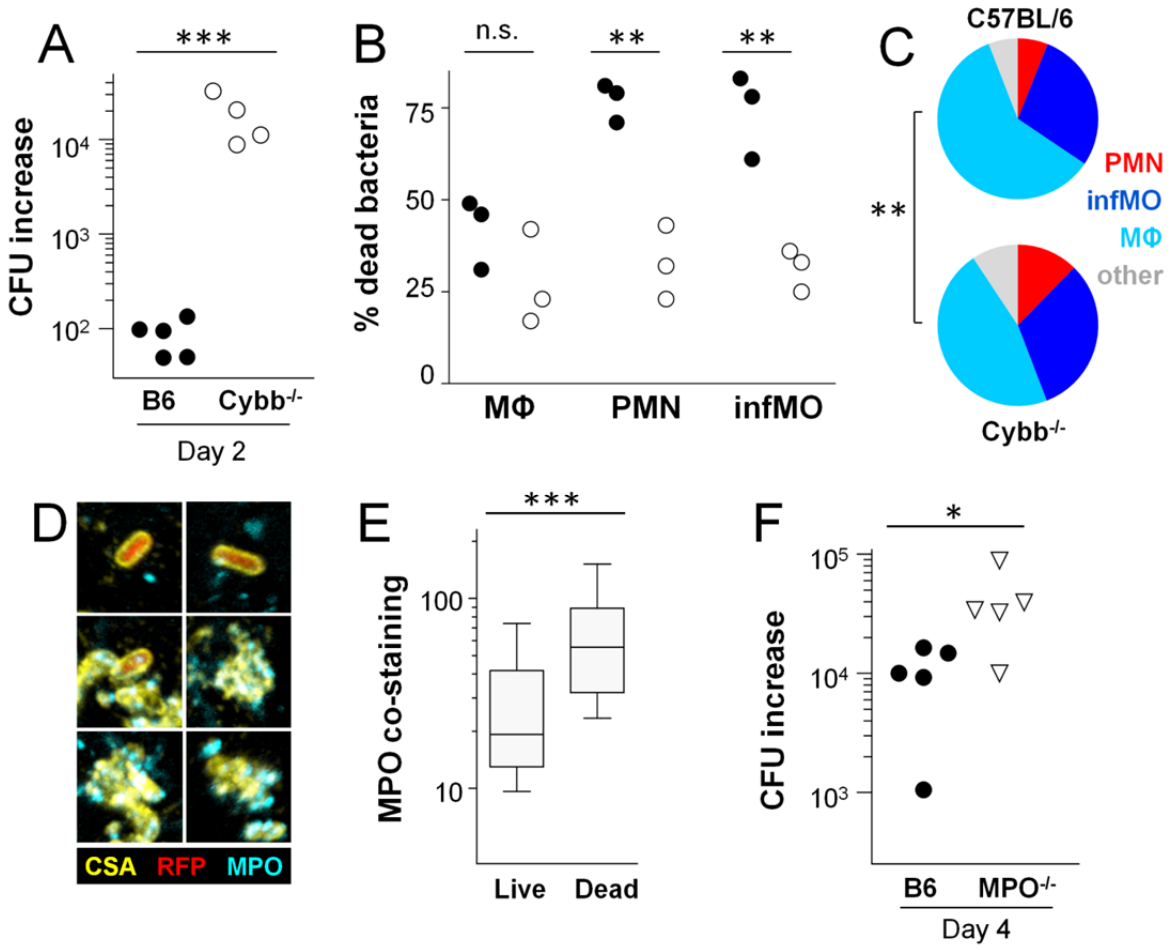

Figure 2: Neutrophils and monocytes kill *Salmonella* through oxidative stress.

A, *Salmonella* growth in C57BL/6 (B6) and congenic *Cybb*$^{-/-}$ mice. Data represent *Salmonella* spleen loads of individual mice at day 2 divided by the inoculum dose (***, $P< 0.001$, two-tailed t-test of log-transformed data). **B**, Proportion of live *Salmonella* in neutrophils (PMN), inflammatory monocytes (infMO), and resident macrophages (MΦ) in C57BL/6 (filled circles, N = 613) and Cybb$^{-/-}$ mice (open circles, N = 579). **C**, Distribution of live *Salmonella* among different host cell types in C57BL/6 and *Cybb*$^{-/-}$ mice. The data represent averages from three mice (**, $P= 0.0032$, Two-Way Anova). **D**, Colocalization of live and dead *Salmonella* with myeloperoxidase (yellow, common *Salmonella* antigen, CSA; red, RFP; cyan, MPO). The scale bar represents 3 µm. Similar observations were made for three mice.

E, Myeloperoxidase (MPO) concentrations around live and dead *Salmonella*. The data are represented as box plots (central line is the median; the box includes the central 50%; whiskers, 10-90 percentile; ***, $P< 0.001$; Mann-Whitney-U test; total N = 159). **F**, *Salmonella* growth in C57BL/6 (B6) and congenic *MPO*$^{-/-}$ mice. Data represent *Salmonella* spleen loads of individual mice at day 4 divided by the inoculum dose (*, $P= 0.042$, two-tailed t-test of log-transformed data).

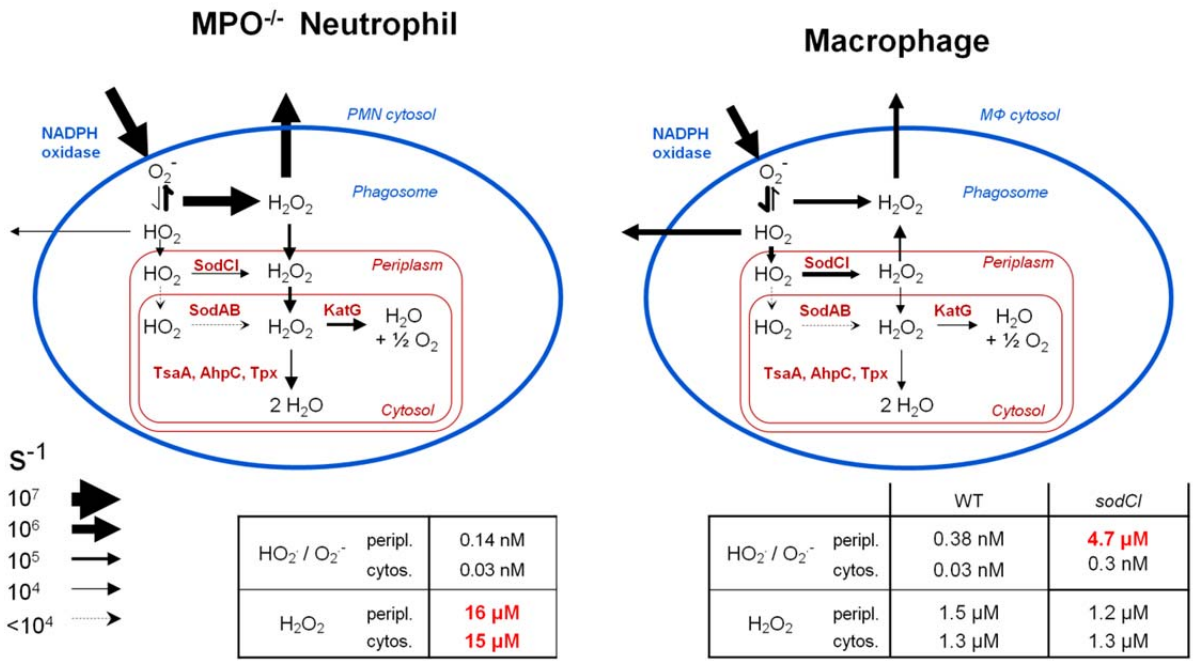

Figure 3: Computational model of *Salmonella* oxidative stress in phagosomes of myeloperoxidase-deficient neutrophils and wild-type macrophages. *Salmonella* membranes and detoxifying enzymes are shown in red. Predicted concentrations for superoxide and hydrogen peroxide in wild-type (WT) *Salmonella* in MPO-deficient neutrophils, and wild-type (WT) *Salmonella* or the *sodCI* mutant inside macrophages are also shown.

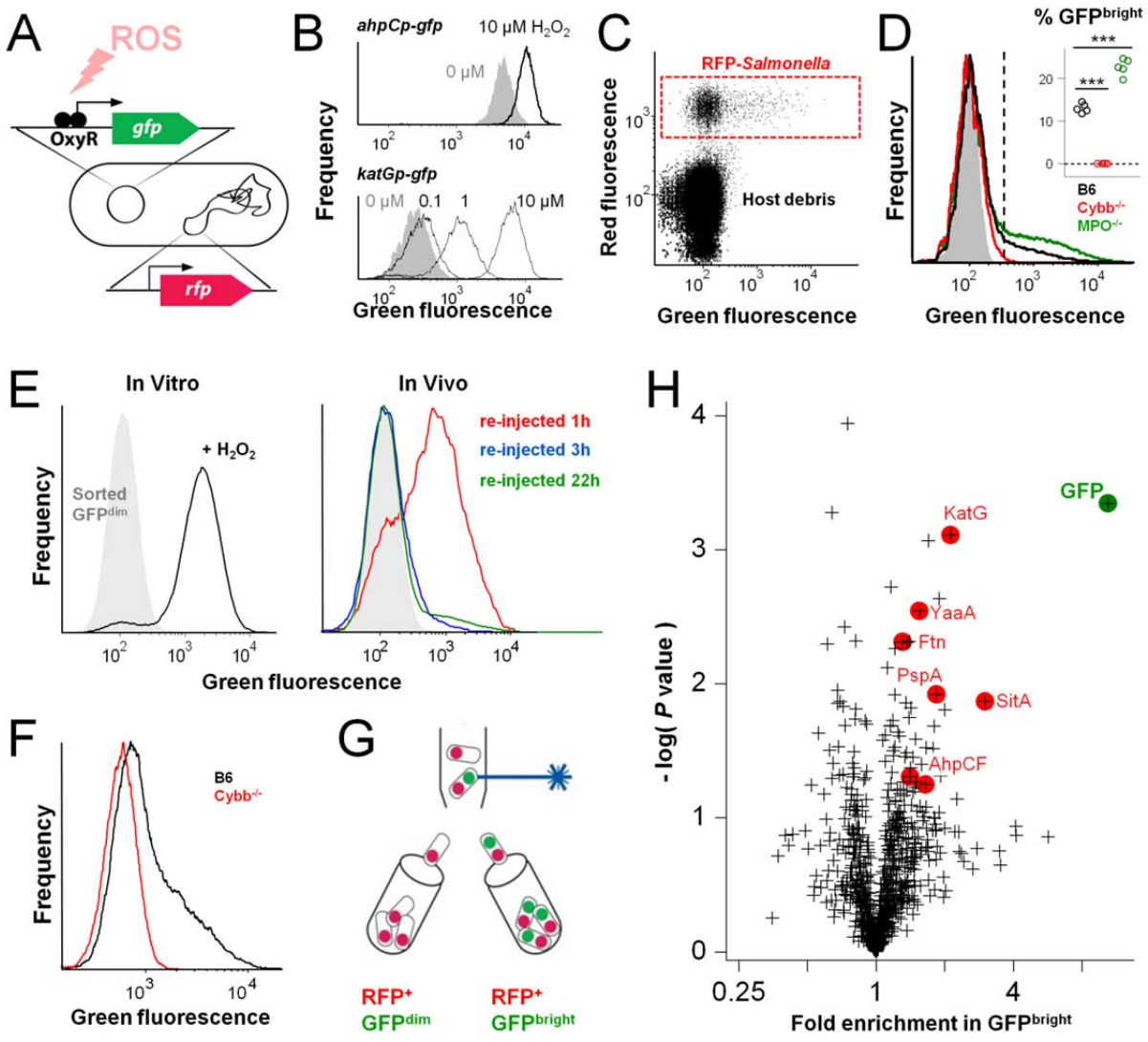

Figure 4: *Salmonella* responses to sub-lethal oxidative bursts (see also Figure S2 and Table S1).

A, ROS biosensor *Salmonella* expressing the green fluorescent protein (GFP) from an OxyR-activated promoter, and the red fluorescent protein mCherry (RFP) from a constitutively active chromosomal promoter. **B**, *In vitro* responses of ROS biosensor *Salmonella* carrying different promoter-*gfp* fusions to H_2O_2 as determined by flow cytometry. **C**, Detection of RFP-expressing biosensor *Salmonella* in infected spleen homogenates using two-color flow cytometry. **D**, Green fluorescence intensities of ROS biosensor *Salmonella* in C57BL/6 (B6),

Cybb$^{-/-}$, and *MPO*$^{-/-}$ mice. The shaded area corresponds to *Salmonella* without GFP. The inset shows the proportion of bright bacteria in individual mice (***, $P< 0.001$, two-tailed t-test). **E**, Re-stimulation of ex vivo isolated GFP^{dim} biosensor *Salmonella* (shaded grey area) *in vitro* (left), or *in vivo* at different times post re-injection into mice already infected with non-fluorescent *Salmonella* (right). **F**, Fluorescence intensities of ROS biosensor *Salmonella* expressing a stable GFP variant under control of the *katGp* promoter in C57BL/6 (B6) and *Cybb*$^{-/-}$ mice. Similar data were obtained for two mice of each line. **G**, Schematic representation of ex vivo purification of GFP^{bright} and GFP^{dim} biosensor *Salmonella* using flow cytometry. **H**, Proteome comparison of purified GFP^{bright} and GFP^{dim} ROS biosensor *Salmonella*. Data represent averages of independent samples purified from 3 to 4 BALB/c mice. Proteins labeled in red have been associated with ROS.

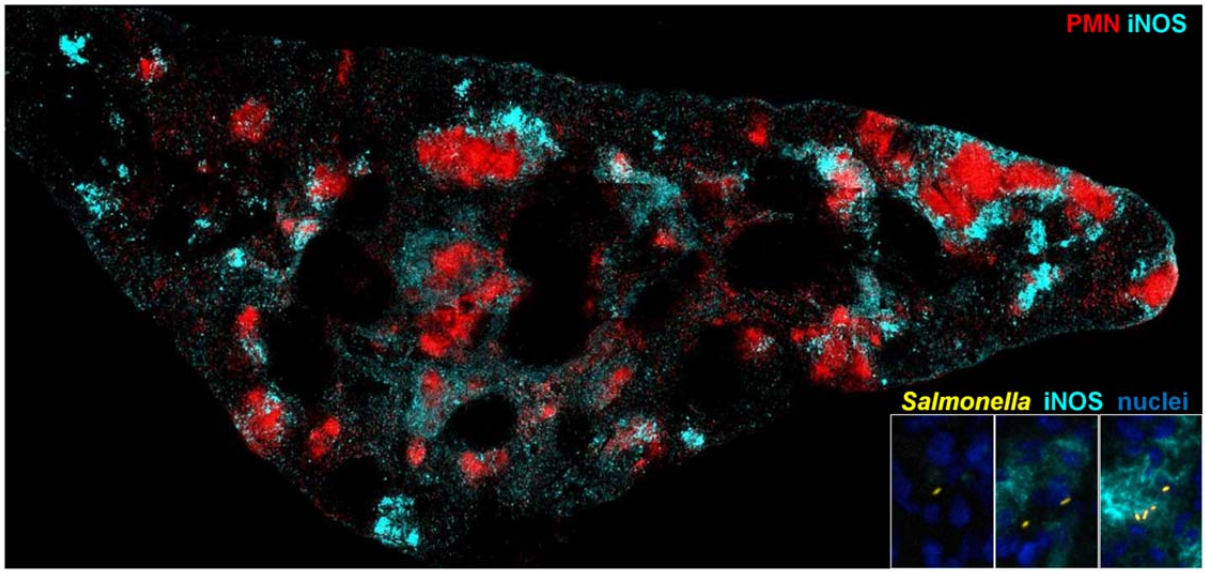

Figure 5: iNOS expression in infected spleen.

Infected mouse spleen immunohistochemistry with a marker for polymorphonuclear neutrophils (PMN, Ly-6G), and an antibody to inducible nitric oxide synthase (iNOS). The scale bar represents 500 µm. The insets show higher magnifications (*Salmonella*, LPS; nuclei, DAPI; the scale bar represents 30 µm). Similar observations were made for 4 BALB/c mice and 4 C57BL/6 mice.

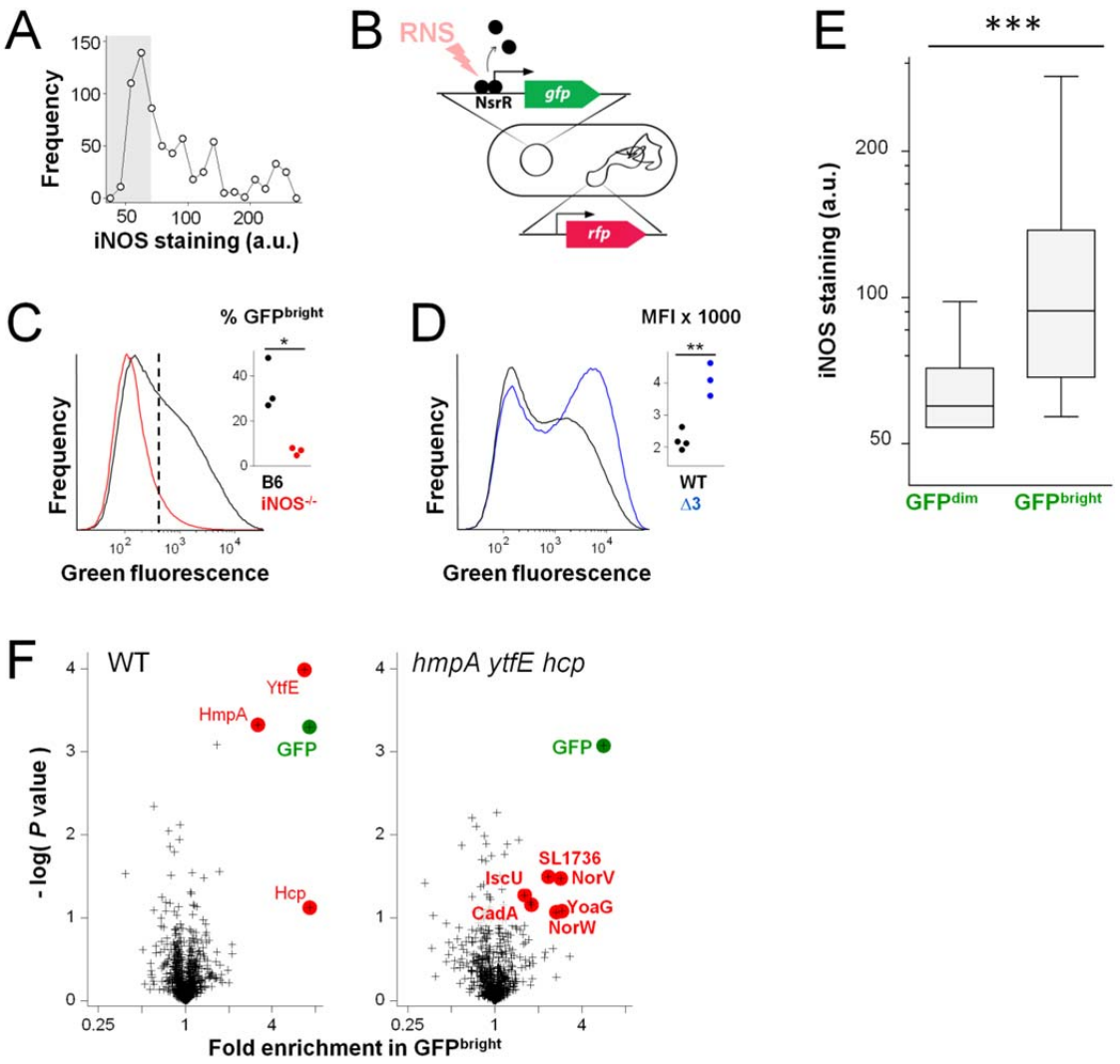

Figure 6: *Salmonella* exposure and responses to nitrosative stress (see also Figures S3,S4 and Table S2).

A, Distribution of *Salmonella* among tissue regions with different iNOS concentrations. The shaded area represents background staining as observed for an *iNOS*$^{-/-}$ mouse. **B**, RNS biosensor *Salmonella* expressing the green fluorescent protein (GFP) from a NsrR-repressed promoter, and the red fluorescent protein mCherry (RFP) from a constitutively active chromosomal promoter. **C**, Green fluorescence intensities of RNS biosensor *Salmonella* in C57BL/6 (B6) and *iNOS*$^{-/-}$ mice. The inset shows the proportion of bright bacteria in

individual mice (*, P= 0.013, two-tailed t-test). **D**, Green fluorescence intensities of RNS biosensors in wild-type *Salmonella* (WT) and *Salmonella hmpA ytfE hcp* (Δ3). The inset shows the mean fluorescence intensities in individual mice (**, P= 0.0016, two-tailed t-test). **E**, Inducible nitric oxidase (iNOS) concentrations around GFP^{dim} and GFP^{bright} RNS biosensor *Salmonella*. The data are represented as box plots (central line is the median; the box includes the central 50%; whiskers, 10-90 percentile; ***, P< 0.001; Mann-Whitney-U test; total N = 690). **F**, Proteome comparison of purified GFP^{bright} and GFP^{dim} RNS biosensor in wild-type *Salmonella* (left), or *Salmonella hmpA ytfE hcp* (right). Data represent averages of independent samples from 3 to 4 BALB/c mice for each *Salmonella* strain. Proteins labeled in red have been associated with RNS.

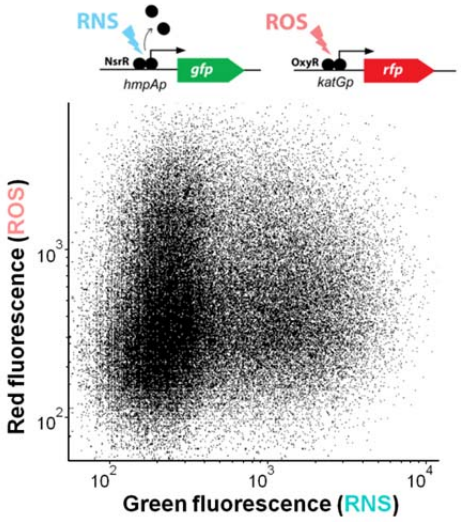

Figure 7: Exposure of individual *Salmonella* to oxidative and nitrosative stresses.

Fluorescence intensities of a dual RNS ROS biosensor *Salmonella* expressing the green fluorescent protein (GFP) from a NsrR-repressed promoter, and the red fluorescent protein mCherry (RFP) from an OxyR-activated promoter in infected spleen. Similar observations were made for 5 mice.

Supplementary Information

Figures S1-S3

Figure legends S1-S3

Extended experimental procedures

Fig. S1

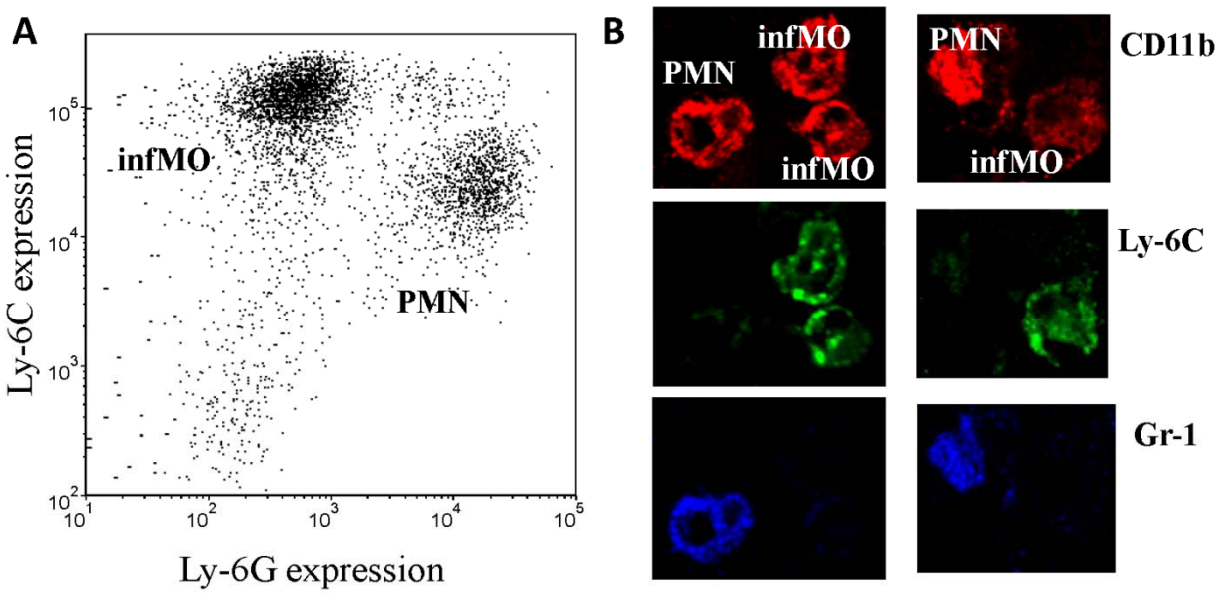

Figure S1: **Staining patterns for markers anti-CD11b, Ly-6C, Ly-6G, and Gr-1**. **Related to Figure 1.**

A) Unfixed infected spleen suspensions as analyzed by flow cytometry (gated for $CD11b^{hi}$), $CD11b^{hi}$ cells consisted almost exclusively of Ly-$6C^{hi}$ inflammatory monocytes (infMO) and Ly-$6G^{hi}$ neutrophils (PMN). B) Unfixed infected spleen section as analyzed by confocal microscopy. Although Gr-1 principally recognizes both Ly-6C and L-6G antigens, its staining intensity was low for Ly-$6C^{hi}$ cells. Since Ly-6C staining of fixed specimens showed inconclusive patterns, we detected inflammatory monocytes as $CD11b^{hi}$ Gr-1^{lo} cells [194].

Fig. S2

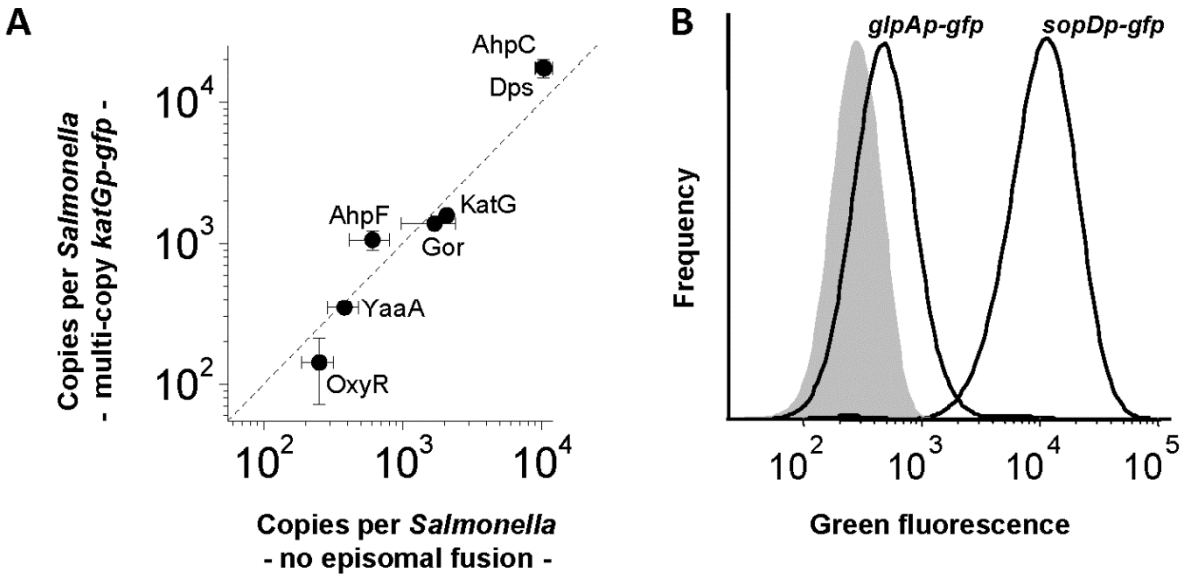

Figure S2 *Salmonella* responses to reactive oxygen species. Related to Figure 3

A) Abundance of OxyR-regulated proteins in wild-type *Salmonella* and ROS biosensor *Salmonella* carrying multi-copy *katGp*. Values represent average copy numbers per *Salmonella* cell ± SD in samples isolated from 3 to 4 independently infected BALB/c mice. The dashed line represents equal abundance in both *Salmonella* strains. B) Green fluorescence intensities of *Salmonella* carrying transcriptional fusions to promoters *glpAp* or *sopD2p* in infected BALB/c mice.

Fig. S3

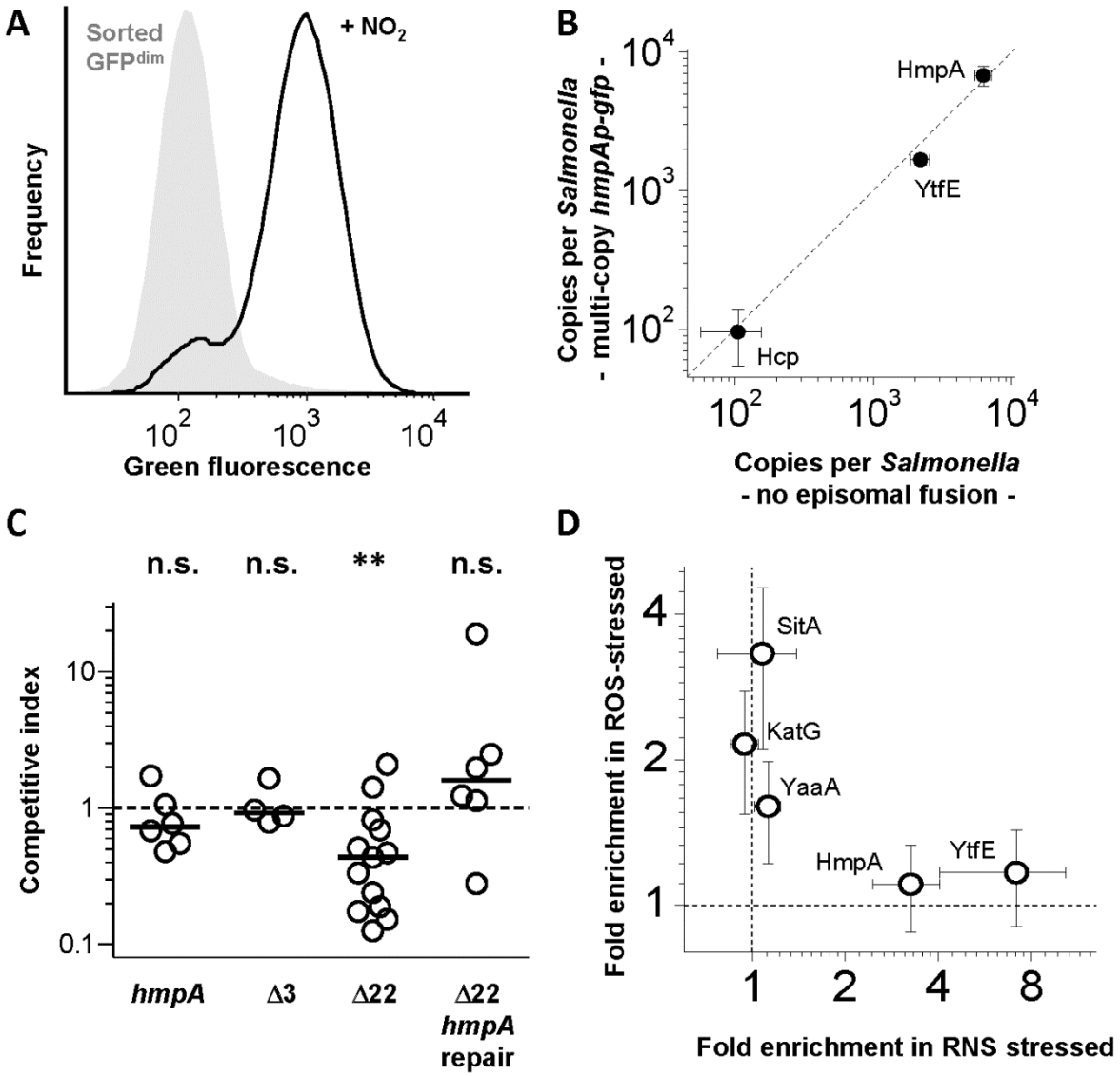

Figure S3: ***Salmonella* exposure and responses to reactive nitrogen species. Related to Figure 4**.

A) Fluorescence intensities after *in vitro* re-stimulation of ex vivo isolated GFP^{dim} RNS biosensor *Salmonella* (shaded grey area) with 1 mM acidified nitrite pH 5.7. B) Abundance of NsrR-regulated proteins in wild-type *Salmonella* and RNS biosensor *Salmonella* carrying multi-copy *hmpAp*. Values represent average copy numbers per *Salmonella* cell ± SD in samples isolated from 3 to 4 independently infected BALB/c mice. The dashed line represents equal abundance in both *Salmonella* strains. C) Competitive indices of various *Salmonella*

mutants with defects in RNS defense. The data represent mutant spleen CFU counts compared to co-infected wild-type *Salmonella* in individual mice (the *hmpA* data were obtained with the same method in a previous study [195]). A value of 1 corresponds to full virulence of a mutant (**, $P = 0.003$; n.s., not significant; two-tailed t-test of log-transformed data). D) Abundance of ROS- and RNS-induced proteins in *Salmonella* subpopulations exposed to high or low ROS / RNS stresses. Values represent average ratios in copy numbers per *Salmonella* cell ± SD in paired samples isolated from 3 to 4 independently infected BALB/c mice. The dashed lines represent fully independent responses to ROS and RNS.

Extended experimental procedures

Bacterial genetics.

Salmonella strains used in this study were derived from *Salmonella* enterica serovar Typhimurium SL1344 hisG rpsL xyl [196, 197]. *Salmonella* were cultured at 37°C with aeration (200 rpm) in Lennox LB with addition of 90 μg ml^{-1} streptomycin; 100 μg ml^{-1} ampicillin; 50 μg ml^{-1} kanamycin; 25 μg ml^{-1} chloramphenicol, where appropriate.

Promoter regions of interest, *ahpCp* (SL1344_0596; positions with respect to start-ATG, -534 to + 149); *hmpA* (SL1344_2518; -403 to +73); *glpA* (SL1344_2253; -343 to +127); *sopD2p* (SL1344_0909; -388 to +218); *katGp* (SL1344_4056; -240 to +61) were PCR amplified, ligated into a *Bam*HI, *Xba*I digest of the pBR322 derivative pMW82[198], and confirmed by sequencing. The finished constructs were expected to produce "operon-like" fusions, in which the transcribed mRNA codes for a short peptide corresponding to the start of the gene downstream of the promoter of interest, prior to a stop codon, followed by a strong ribosome binding site and *gfp_ova* (or *gfpmut2*, *mCherry*). For generating a dual biosensor, a pBR322-compatible pSC101-derived vector was constructed by PCR amplifying the full *hmpAp::gfp_ova* construct and ligating this into a *Bam*HI, *Sbf*I digest of pUA66[199].

Gene replacement mutagenesis of *Salmonella* was carried out as described[200]. All mutations were purified by generalized P22 *int*-transduction. A chromosomal fusion of the native *sifB* promoter with *rfp* encoding the red fluorescent protein mCherry (RFP), or with *cfp* encoding the cyan fluorescent protein (CFP) was constructed as described for a similar *gfp* fusion at this locus[201]. Expression of RFP or CFP was verified by growing cells overnight in inducing media (MOPS media[202] buffered to pH5.5 with 100mM 2-(N-morpholino)ethanesulfonic acid (MES; Sigma-Aldrich), and containing 10μM $MgCl_2$).

Mice infections.

All animal experiments were approved (license 2239, Kantonales Veterinäramt Basel-Stadt) and performed according to local guidelines (Tierschutz-Verordnung, Basel-Stadt) and the Swiss animal protection law (Tierschutz-Gesetz).

Female 10-14 weeks old BALB/c mice (Charles River Laboratories), B6.129S6-Cybb$^{tm1Din/J}$, B6.129X1-MPO$^{tm1Lus/J}$, B6.129P2-Nos2^{tm1Lau}/J, and age- and sex-matched C57BL/6J congenic control mice (Jackson Laboratory) were infected by tail vein injection of 400-2000 *Salmonella* in 100µl PBS and euthanized at 4-5 days post infection, except for infections in Cybb$^{-/-}$ mice and respective C57BL/6 control mice that were euthanized already at day 2 to prevent lethal infections (in this case, control mice were injected with ca. 10'000 CFU to reach comparable spleen loads).Competitive indices for *Salmonella* mutants vs. wild-type at day 4 post infection were determined by plating on selective media, as described[203].

Immunohistochemistry.

2-3mm thick spleen portions were fixed with fresh 4% paraformaldehyde at 4°C for 4 h, followed by incubating in increasing sucrose concentrations from 10%-40% at 4°C. After overnight incubation in 40% sucrose, tissue was rapidly frozen in embedding media (Tissue-Tek® O.C.T; Sakura), left overnight at -80°C, and then stored at -20°C. 10-20 µm thick cryosections were dried onto coated coverslips (BD BioCoat™), blocked in 1% blocking reagent (Invitrogen) and 2% mouse serum (Invitrogen) in TBST (0.05% Tween in 1X TBS pH7.4), and stained with primary and secondary antibodies (rat anti-CD11b, BD clone M1/70; goat anti-CSA1, KPL 01-91-99-MG; rat F4/80, Serotec clone CI:A31; rabbit anti-iNOS, Acris antibodies iNOS-A; rat Gr-1, BD 553124; goat anti-4-HNE, Alpha Diagnostics HNE12-S; rabbit anti-LPS *Salmonella*, Sifin REF TS 1624; rat Ly6C-PE, BD clone AL-21; rat Ly-6G, BD clone 1A8; rabbit anti-myeloperoxidase, abcam 9535). A variety of secondary antibodies

were used depending on the application (Molecular probes; Cat. A-21443; S11225, S21374; A-21206; A11096, D20698, Invitrogen A31556, Santa CruzBT sc-362245). In the case of anti-4-HNE staining, we incubated sections with primary antibody overnight and used a horseradish peroxidase kit (Molecular probes; Cat: T-20936) to amplify the signal. Sections were mounted in 90% glycerol, 24.5mg/ml DABCO, PBS pH7.4, and examined with Leica SP5 or Zeiss LSM 700 confocal microscopes (Biozentrum, Imaging Core Facility), using glycerol 20X, 40X, and 63X objectives. Images were analyzed with FIJI and Imaris.

Flow cytometry and proteomics.

Spleen homogenates were prepared for flow cytometry as described[195]. Relevant spectral parameters of 10,000 to 50,000 *Salmonella* were recorded in a FACS Fortessa II equipped with 445 nm, 488 nm and 561 nm lasers (Becton Dickinson), using thresholds on SSC and FSC to exclude electronic noise (channels: CFP, excitation 445 nm, emission 499-529 nm; GFP, excitation 488 nm, emission 502-525; RFP, excitation 561 nm, emission 604-628 nm; yellow autofluorescence channel, excitation 455 nm, emission 573-613 nm; infrared autofluorescence channel, excitation 561 nm, emission 750-810 nm). Data processing was done in FlowJo and FCS Express.

Salmonella subpopulations were sorted in a FACS Aria III equipped with 488 nm and 561 nm lasers (Becton Dickinson) and processed for proteome analysis as described[146]. Processed peptides were analyzed by nLC-MS/MS and absolute protein amounts were determined using a label-free approach with calibration by isotope-labeled AQUA peptides as described[146]. We only considered proteins with two identified peptides (at a 1% false-discovery rate) that were detected in at least two independent samples.

Computational modeling of *Salmonella* ROS defense.

We build a diffusion-reaction model (Fig. 2G) based on a previous neutrophil phagosome model[145] combined with experimental data on *Salmonella* protective enzyme expression as obtained by ex vivo proteomics[146] (SodCI, 39'800 ± 8'300 copies per *Salmonella* cell; SodCII, 370 ± 200; SodA, 4'000 ± 1'000; SodB, 10'200 ± 2'100; KatG, 2'600 ± 500; KatE and KatN, below detection limit; Tpx, 22'000 ± 4'000; AhpC, 15'200 ± 3'500; AhpF, 1'000 ± 400; TsaA, 21'700 ± 3'600), kinetic parameters (SodCI, SodCII, $k_{cat}/K_M = 4x10^9$ $M^{-1}s^{-1}$ diffusion-limited[204]; SodA, SodB, $k_{cat}/K_M = 7x10^9$ $M^{-1}s^{-1}$ diffusion-limited[205]; KatG, k_{cat} = 14'000 s^{-1}, K_M = 5.9 mM[206]; Tpx, k_{cat} = 76 s^{-1}, K_M = 1.7 mM[207]; AhpC (and TsaA), k_{cat} = 55.1 s^{-1}, K_M = 1.4 µM[208]; AhpF, k_{cat} = 25.5 s^{-1}, K_M = 14.3 µM[208]), rate constants for spontaneous dismutation of superoxide (pH 7.4, 1.28 x 10^5 M^{-1} s^{-1}; pH 7.4, $9.01x10^6$ M^{-1} s^{-1})[209, 210], membrane permeabilities for hydrogen peroxide ($3.2x10^{-5}$ m s^{-1})[148] and $HO_2^{\cdot}$ ($9x10^{-6}$ m s^{-1})[147], *Salmonella* endogenous generation of hydrogen peroxide (10 µM s^{-1}, dismutation of endogenous superoxie was deducted)[211] and superoxide (cytosol, 5 µM s^{-1}; periplasm, 5 µM s^{-1})[154], and *Salmonella* dimensions modeled after *E. coli* as given in the CCDB database (ccdb.wishartlab.com/CCDB/intron_new.html). Modeling was done using the Simulink feature of MATLAB. The corresponding MATLAB files are available upon request.

2.2 Myeloperoxidase focusses intense oxidative attacks on pathogens and prevents collateral tissue damage

Nura Schürmann[1]‡, Pascal Forrer[3]‡, Olivier Casse[1], Boas Felmy[4], Anne-Valérie Burgener[3], Nikolaus Ehrenfeuchter[2], Wolf-Dietrich Hardt[4], Mike Recher[3], Christoph Hess[3], Astrid Tschan-Plessl[3], Nina Khanna[3], Dirk Bumann[1]*

[1]Focal Area Infection Biology, Biozentrum, University of Basel, CH-4056 Basel

[2]Imaging Core Facility, Biozentrum, University of Basel, CH-4056 Basel

[3]Department Biomedicine, University of Basel, CH-4056 Basel

[4]Institute of Microbiology, ETH Zurich, CH-8093 Zurich

‡These authors contributed equally to the work.

*Corresponding Author

The current version of the manuscript was submitted to Nature medicine.

Statement of my work:

Design of experiments

Immunohistochemistry staining and Analysis (Fig. 1e, 3c, 4 Supplementary Fig. 4, 5)

In vitro assays of H_2O_2 release, MPO measurement and oxygen consumption (Fig 2, Supplementary Figure 1, 2, 3b) (Oxygen measurements together with P.F.)

Flow cytometry and Analysis (Fig. 3b)

Manuscript writing and revision with D.B.

The references of the manuscript are included with the references of the main text.

Myeloperoxidase focusses intense oxidative attacks on pathogens and prevents collateral tissue damage

Nura Schürmann[1]*, Pascal Forrer[3]*, Olivier Casse[1], Boas Felmy[4], Anne-Valérie Burgener[3], Nikolaus Ehrenfeuchter[2], Wolf-Dietrich Hardt[4], Mike Recher[3], Christoph Hess[3], Astrid Tschan-Plessl[3], Nina Khanna[3], Dirk Bumann[1]

Abstract:

Pathogen killing with reactive oxygen species (ROS) is crucial for host defense against infection, but ROS can also cause serious tissue damage. Here, we show that neutrophils use their most abundant protein, myeloperoxidase, to solve the challenging problem of targeting ROS specifically to pathogens. A computational reaction-diffusion model of neutrophil oxidative bursts against *Salmonella* predicted that myeloperoxidase at the *Salmonella* surface efficiently scavenges diffusible hydrogen peroxide and converts it into highly reactive HOCl (bleach), causing most damage within a radius of only 0.1 μm. At low myeloperoxidase levels, hydrogen peroxide was predicted to accumulate to high concentrations sufficient for *Salmonella* killing, but also massive leakage to the surroundings. *Salmonella* stimulation of neutrophils from normal and myeloperoxidase-deficient human donors experimentally confirmed an inverse relationship between myeloperoxidase activity and extracellular peroxide release. Moreover, myeloperoxidase-deficient mice infected with *Salmonella* had elevated hydrogen peroxide levels and exacerbated oxidative damage of host lipids and DNA in spite of almost normal *Salmonella* control, as predicted. The previously enigmatic enzyme myeloperoxidase thus enables oxidative attacks against pathogens with high local intensity but minimal collateral tissue damage, by converting diffusible long-lived H_2O_2 into highly reactive HOCl at the *Salmonella* surface.

Myeloperoxidase (MPO) is a key innate immunity protein that humans produce in daily amounts of hundreds of milligrams [45]. MPO is mostly expressed in neutrophils and monocytes, and is widely used as a marker for these cells and inflammation in general [212]. MPO can generate hypohalites (predominantly HOCl, bleach; but also HOBr) [45]. These molecules are kinetically and thermodynamically highly reactive oxidants [213] with potent antimicrobial efficacy, but also detrimental effects in cardiovascular diseases and other indications [214]. In addition, MPO can catalyze several other reactions including dismutation of superoxide O_2^- to H_2O_2 and molecular oxygen. However, the physiological relevance of this remarkable enzyme remains still unclear. Human individuals with MPO deficiencies are surprisingly frequent (around 1 in 2000 to 4000 in Europe), and most of them have unremarkable infectious disease histories [45]. Similarly, mice lacking MPO have only mild defects in controlling various infections.

During oxidative bursts, several reactive oxygen species (ROS) occur. NADPH oxidase initially generates O_2^-, which spontaneously dismutates to H_2O_2. MPO accelerates this dismutation and converts the resulting H_2O_2 into HOCl. Alternatively, HO_2 (protonated superoxide) and H_2O_2 can diffuse out of the phagosome. When oxidative bursts are targeted against microbial pathogens, ROS chemistry becomes even more complex due to the action of detoxifying microbial enzymes such as superoxide dismutases, catalases, and peroxidases [215]. To quantitatively estimate the role of MPO during interaction of neutrophils with *Salmonella*, we built a computational model combining oxidative bursts in neutrophil phagosomes [44] and *Salmonella enterica* serovar Typhimurium ROS defense [216] based on reported experimental parameters (Fig. 1a). This model included 8 small molecules, 10 host and bacterial enzymes, and 27 different reactions. At normal MPO concentrations (around 1 mM in the phagosome) [44], this model predicted efficient conversion of O_2^- to HOCl (80% compared to the optimal theoretical yield of ½ HOCl per O_2^-) in close agreement with previous experimental [45] and modeling results [44], as well as about 10% leakage of other ROS (mostly H_2O_2, some HO_2) from the phagosome (Fig. 1b). HOCl is highly reactive and thus has short lifetime and short reach (around 0.1 μm [44]). These properties confine HOCl and its damaging action to the phagosome [46]. In neutrophil phagosomes, MPO localizes mostly to the *Salmonella* surface (Fig. 1e)

as previously observed for other bacteria [45], possibly causing localized HOCl generation and *Salmonella* damage. HOCl would indeed be responsible for most of the potent neutrophil oxidative killing action [216] , since the predicted efficient scavenging of O_2^- and H_2O_2 by MPO would limit their concentrations to levels (17.4 μM, 1.2 μM) that *Salmonella* detoxification through peroxidases and catalase could easily handle (internal H_2O_2 concentration, 0.77 μM; well below the toxicity threshold of about 2 μM [148]; Fig. 1c,d).

With decreasing MPO content, predicted HOCl yield declined and H_2O_2 leakage increased (Fig. 1b). At MPO levels below 0.13 mM, leakage would prevail over HOCl production. At the same time, less efficient scavenging by MPO would lead to elevated phagosomal concentrations of O_2^- and in particular H_2O_2 (Fig. 1c). *Salmonella* detoxification of H_2O_2 through peroxidases (AhpC, Tsa, Tpx) would be saturated at all MPO concentrations, but catalase (KatG) activity would strongly increase with lower MPO/higher H_2O_2 (Fig. 1d), as expected based on the respective enzyme kinetics [154]. However, at MPO levels below 40% of normal levels, this detoxification would be insufficient to keep H_2O_2 concentration in *Salmonella* cytosol below the lethality threshold (Fig. 1c). The computational model thus predicted that MPO deficiency alters the bactericidal mechanisms (HOCl vs. H_2O_2), but might have little impact on overall *Salmonella* killing (Fig. 1f). These predictions might explain the unremarkable infectious disease history of MPO-deficient individuals [45, 216]. On the other hand, however, low MPO levels likely cause massive H_2O_2 leakage from neutrophil phagosomes (Fig. 1b).

H_2O_2 leaking into the neutrophil cytosol has been assumed to be largely scavenged by neutrophil redox protection mechanisms such as glutathione peroxidase [44]. This was based on early experimental data showing only minor extracellular H_2O_2 release in the first few minutes after stimulation of neutrophils with large amounts of microbes, and only moderate differences between stimulated neutrophils with normal or low levels of MPO [217, 218]. We revisited this issue using purified human neutrophils *in vitro*. Stimulation with heat-killed *Salmonella* resulted in typical neutrophil oxygen consumption kinetics with peaks at 20 to 40 min (Fig. 2a), which closely agreed with luminol oxidation (a specific chemoluminescence read-out for HOCl production [219]). An

assay using horseradish peroxidase and Amplex Red that reports H_2O_2 in the extracellular medium, indicated neutrophil leakage of H_2O_2 throughout the entire oxidative burst response (Fig. 2a).

The specific MPO-inhibitor ABAH [220] blocked HOCl production (as measured by luminol oxidation; Fig. 2b). This required rather high concentrations (IC_{50} about 200 μM under our assay conditions) compared to much lower inhibitory concentrations (IC_{50} = 3 μM) for neutrophil lysates (Supplementary Fig. 1). Some 50-fold higher IC_{50} values for MPO in intact cells vs. freely accessible MPO were consistent with previous reports [219, 220], and might reflect low saturation of MPO with endogenously generated H_2O_2 in phagosomes and/or poor intracellular drug penetration. Interestingly, partial MPO inhibition with ABAH significantly enhanced extracellular H_2O_2 leakage (Fig. 2b) while oxygen consumption was not significantly affected (Supplementary Fig. 2a). Donors with low MPO activities as measured by standard clinical cytometry (Fig. 2d) had low levels of luminol oxidation that correlated with the clinical parameter "mean peroxidase index" (Fig. 2b,d). At the same time, such neutrophils showed substantially higher H_2O_2 leakage upon *Salmonella* stimulation (Fig. 2b). As a control, the NADPH oxidase inhibitor DPI (which blocks generation of O_2^-) abolished both luminol oxidation and H_2O_2 leakage. Overall, there was an inverse relation between HOCl production (as measured by luminol chemoluminescence) and H_2O_2 leakage after stimulation with heat-killed or live *Salmonella* (Fig. 2c), as predicted by our computational model (Fig. 1b). In contrast, oxygen consumption and H_2O_2 release were not correlated (Supplementary Fig. 2b). Similar data were also obtained using stimulation with live *Salmonella* or the fungal pathogen *Candida albicans* (Supplementary Fig. 3). These data demonstrated that neutrophils cannot completely quench hydrogen peroxide leaking from phagosomes, and that higher amounts of H_2O_2 are released by MPO-deficient neutrophils as predicted by our model. This supports a role of MPO in confining ROS to intracellular compartments during oxidative antimicrobial responses.

To investigate MPO functions in infected tissues, we employed a well-characterized mouse model of systemic salmonellosis that mimics important aspects of human typhoid fever [221]. In this model, neutrophils kill a large proportion of *Salmonella* through NADPH oxidase-mediated mechanisms, suggesting a key importance of oxidative bursts and ROS [216]. However, MPO-

deficient mice have only slightly higher *Salmonella enterica* serovar Typhimurium loads after four days of infection, indicating a largely dispensable role of MPO-mediated ROS conversion for *Salmonella* control [216]. In this study, we infected MPO-mice with an 2-3 fold lower dose than congenic wild-type mice and obtained equivalent *Salmonella* spleen loads at day 4 (log(CFU), 7.0 ± 0.3 vs. 6.8 ± 0.3; n = 8, t-test, n.s.). This minimized potential artefacts due to differential bacterial loads. We used a sensitive and specific *Salmonella* H_2O_2 biosensor carrying a transcriptional fusion of the *katGp* promoter to *gfp* in addition to constitutively expressed mCherry [216] (Fig. 3a). *katGp* is controlled by the transcription factor OxyR that is activated by direct reaction of cysteines with H_2O_2 [222]. The biosensor *Salmonella* thus show always red fluorescence when alive, and additional green fluorescence when exposed to H_2O_2 at levels above 0.1 μM , while dead *Salmonella* rapidly loose fluorescence [216] (Fig. 3a). Flow cytometry of infected spleen homogenates from wild-type mice revealed that about 10% of live *Salmonella* biosensor cells were exposed to H_2O_2. In MPO-deficient mice this fraction doubled (Fig. 3b) as reported previously [216]. Interestingly, immunohistochemistry revealed that 68 ± 3% of these numerous H_2O_2-exposed GFP-positive *Salmonella* in MPO-deficient mice resided in F4/80^{hi} red pulp macrophages (Fig. 3c; N = 642, three mice). This was initially surprising since MPO is selectively expressed in neutrophils and monocytes, and absence of MPO should thus primarily affect *Salmonella* residing in these cells instead of red pulp macrophages [45],[223]. However, neutrophils and monocytes efficiently kill most intracellular *Salmonella* and destroy their fluorescent proteins (GFP and mCherry), making biosensor activities undetectable **[216]**. In contrast, the majority of live *Salmonella* with detectable fluorescent proteins resided in red pulp macrophages [216] where they reported increased H_2O_2-exposure. These findings were consistent with increased H_2O_2 release from MPO-deficient neutrophils (and monocytes), followed by diffusion into the surrounding tissue where H_2O_2 was sensed by live *Salmonella* in macrophages (together with some H_2O_2 generated during sub-lethal oxidative bursts in macrophages [216]). Together, these data support a role of MPO in locally confining ROS during infection *in vivo*.

While less reactive compared to HOCl, H_2O_2 is still a strong oxidizing reagent that can damage a large range of biomolecules (especially when in contact with metals, nitric oxide, etc.)

[215]. To determine if increased release of H_2O_2 in absence of MPO cause enhanced oxidative tissue damage, we quantified host lipid peroxidation with an antibody to the reaction product 4-HNE [224, 225] (Fig. 4a), and oxidative DNA damage with an antibody to 8-OHdG [225] in sections of *Salmonella*-infected spleen (Supplementary Fig. 4a). As expected [216], at day 4 post infection neutrophils and monocytes (which are both $CD11b^{hi}$ [216]) where detected almost exclusively in the red pulp, where also almost all *Salmonella* resided. In these areas, MPO-deficient mice had strongly exacerbated lipid peroxidation (Fig. 4a,b), and slightly but significantly increased DNA damage (Supplementary Fig. 4a,c), compared to wild-type mice (uninfected mice had no detectable damage). These damages occurred in $CD11b^{hi}$ cells, as well as $CD11b^{low}$ bystander cells (Fig. 4a, inset; Supplementary Fig. 4b) consistent with ROS leakage and diffusion through the tissue. These data suggested that without the confining action of MPO, ROS were released and caused excacerbated collateral tissue damage.

Several pathogens such as *Salmonella* have evolved versatile defense mechanisms against diverse host stresses. Killing these sturdy pathogens requires aggressive immune attacks with high local intensity, but this inevitably poses a risk of excessive self-damage of host tissues. Our data show how host immunity can solve this fundamental problem for a crucial antimicrobial mechanism, the employment of reactive oxygen species (ROS). During oxidative bursts, neutrophils use NADPH oxidase to generate high fluxes of superoxide, which spontaneously dismutates to H_2O_2. The amount of H_2O_2 thus generated is sufficient to kill even microbes with sophisticated redox defenses such as *Salmonella*. The primary objective - microbial target destruction – is thus achieved by this pathway. However, H_2O_2 can also readily diffuse through membranes and leaks out of cells to the surrounding host tissue where it causes substantial collateral damage. Neutrophils solve this problem with MPO, which rapidly converts H_2O_2 into HOCl. This molecule is even more toxic to microbes compared to H_2O_2 and has a much shorter reach (in the range of 0.1 μm) until it reacts with various biomolecules. This chemical conversion is thus an effective mechanism to concentrate and accurately position intense oxidative attacks on pathogens and to mitigate the risk of collateral damage (Fig. 4c). MPO is thus not essential for pathogen destruction but for self-protection, explaining the unremarkable

infectious disease histories of MPO-deficient individuals. However, if MPO-deficient humans accumulate oxidative damage such as lipid peroxidation and DNA oxidation during infection, similar to what we observed in mice, this could increase the risk for long-term sequelae such as accelerated aging and cancer [226, 227]. Future epidemiological studies in countries with high incidence of infections might test this association. In contrast, the self-protective role of MPO might be less obvious in developed countries, where infections and inflammation have become greatly reduced in modern times [228].

Methods

Modeling of oxidative bursts in neutrophil phagosomes

We build a diffusion-reaction model based on a previous neutrophil phagosome model [44] and our previous model of *Salmonella* oxidative stress defense [216] that are both based on experimentally determined parameters. The model covers O_2^- generation by NADPH oxidase; O_2^- protonation equilibrium; spontaneous O_2^- dismutation; reactions of O_2^- catalyzed by myeloperoxidase or *Salmonella* superoxide dismutases SodA, SodB, SodCI; reactions of H_2O_2 catalyzed by myeloperoxidase or *Salmonella* catalase KatG or peroxidases AhpC, Tsa, Tpx; generation of HOCl by reaction of MPO compound I with chloride; and diffusion of HO_2 and H_2O_2 across the phagosomal membrane as well as *Salmonella* outer and inner membranes. Simulations using the Simulink feature of MATLAB were run until steady state concentrations were reached.

Code availability: Code is available upon request from the corresponding author.

Pathogen cultures

Salmonella strains used in this study were derived from *Salmonella enterica* serovar Typhimurium *SL1344 hisG rpsL xyl* [197, 229]. The H_2O_2 biosensor construct p*katGp-gfp* was described previously [216]. *Salmonella* were cultured at 37°C with aeration (200 rpm) in Lennox LB with addition of 90 μg ml^{-1} streptomycin with or without 100 μg ml^{-1} ampicillin. For *in vitro* experiments, stationary phase *Salmonella* were opsonized in 10% human serum in PBS for 20min at 37°C, washed with PBS, and diluted to MOI 30 for immediate use (live *Salmonella*). Alternatively, *Salmonella* were grown to mid-log phase, washed twice in PBS and heat-inactivated at 99°C for 15 min. Heat-inactivated *Salmonella* were opsonized in 10% human serum in PBS for 20 min at 37°C, washed with PBS, and diluted to MOI 200 for immediate use (heat-inactivated *Salmonella*).

Candida albicans SC5314 was grown overnight in yeast peptone dextrose (YPD, BD Difco) media at 37°C. A subculture was inoculated 1:100 and grown to mid-log phase. *C. albicans* was washed twice with 0.9% NaCl and heat-inactivated at 95°C for 1 h. *C. albicans* was opsonized in 10% human serum in PBS for 20 min at 37°C, washed with PBS and diluted to MOI 1 for immediate use.

Human PMN isolation

Human PMN were isolated as previously described[230]. In brief, human peripheral blood was collected in 7.5 ml polyethylene tubes containing 1.6 mg EDTA/ml blood (Sarsted), mixed with 3% Dextran (Pharmacia)/ NaCl solution supplemented with 10 ug/ml Polymyxin-B (Calbiochem) in a ratio of 2:1. Erythrocyte sedimentation occurred after incubation for 30 min at 37°C in a 5% CO_2 incubator. Then the leukocyte-rich plasma was aspirated and centrifuged for 7 min at 1400 rpm, 4°C. The pellet was resuspended and transferred to a discontinuous Percoll gradient with 53% and 67% Percoll (GE Healthcare). Percoll Gradient centrifugation was performed for 30 min at 1400 rpm, 4°C, no braking. The visible ring containing PMN fraction was collected and washed in 0.9% NaCl, resuspended in RPMI (Invitrogen Gibco) + 10% FBS and counted manually with Türk solution and an automatic cell counter system ADAM (Digital Bio). Purity and Viability was >97% respectively >99%. If necessary, hypotonic erythrocyte lysis was performed with erythrocyte lysis buffer (Biolegend). Neutrophils were distributed and rested for 15 min before stimulation.

MPO-deficient patients and healthy volunteers

The study was approved by the responsible Ethics Committee (EKNZ 2015-187) and in compliance with the Declaration of Helsinki. Study participants signed an informed consent form.

Fresh venous blood was drawn in 2.7 ml polyethylene tubes containing 1.6mg EDTA/ml blood (Sarsted) and analyzed within two hours on full-automated Advia 2120 hematological analyzer (Bayer) at Hematology Routine Diagnostics Laboratory, University Hospital Basel. MPO level was determined from a Perox diagram according to cell size and peroxidase activity. MPO Index (MPXI) was calculated according to the formula: MPXI=121.1-2.38 x A(degrees), where A(degrees) describes the angle through the centre of the deficient cluster and the baseline of the diagram [231].

Luminol-enhanced Chemiluminescence

Hypochlorous acid (HOCl) production of PMN was measured using luminol-enhanced chemiluminescence. In brief, $2x10^5$ cells were incubated in RPMI+10% FCS for 1h at 37°C, 5% CO_2

without inhibitors, or with 500 μM ABAH or 10 μM DPI. Neutrophils were stimulated with opsonized *Salmonella* or *Candida albicans* in the presence of 10% human serum and 100 μM luminol (Fluka) in HBSS (Invitrogen, Gibco) + 0.1% glucose (Braun).

Chemiluminescence was measured at 5min intervals at 37°C with a luminometer (Microlumat Plus, Berthold Technologies). Values were corrected against unstimulated control and initial time points.

Hydrogen peroxide release of human neutrophils

Extracellular H_2O_2 release was measured by the production of Resofurin from Amplex Red (Invitrogen). In brief, $1x10^5$ cells/well were treated with or without inhibitors in RPMI+10% FCS for 1h at 37°C, 5% CO_2. Cells were washed once and reaction mixture was added (50μM Amplex Red +0.1U/mL horse radish peroxidase (HRP, Sigma) in KRPG buffer 145 mM NaCl, 5.7 mM sodium phosphate, 4.86 mM KCl, 0.54 mM $CaCl_2$, 1.22 mM $MgSO_4$, 5.5 mM glucose, pH 7.35). As a negative control, HRP was omitted. Neutrophils were stimulated with *Salmonella* or *Candida albicans* and fluorescence was measured at 5 min intervals at 37°C with a fluorescence plate reader (490 nm excitation, 590 nm emission). Values were corrected against HRP-negative control and initial time points. H_2O_2 concentration was determined using standard curves obtained with defined H_2O_2 concentrations.

Oxygen Consumption Rate

Oxygen Consumption Rate was measured with a Seahorse XF-96 metabolic extracellular flux analyzer (Seahorse Bioscience). Human peripheral blood derived neutrophils pretreated or not with inhibitors were resuspended in KRPG buffer and plated onto Seahorse cell plates (3×10^5 cells per well) coated with Cell-Tak (BD Bioscience). Heat-killed *C. albicans* SC5314 (MOI=2) or heat-killed *Salmonella* Typhimurium SL1344 (MOI=200) was directly applied onto plated cells via the instrument's injection port. The experimental parameters were set at 3 min mixture / 0 minutes wait / 3 min measurement for 23 cycles.

Peroxidation activity of MPO in intact and lysed neutrophils

Peroxidation activity was quantified by the production of Resofurin from Amplex Red in the supernatant of neutrophils. To determine MPO activity of neutrophil lysates $1x10^5$ cells/well were lysed with 1x lysis buffer (Cell signaling, No. 9803) and treated with increasing ABAH concentrations (0 μM to 500 μM) in RPMI+10% FCS. 50 μM Amplex Red + 5 μM H_2O_2 were added and fluorescence was measured after 30 min incubation at 37°C. To determine MPO activity of intact neutrophils $1x10^5$cells/well were washed 3 x with PBS after 1h treatment of increasing ABAH concentrations (0 μM to 500 μM) in RPMI+10% FCS. 50 μM Amplex Red + 5 μM H_2O_2 were added and fluorescence was measured after 30 min incubation at 37°C. MPO activity was determined using standard curves obtained with defined MPO (Sigma M6908) concentrations.

Mouse Infections and Tissue Collection

All animal experiments were approved (license 2239, Kantonales Veterinäramt Basel) and performed according to local guidelines (Tierschutz-Verordnung, Basel) and the Swiss animal protection law (Tierschutz-Gesetz).

Female 8-10 weeks old B6.129X1-MPO$^{tm1Lus/J}$ as well as age- and sex-matched C57BL/6J congenic mice, were infected by tail vein injection of 800-2800 *Salmonella* in 100 μl PBS and euthanized at 4 days post infection. Spleen tissue was collected from each mouse and dissected into several pieces. CFU counts were determined by plating. We estimated sample size by a sequential statistical design. We first infected 4 mice each based on effect sizes and variation observed in our previous study [216]. Biosensor responses and oxidative tissue damage analysis suggested that with 4 additional mice in each would be sufficient to determine statistical significance with sufficient power. This was indeed the case (see text). We did neither randomice or blind the experiments. However, image analysis of stained section was carried out using an automated unbiased approach (see Image Analysis section).

Immunohistochemistry

2-3mm thick spleen sections were fixed with fresh 4% paraformaldehyde at 4°C for 4 h, followed by incubating in increasing sucrose concentrations from 10%-40% at 4°C. After overnight incubation in 40% sucrose, tissue was rapidly frozen in embedding media (Tissue-Tek® O.C.T; Sakura), left overnight at -80°C, and then stored at -20°C. Unfixed tissue was immediately frozen in embedding media, left overnight at -80°C, and then stored at -20°C. 10-14 μm thick cryosections were cut, put on coated glass cover slips (Thermo Scientific) and dried in a desiccator. After blocking with 1% blocking reagent (Invitrogen) and 2% mouse serum (Invitrogen) in PBST (0.05% Tween in 1X PBS pH7.4), sections were stained with primary antibodies (rat anti-CD11b, BD clone M1/70; goat anti-CSA1, KPL 01-91-99-MG, goat anti-4-HNE, Alpha Diagnostics HNE12-S, rabbit anti-myeloperoxidase, abcam 9535, goat anti-8 Hydroxyguanosine abcam 10802; rat F4/80, Serotec clone CI:A31). A variety of secondary antibodies were used depending on the application (Molecular probes; Cat. A-21443; S11225, S21374; A-21206; A11096, D20698, Invitrogen A31556, Santa CruzBT sc-362245). In the case of anti-4-HNE and 8-Hydroxyguanosine (8-OHdG) staining, we used fresh unfixed sections and a horseradish peroxidase kit (Molecular probes; Cat: T-20936) to amplify the signal. Sections were mounted in fluorescence mounting medium (Dako or Vectashield), and examined with a Zeiss LSM 700 confocal microscope using glycerol 25X, 40X, and 63X objectives. Tiles covering an entire spleen section were stitched together. High resolution images were obtained using Zeiss LSM 800 Airy Scanning.

Image Analysis

For quantitative analysis of lipid peroxidation and DNA damage on antibody-stained spleen sections, we used an unbiased, automated protocol in the bioimage informatics platform icy [232]. This protocol was established to minimize the impact of differences in staining intensities between individual samples. Each image consisted of 3 channels (DAPI, nuclei; 4-HNE, lipid peroxidation or 8-OHdG, DNA damage; CD11b, infiltrating neutrophils and monocytes). In a first step, the whole tissue area was segmented using the combined intensities from all three channels. In a next step a threshold was

applied to create a segmentation of $CD11b^{hi}$ regions. The threshold value was set using Huang's method, which tries to minimize the measures of fuzziness [233], therefore providing a robust method to avoid over-segmentation of noisy regions, especially at segmentation borders. Next the $CD11b^{hi}$ area was subtracted from the whole tissue area to create a segmentation of $CD11b^{lo}$ regions. For detecting the proportion of $4\text{-}HNE^{hi}$ (or $8\text{-}OHdG^{hi}$) pixels in the $CD11b^{hi}$ and $CD11b^{lo}$ regions, we used as threshold the sum of the mean 4-HNE signal over the entire tissue section + 3 times the standard deviation. The staining index was then determined as the ratio of $4\text{-}HNE^{hi}$ pixels proportions in $CD11b^{hi}$ over $CD11b^{lo}$ regions. AS a much simpler alternative, we also used a simple threshold of 100 across all samples with essentially very similar results (Supplementary Fig. 5).

Flow Cytometry

Spleen homogenates were prepared for flow cytometry as described [216]. Relevant spectral parameters of 10,000 to 50,000 *Salmonella* were recorded in a FACS Fortessa II equipped with 445 nm, 488 nm and 561 nm lasers (Becton Dickinson), using thresholds on SSC and FSC to exclude electronic noise (channels: CFP, excitation 445 nm, emission 499-529 nm; GFP, excitation 488 nm, emission 502-525; RFP, excitation 561 nm, emission 604-628 nm; yellow autofluorescence channel, excitation 455 nm, emission 573-613 nm; infrared autofluorescence channel, excitation 561 nm, emission 750-810 nm). Data processing was done with FlowJo.

Acknowledgements

We thank Kathrin Ullrich and Richard Kühl for taking blood from human donors and all donors for blood donations. We thank Ingo Bartholomaeus and Andreas Martin for support with confocal microscopy. This study was supported in part by grants from Swiss National Foundation (PP00P3_144863 to M.R. and 310030_156818 to D.B.).

Author contributions

D.B. conceived the study. D.B., N.S., P.F., N.K., W.-D.H. designed the experiments. N.S., P.F., B.F., N.E., A.T.P., D.B. performed experiments and analyzed the data. O.C. and D.B. wrote code and ran the models. A.V.B., C.H. and M.R. recruited patients. D.B. and N.S. wrote the paper with input from all authors.

Author information

The authors declare no competing financial interests.

Correspondence and requests for materials should be addressed to dirk.bumann@unibas.ch.

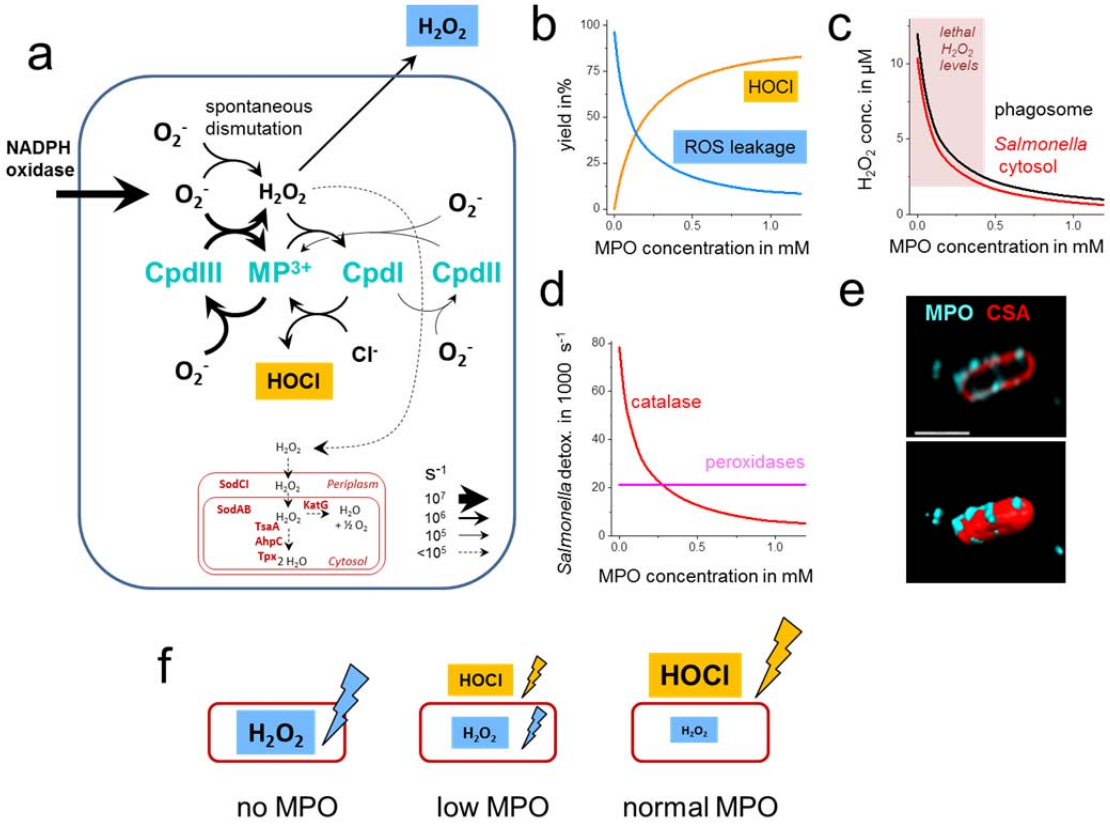

Fig. 1: Reactive oxygen species generation and leakage in neutrophil phagosomes containing *Salmonella* enterica. a) Computational model with enzymatic reactions of myeloperoxidase (MPO) species (cyan; Cpd, Compound; MP3+, native MPO) and *Salmonella* detoxification enzymes (red). Only the most relevant reactions are shown for conditions with partial MPO deficiency (13% of normal, 0.13 mM). b) Predicted HOCl production and leakage of reactive oxygen species (ROS, mostly H_2O_2) for various MPO concentrations in the phagosome. c) Impact of MPO concentration on H_2O_2 concentrations in the phagosome lumen and the *Salmonella* cytosol. Concentrations above the Salmonella lethality threshold are also shown. d) *Salmonella* detoxification of H_2O_2 through catalase (KatG) and peroxidases (AhpC, Tsa, Tpx). e) Micrograph of *Salmonella* in infected mouse spleen stained for MPO and common *Salmonella* antigen (CSA). The right panel shows a 3-dimensional surface rendering of the confocal stack. The scale bar represents 2 µm. f) Schematic model of bactericidal reactive oxygen species at various MPO levels.

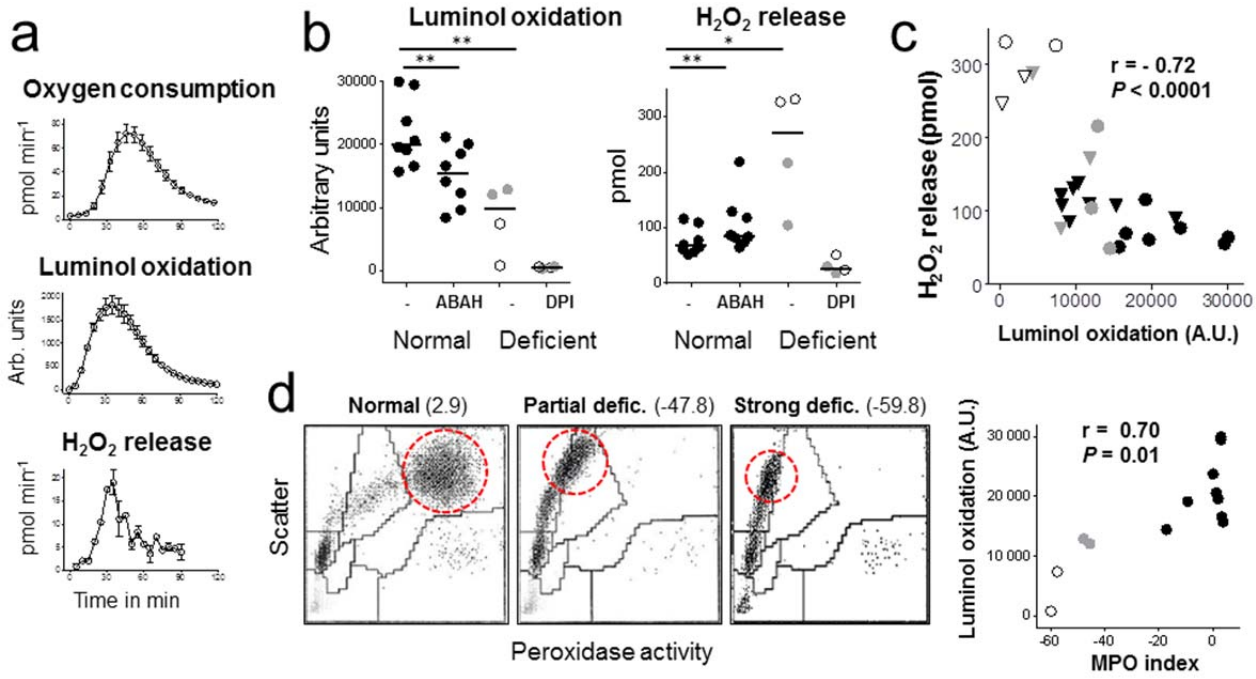

Fig. 2: Neutrophil production of reactive oxygen species *in vitro* upon stimulation with *Salmonella*. **a**) Kinetics of oxygen consumption, luminol oxidation (a chemoluminescence read-out for HOCl production), and extracellular H_2O_2 release for one normal human donor (measured in different platforms). **b**) Luminol oxidation and H_2O_2 release for eight different normal donors in presence/absence of the MPO inhibitor ABAH as well as two partially deficient (grey) and strongly deficient donors (open circles) without or with the NADPH oxidase inhibitor DPI (Wilcoxon test or Mann-Whitney-U test, respectively; *, $P< 0.05$; **, $P< 0.01$; ***, $P< 0.001$). **c**) Relationship between luminol oxidation and H_2O_2 release for normal and deficient donors after stimulation with heat-killed (circles) or live *Salmonella* (triangles) (r, Spearman correlation coefficient; other symbols as in B). **d**) Leukograms of normal and deficient donors. The numbers in parenthesis show the mean peroxidase index. The red circles contain the granulocyte populations. The right panel shows the relationship between the mean peroxidase index as determined by leukograms and luminol oxidation upon *Salmonella* stimulation.

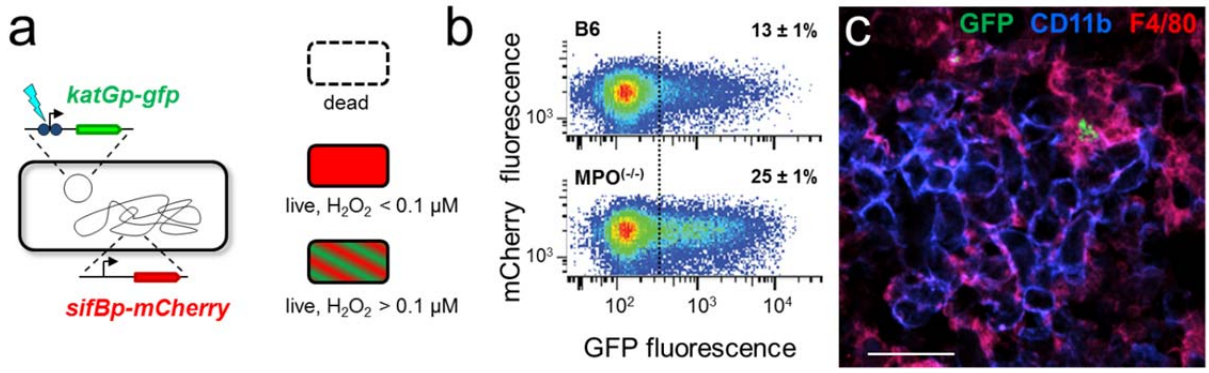

Fig. 3: H_2O_2 exposure of *Salmonella* in spleen of wild-type and MPO-deficient mice as revealed by a *Salmonella* biosensor strain. **a**) Biosensor properties. The strain constitutively expresses mCherry from a chromosomal cassette. In presence of H_2O_2, GFP is expressed from an inducible episomal cassette. Killed *Salmonella* rapidly loose fluorescence. **b**) Flow cytometry of *Salmonella* biosensor in spleen homogenates. All *Salmonella* contain mCherry and some also contain GFP, a reporter for H_2O_2 exposure. The numbers show averages ± SD of GFP^{hi} *Salmonella* (N = 8; t-test, $P < 0.001$). **c**) Localization of GFP^{hi} biosensor *Salmonella* in $F4/80^{hi}$ macrophages in the vicinity of $CD11b^{hi}$ neutrophils/inflammatory monocytes. The scale bar represents 20 µm.

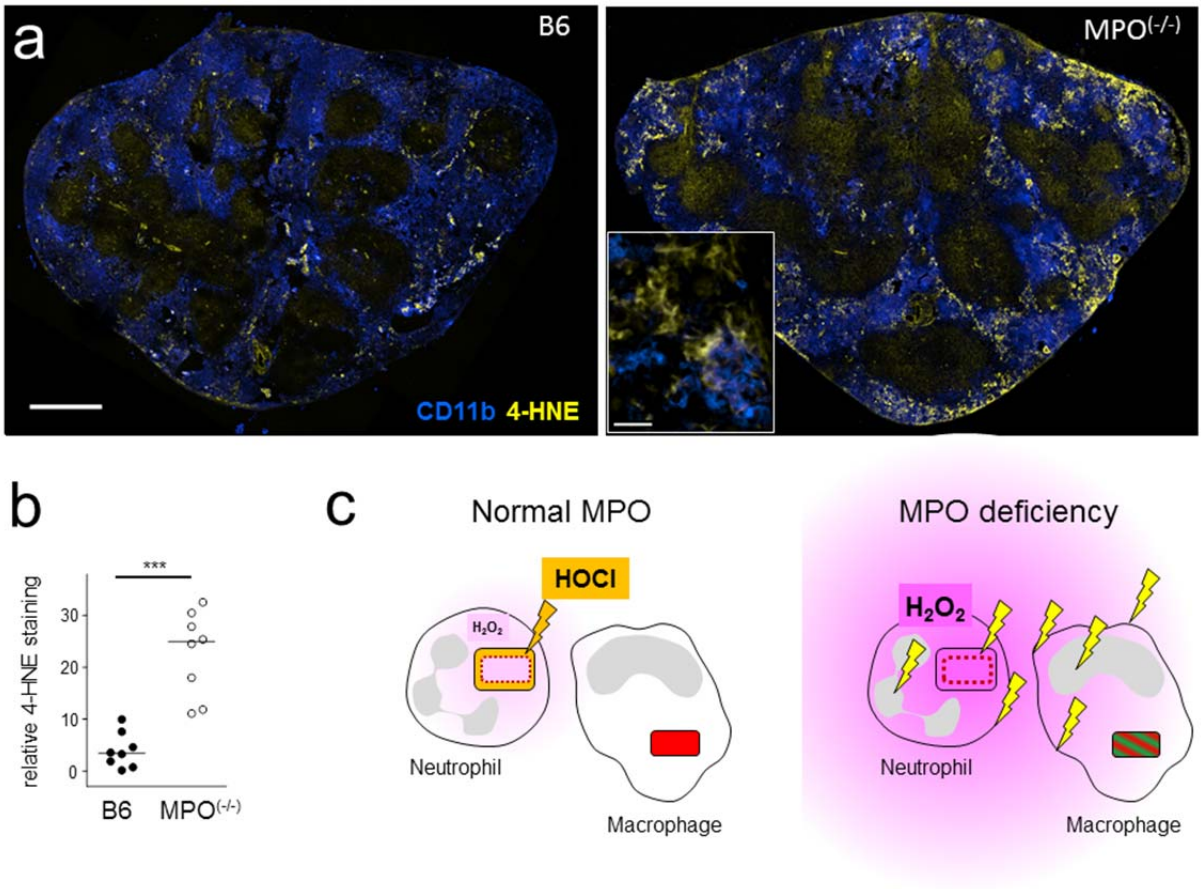

Fig. 4: Collateral damage in absence of myeloperoxidase (MPO). **a**) Lipid peroxidation in infected spleen as determined by 4-hydroxynonenal (4-HNE) immunohistochemistry. Representative micrographs of infected spleen cross-sections from wild-type B6 mice or MPO-deficient mice imaged at identical microscopy settings are shown. The scale bar represents 500 µm. The inset shows a representative area at higher magnification. Lipid peroxidation was detectable in $CD11b^{hi}$ neutrophils/inflammatory monocytes but also in neighboring CD11b-negative cells. The scale bar represents 20 µm. **b**) Quantification of 4-HNE staining corrected for different background intensities as described in the Methods (Mann-Whitney-U test; ***, $P< 0.0001$). For an alternative simple analysis see Supplementary Fig. 5. **c**) Schematic model for the role of MPO. At normal MPO levels (left), ROS generated in the neutrophil phagosome are efficiently converted into HOCl that remains confined to the phagosome and kills the ingested pathogen. In MPO-deficient individuals (right), ROS are still produced at high levels but instead of HOCl, H_2O_2 accumulates and kills the pathogen.

However, a substantial fraction of H_2O_2 leaks out from the phagosome and diffuses through the tissue where it causes exacerbated collateral damage.

Supplementary Figures

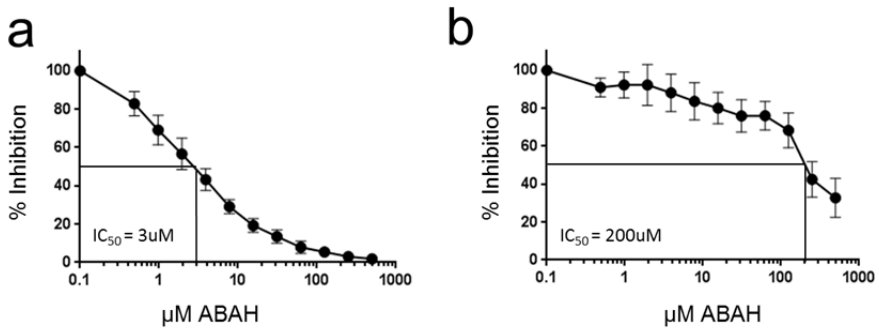

Supplementary Fig. 1: Inhibition of myeloperoxidase activity by ABAH in human neutrophil lysates (**a**) or intact neutrophils (**b**).

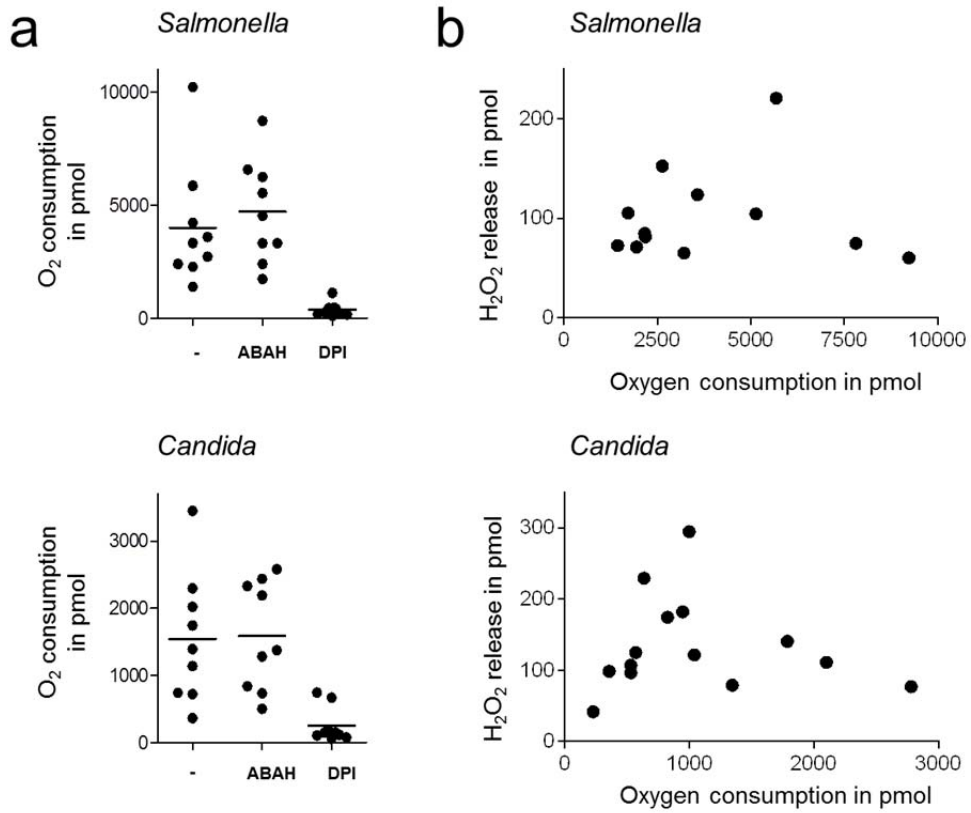

Supplementary Fig. 2: Oxygen consumption (**a**) and its relation to H_2O_2 release (**b**) in human neutrophils stimulated with heat-killed *Salmonella enterica* or heat-killed *Candida albicans*. Values for 100'000 neutrophils from individual donors are shown. ABAH treatment did not significantly affect oxygen consumption in either stimulation (Wilcoxon test).

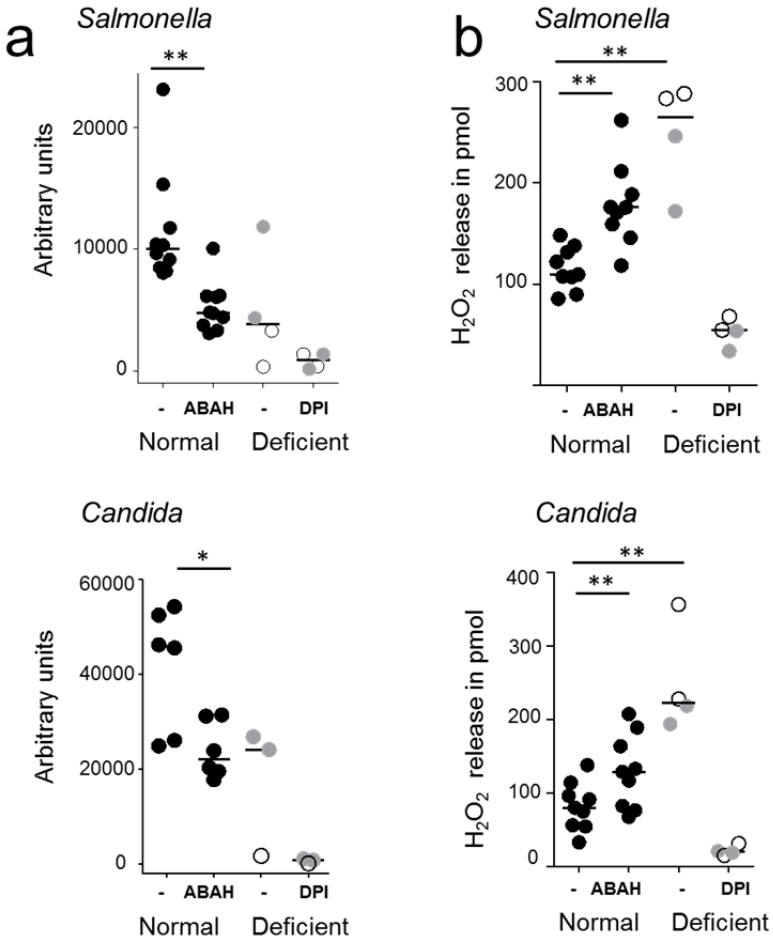

Supplementary Fig. 3: Luminol oxidation (**a**) and H_2O_2 release (**b**) in human neutrophils stimulated with live *Salmonella enterica* or heat-killed *Candida albicans*. Values for 100'000 neutrophils from individual donors are shown (Wilcoxon test or Mann-Whitney-U test, respectively; *, $P< 0.05$; **, $P< 0.01$).

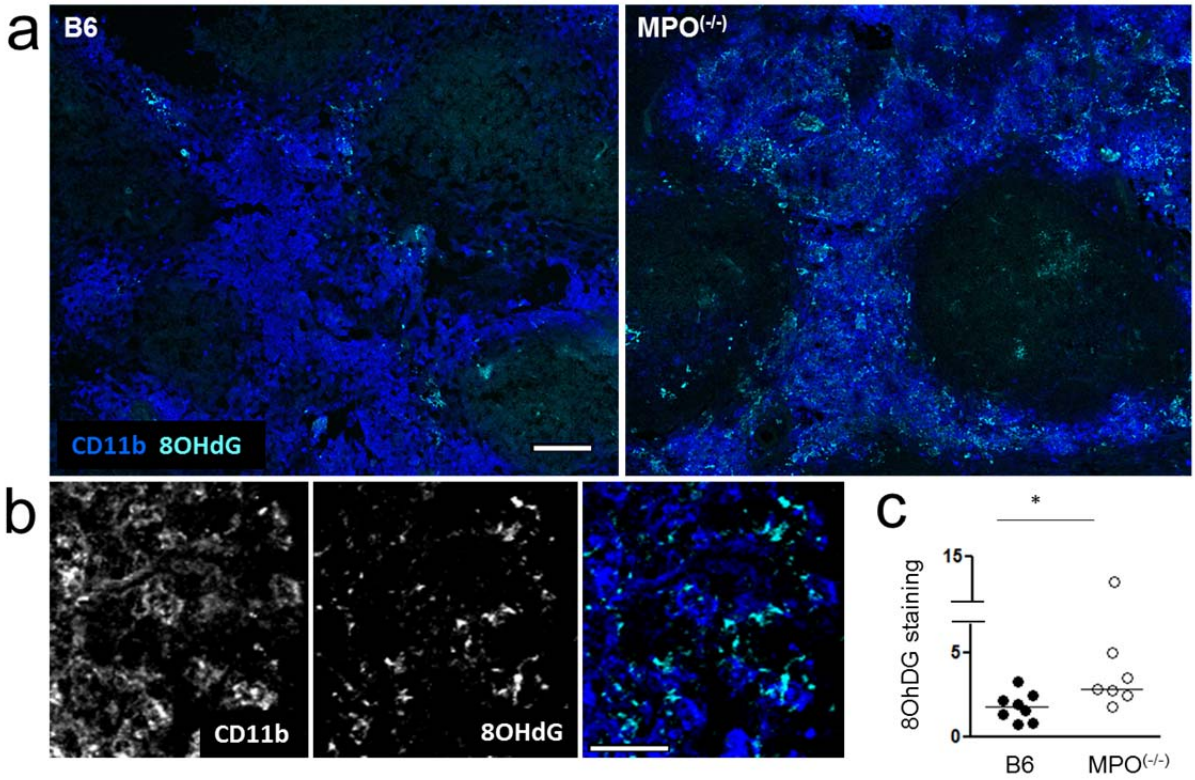

Supplementary Fig. 4: Collateral damage in absence of myeloperoxidase (MPO). **a**) DNA oxidation in infected spleen as determined by 8-OHdG immunohistochemistry. Representative micrographs of infected spleen cross-sections from wild-type B6 mice or MPO-deficient mice imaged at identical microscopy settings are shown. The scale bar represents 500 µm. **b**) Individual image channels and merged micrograph at higher magnification. The scale bar represents 20 µm. DNA peroxidation was detectable in $CD11b^{hi}$ neutrophils/inflammatory monocytes but also in neighboring CD11b-negative cells. **c**) Quantification of 4-HNE staining corrected for different background intensities as described in the Methods (N = 8; t-test; *, $P< 0.05$).

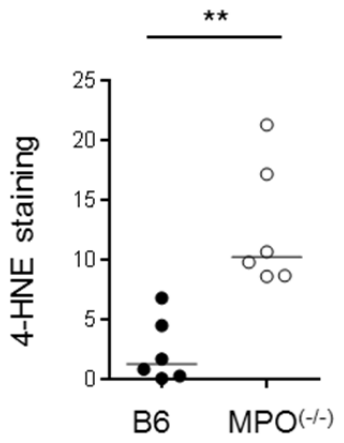

Supplementary Fig. 5: Quantification of lipid peroxidation in spleen sections from *Salmonella*-infected wild-type B6 mice or MPO-deficient mice. In this simple analysis, we used a common threshold for detecting the fraction of 4-HNE^{hi} pixels in all 12 samples (Mann-Whitney-U test; **, $P<$ 0.01). For a more sophisticated analysis in which we corrected for differences in background intensities between samples see Fig. 4b.

2.3 Dietary fat induces lipid accumulation in inflammatory monocytes, and drives lethal pro-inflammatory cytokine production during sepsis

Mauricio Rosas-Ballina[1], **Nura Schürmann[1],** Beatrice Claudi[1], Janine Zankl[2], Alexander Schmidt[3], Giuseppe Danilo Norata[4] Dirk Bumann[1]*

[1] Focal Area Infection Biology, Biozentrum, University of Basel, 4056 Basel, Switzerland.

[2] FACS Core Facility, Biozentrum, University of Basel, 4056 Basel, Switzerland.

[3] Proteomics Core Facility, Biozentrum, University of Basel, 4056 Basel, Switzerland.

[4] Department of Pharmacological and Biomolecular Sciences, Università degli Studi di Milano, Milan, Italy.

*Corresponding Author

Manuscript in preparation

Statement of my work:

Design of experiments

Immunohistochemistry staining + Analysis (Fig. 1A, B; Fig 2A, B)

The following parts contain only the abstract, figures and experimental procedures to which I contributed. The contribution of my work showed that neutral lipid accumulates in inflammatory monocytes and neutrophils located within spleen inflammatory lesions of mice infected with *Salmonella*.

Dietary fat induces lipid accumulation in inflammatory monocytes, and drives lethal pro-inflammatory cytokine production during sepsis

Mauricio Rosas-Ballina, Nura Schürmann, Beatrice Claudi, Janine Zankl, Alexander Schmidt, Giuseppe Danilo Norata, Dirk Bumann

Abstract

Sepsis, the inflammatory response to infection, remains an important source of morbidity and mortality world-wide. Besides the overwhelming levels of pro-inflammatory cytokines, sepsis is characterized by systemic derangements in lipid metabolism. Lipid accumulation is a key feature of pro-inflammatory activation of phagocytes, but neither the cell type accumulating lipid nor the function of this accumulated lipid has been established. Here we show that neutral lipid accumulates in inflammatory monocytes and neutrophils located within spleen inflammatory lesions of mice infected with *Salmonella*. Increased neutral lipid content in these immune cells is accompanied by elevated cholesterol and decreased TAG plasma levels, and changes in lipoprotein composition suggestive of reduced reverse cholesterol transport. Metabolic studies suggest that spleen inflammatory monocytes from septic mice have and increased respiratory rate due to enhanced mitochondrial beta-oxidation, which in turn drives elevated reactive oxygen species levels. Our findings establish a functional connection between systemic lipid levels and the metabolic state of inflammatory monocytes in sepsis.

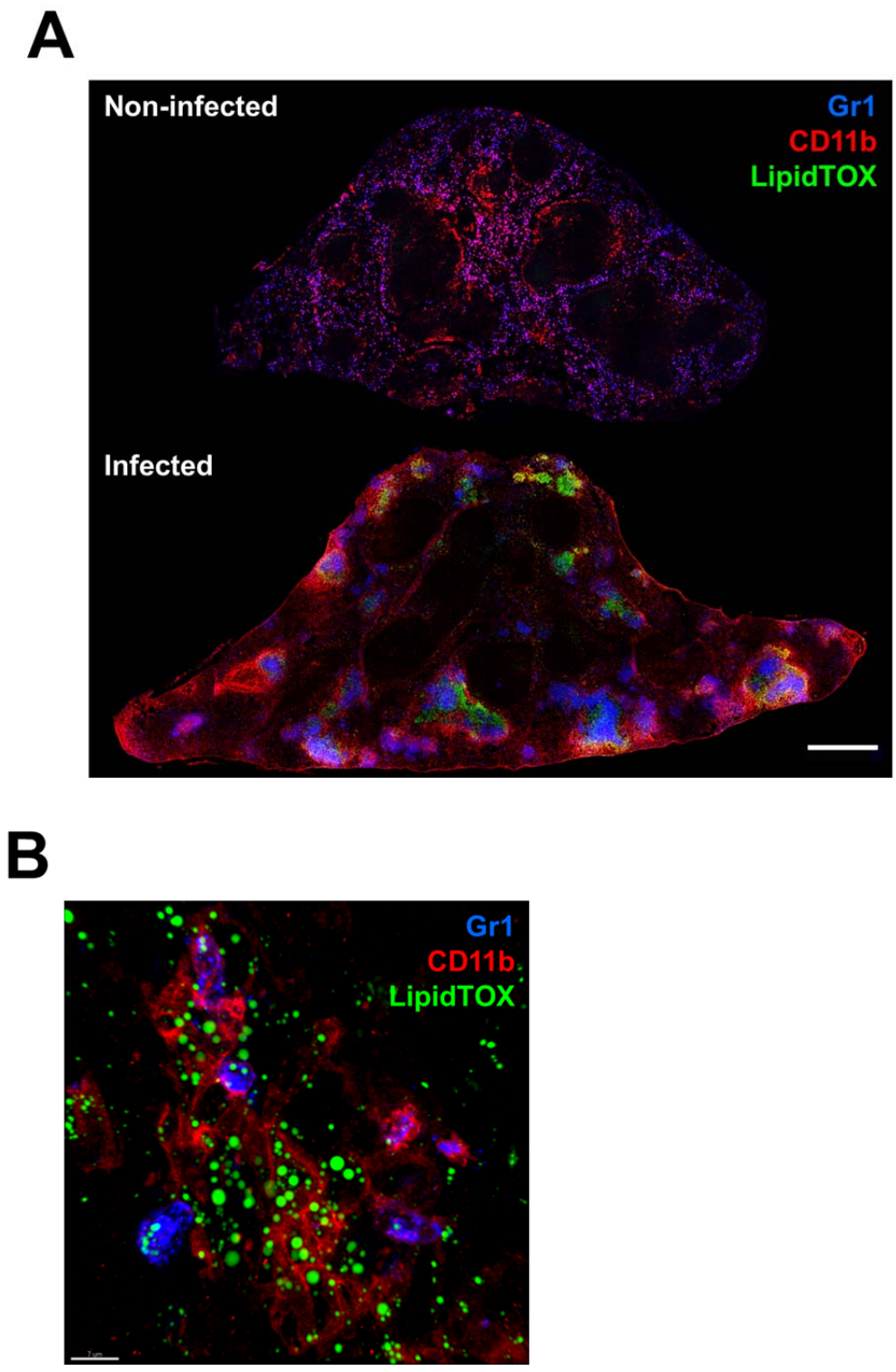

Figure 1 Neutral lipid accumulation in spleen. Inflammatory monocytes and PMNs

A) Mouse spleen immunohistochemistry with markers for neutrophils ($Gr1^{hi}$, $CD11b^{hi}$), inflammatory monocytes ($Gr1^{low}$, $CD11b^{hi}$) and neutral lipids (lipidtox). The scalebar represents 500 µM B) Higher magnification of A) infected spleen. The scale bar represents 7 µM

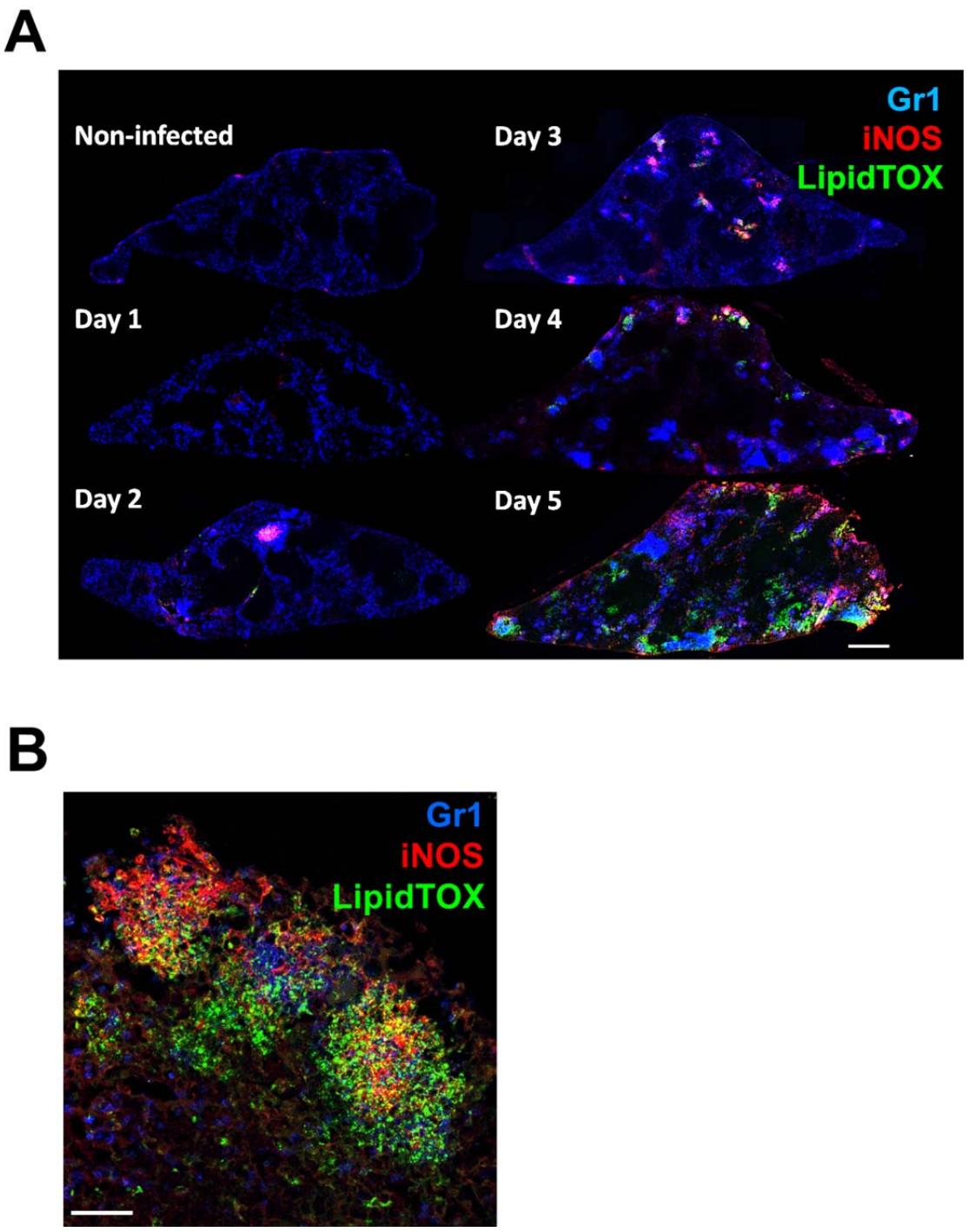

Figure 2 Neutral lipid accumulation in inflammatory monocytes and neutrophils is not dependent on iNOS

A) Mouse spleen immunohistochemistry with markers for neutrophils ($Gr1^{hi}$, $CD11b^{hi}$), inducible nitric oxide synthase (iNOS) and neutral lipids (lipidtox) at different time points of infection. The scale bar represents 500 µM B) Higher magnification of A) infected spleen Day 4. The scale bar represents 50 µM

EXPERIMENTAL PROCEDURES

Immunofluorescence

Following fixation in formaldehyde 4% and dehydration with sucrose-containing PBS, spleen was embedded in OCT compound, frozen and kept at -80 °C until further analysis. 10-14 µm-thick sections were blocked in 1% blocking reagent (Invitrogen) and 2% mouse serum in TBST (0.05% Tween in 1X TBS pH7.4) and stainined with combinations of the following primary antibodies: anti-Gr-1 (clone RB6-8C5, BD Biosciences), anti-CD11b (clone M1/70, BD Biosciences), anti-F4/80 (clone CI:A3-1, BD Biosciences), and anti-iNOS (Abcam, ab15323). The anti-Gr-1 antibody recognizes Ly6G and Ly6C. However, Gr-1 readily stains Ly6G but stains Ly6C poorly in fixed spleen sections, as previously shown by us (Burton et al., 2014). On this basis, neutrophils were identified as Gr-1+ and CD11b+, and inflammatory monocytes as CD11b+. Neutral lipids were visualized with 1:500 HCS LipidTOX Green Neutral Lipid Stain (LifeTechnologies). Sections were visualized and pictures taken with a Leica SP5, Zeiss LSM 700 confocal microscope, and images were analyzed with Imaris and Fiji.

2.4 Caspase-11 activation requires lysis of pathogen-containing vacuoles by interferon-induced GTPases

Etienne Meunier[1], Mathias S. Dick[1], ‡, Roland F. Dreier[1], ‡, **Nura Schürmann[1]**, Daniela Kenzelmann Broz[2], Søren Warming[4], Merone Roose-Girma[4], Dirk Bumann[1], Nobuhiko Kayagaki[4], Kiyoshi Takeda[3], Masahiro Yamamoto[3] and Petr Broz[1]*

[1]Focal Area Infection Biology, Biozentrum, University of Basel, Basel, Switzerland

[2]Department Biomedicine, University of Basel, Basel, Switzerland

[3]Department of Microbiology and Immunology, Osaka University, Yamadaoka, Suita, Osaka 565-0871, Japan

[4]Genentech Inc., South San Francisco, California, USA.

‡These authors contributed equally

*Corresponding Author

The manuscript was published in Nature 508, 366-370, 15 May 2014

doi:10.1038/nature13157

Statement of my work:

Design of experiments

Immunohistochemistry and quantification of GBPs and *Salmonella* in infected mouse spleen

(Figure 2 e, f, g)

Supplementary Figure (not included in the paper)

The following parts contain only the abstract and the figures to which I contributed. The contribution of my work showed that GBPs play a relevant role for *Salmonella* killing by macrophages *in vivo*.

Caspase-11 activation requires lysis of pathogen-containing vacuoles by interferon-induced GTPases

Etienne Meunier, Mathias S. Dick, Roland F. Dreier, Nura Schürmann, Daniela Kenzelmann Broz, Søren Warming, Merone Roose-Girma, Dirk Bumann, Nobuhiko Kayagaki, Kiyoshi Takeda, Masahiro Yamamoto and Petr Broz

Abstract

Lipopolysaccharide (LPS) from Gram-negative bacteria is sensed in the host cell cytosol by a non-canonical inflammasome pathway that ultimately results in caspase-11 activation and cell death[234-236]. Activation of this pathway requires the production of type-I-interferons[182, 237], indicating that interferon-induced genes play a critical role in initiating this pathway. Here we report that a cluster of small, interferon-inducible GTPases, the so-called GBP proteins, is required for the full activity of the non-canonical caspase-11 inflammasome during infections with vacuolar Gram-negative bacteria. We show that GBP proteins are recruited to intracellular bacterial pathogens and are necessary to induce the lysis of the pathogen containing vacuole (PCV). Lysis of the PCV releases bacteria into the cytoplasm, thus allowing the detection of their LPS by a yet unknown LPS sensor. Moreover, recognition of the lyzed vacuole by the danger sensor Galectin-8 initiates the uptake of bacteria into autophagosomes, which results in a reduction of caspase-11 activation and bacterial killing. These results indicate that host-mediated lysis of PCVs is an essential immune function and is necessary for efficient recognition of pathogens by inflammasome complexes in the cytosol.

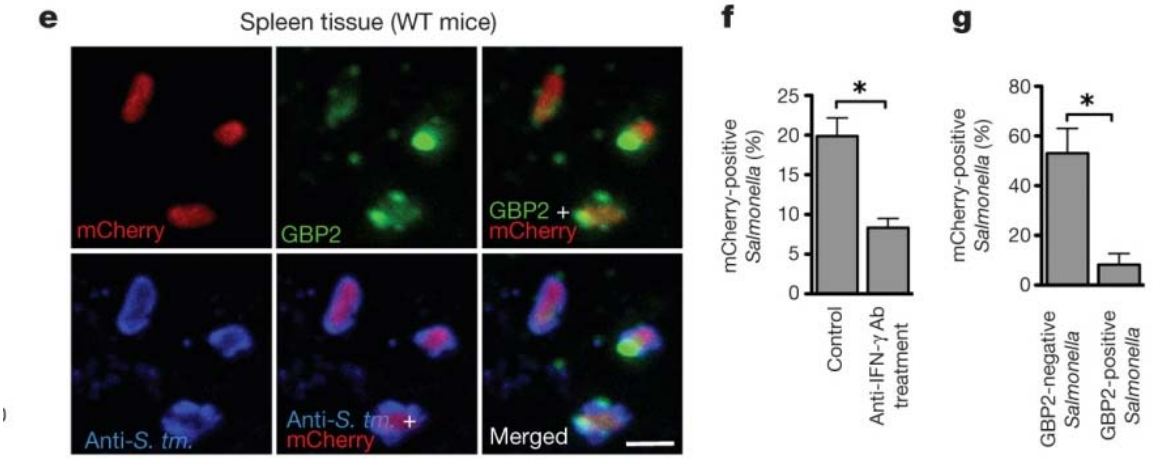

Figure 2 GBP proteins control bacterial replication

e, Immunohistochemistry for GBP2 and *Salmonella* on spleen tissue from *Salmonella* (mCherry-positive)-infected mice (representative of *n* = 3 per group). *S. tm.*, *S. typhimurium*. **f**, **g**, Quantification of GBP-positive *Salmonella* in anti-IFN-γ-treated or control animals (**f**) and live and dead bacteria among GBP2-negative/-positive *Salmonella* (**g**) (*n* = 3 per group). Scale bars, 10 µm

Supplementary Figure (not included in the paper)

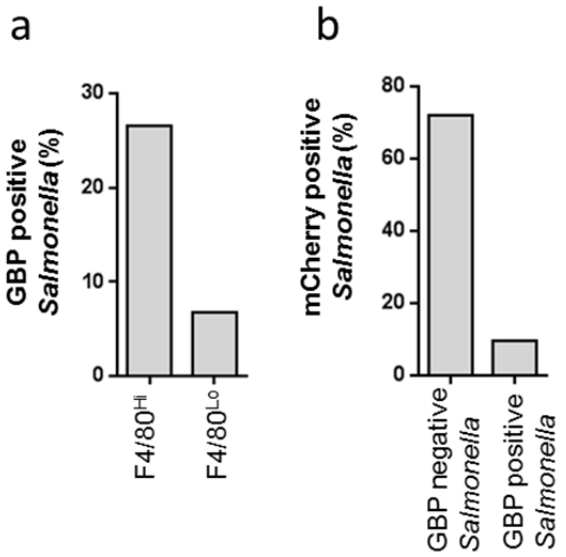

GBPs play a major role in macrophages

a) Quantification of GBP positive *Salmonella* in resident macrophages (F4/80^{Hi}) and inflammatory cells (F4/80^{Lo}) b) and live and dead bacteria among GBP2-negative/-positive *Salmonella* in resident macrophages

2.5 Phenotypic Variation of *Salmonella* in Host Tissues Delays Eradication by Antimicrobial Chemotherapy

Beatrice Claudi[1, 5], Petra Spröte[1, 4, 5], Anna Chirkova[1, 5], Nicolas Personnic[1, 5], Janine Zankl[2], **Nura Schürmann[1]**, Alexander Schmidt[3], Dirk Bumann[1*]

[1] Focal Area Infection Biology, Biozentrum, University of Basel, 4056 Basel, Switzerland

[2] FACS Core Facility, Biozentrum, University of Basel, 4056 Basel, Switzerland

[3] Proteomics Core Facility, Biozentrum, University of Basel, 4056 Basel, Switzerland

[4] BASF SE, 67056 Ludwigshafen, Germany

[5] These authors contributed equally to this work

* Corresponding author

The manuscript was published in Cell Volume 158, Issue 4, 14 August 2014, Pages 722-733

doi:10.1016/j.cell.2014.06.045

Statement of my work:

Design of experiments

Immunohistochemistry and analysis of Timer^{bac} *Salmonella* in infected spleen (Figure S3)

Revision of manuscript with all authors

The following parts contain only the abstract and the figures to which I contributed. The contribution of my work showed that TIMER^{bac} *Salmonella* showed divergent colors in confocal microscopy. *Salmonella* within the same infected host cell had similar colors whereas neighboring infected cells often contained *Salmonella* with different colors (Figure S3A), suggesting a potential impact of individual host cells rather than regional factors. *Salmonella* colors did not correlate with *Salmonella* load or host cell type (Figures S3B, C).

Phenotypic Variation of *Salmonella* in Host Tissues Delays Eradication by Antimicrobial Chemotherapy

Beatrice Claudi[1, 5], Petra Spröte[1, 4, 5], Anna Chirkova[1, 5], Nicolas Personnic[1, 5], Janine Zankl[2], Nura Schürmann[1], Alexander Schmidt[3], Dirk Bumann[1*]

Summary

Antibiotic therapy often fails to eliminate a fraction of transiently refractory bacteria, causing relapses and chronic infections. Multiple mechanisms can induce such persisters with high antimicrobial tolerance *in vitro*, but their *in vivo* relevance remains unclear. Using a fluorescent growth rate reporter, we detected extensive phenotypic variation of *Salmonella* in host tissues. This included slow-growing subsets as well as well-nourished fast-growing subsets driving disease progression. Monitoring of *Salmonella* growth and survival during chemotherapy revealed that antibiotic killing correlated with single-cell division rates. Nondividing *Salmonella* survived best but were rare, limiting their impact. Instead, most survivors originated from abundant moderately growing, partially tolerant *Salmonella*. These data demonstrate that host tissues diversify pathogen physiology, with major consequences for disease progression and control.

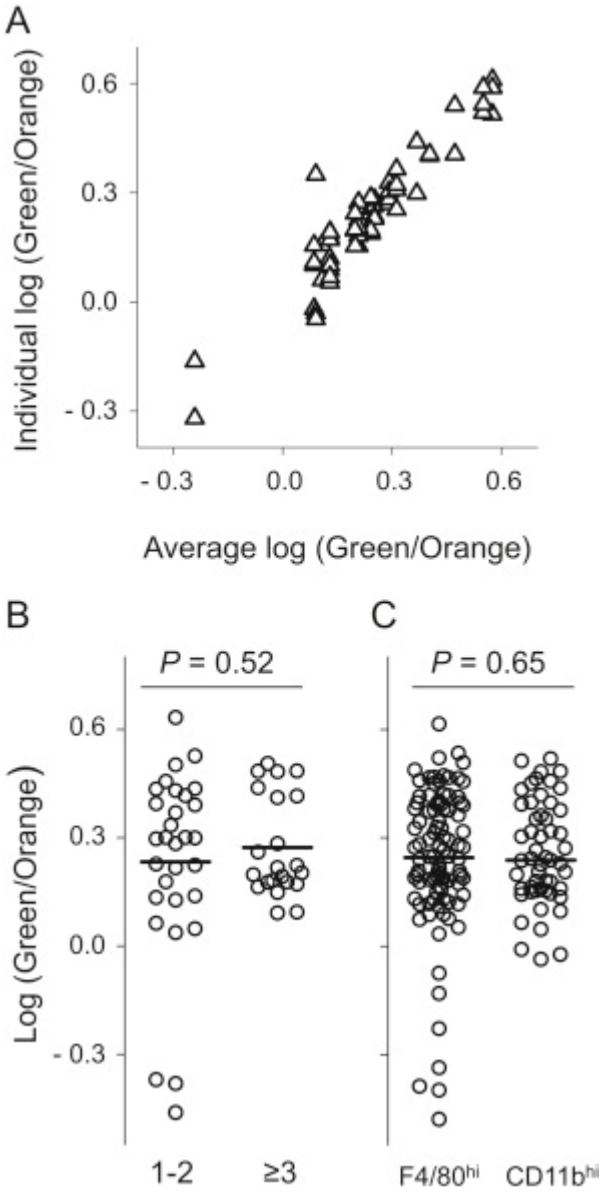

Figure S3 Confocal Microscopy of TIMER^{bac}-*Salmonella*-Infected Spleen

A) Analysis of *Salmonella* colors in single infected host phagocytes. Green/orange ratios of individual *Salmonella* are compared with averages colors of all *Salmonella* in the same cell. Most *Salmonella* had individual colors close to the average for the respective phagocyte.

B) *Salmonella* green/orange ratios in infected cells containing 1-2, or more *Salmonella*.

C) *Salmonella* green/orange ratios in infected F4/80^{hi} resident macrophages and CD11b^{hi} infiltrating host cells.

3 Discussion

An infectious disease is the battle between the immune system of the host and the invading pathogen. The immune system is armed with weapons to eradicate the pathogen, such as phagocytic immune cells and microbicidal molecules, whereas the pathogen has developed counterattack or evading systems. This battle takes place in host tissues with complex anatomy and heterogeneous microenvironments. However, tissue complexity has been largely ignored in infection research. Recently, several studies using fluorescent reporters, in situ RNA hybridization and advanced imaging techniques showed remarkable host-pathogen heterogeneity in the tuberculosis model. But functional consequences are difficult to study in *Mycobacterium tuberculosis*. In comparison, the murine typhoid fever model is more accessible. Nonetheless, methods which determine individual *Salmonella*-host encounters *in vivo* are still largely lacking. In this work the combination of fluorescent *Salmonella* biosensors with high-resolution confocal imaging was used to reveal the unique fate of *Salmonella* in specific host environments. We showed that the immediate host environment in which *Salmonella* resides is decisive for pathogen survival or death. Overall, our data indicate that the sum of many different individual host-pathogen interactions determines disease outcome.

3.1 Alteration of infected host environments

Salmonella growth in spleen leads to drastic changes of the host environment arising from the influx of immune cells and the development of pathological lesions. We confirmed that lesions consist of an inner core of neutrophils and an outer core of monocytes [7], both of which produce large amounts of ROS and RNS. Lesion formation was well studied in correlation to *Salmonella* growth (see section 1.2.2 and [7, 30]). These studies suggested that inflammatory lesions are heterogeneous, and different individual immune control mechanisms may act at each lesion. However, experimental evidence has been lacking.

In this work, we analyzed the temporal and spatial relationship between developing lesions, RNS, ROS, and lipids in infected spleen. Specifically, the spatial development of lesions in correlation to iNOS, a marker for nitric oxide stress that is mainly expressed by inflammatory monocytes, and lipidtox, a marker for neutral lipids, was shown over a time course of a 5 day infection. Lipid droplets are also a hallmark of immune activation, but neither the leukocyte subpopulations that accumulate them *in vivo*, nor the spatial relationship to lesions was known. We showed that lipids accumulate mainly in inflammatory monocytes and neutrophils. At day 2 of infection, lesions started to appear,

which correlated with expression of iNOS and lipidtox staining. With an increase in *Salmonella* burden, lesions grew in number (as reported previously [7]) and size, in addition to exhibiting increased amounts of iNOS and neutral lipids. However, *Salmonella* localization did not correlate with nitric oxide and lipids. Interestingly, nitric oxide and lipid expression were not always confined to lesions, but rather heterogeneously distributed within and around lesions. Some advanced (older) lesions did not show nitric oxide or lipid expression at all. In addition, we also showed heterogeneous expression of reactive oxygen stress markers (4-HNE for lipid peroxidation and 8-OHdG for DNA damage) at day 4 of *Salmonella* infection. Location of *Salmonella* also did not correlate with diverse ROS markers. In uninfected spleen, no expression of ROS, RNS or lipids were detected. These data indicated that heterogeneity between lesions included differential expression of ROS, RNS and lipids. Why some lesions produced more lipids, ROS and RNS than others is not completely understood. One explanation could be the different developmental stages of lesions. Large lesions, for example, which often do not express ROS or RNS could have successfully cleared *Salmonella*, similar to sterile granuloma in tuberculosis [187]. However, it is not known why these lesions prevail over a longer time, even though the pathogen has been eradicated. Overall, our data showed that appearance of ROS, RNS and lipids correlated with *Salmonella* growth temporally, but not spatially.

3.2 Distribution of *Salmonella* in host environments

The distribution of *Salmonella* in diverse host compartments was studied mainly by microscopy and flow cytometry. In spleen, *Salmonella* resides in the red pulp and in the marginal zone [97, 102]. Our data confirmed that *Salmonella* resides in the red pulp, but only rarely in the marginal zone. However, we studied mainly day 4 or day 5 after intravenous infection, and *Salmonella* could reside in the marginal zone after oral infection and/or an earlier time point of infection. In the red pulp and the marginal zone *Salmonella* is able to reside in diverse cell types [97-100], nonetheless, there is contradictory evidence as to which environment or cell types are able to promote *Salmonella* replication. Some studies have suggested that *Salmonella* mainly resides and replicates in red pulp macrophages in agreement with our data [97, 102]. One study showed that *Salmonella* may establish a chronic infection via replication in M2 macrophages [103]. We could not locate any *Salmonella* in M2 macrophages (data not shown), however, we only studied early acute *Salmonella* infection, and cannot exclude the possibility that M2 macrophages may become important at a later stage of infection. Some published data even suggested that *Salmonella* replicates in neutrophils [104]. According to our data the majority of live *Salmonella* resides in resident macrophages, and a minority in neutrophils and inflammatory monocytes.

Overall, the cell types in which *Salmonella* predominantly resides and replicates *in vivo* is still controversial. This might be due to experimental conditions, such as different amounts of inoculum, infection route, length of infection, different cell markers, and the inherent difference between the analyzing techniques (flow cytometry vs. microscopy).

3.3 Disparate *Salmonella*-host cell encounters

A method to systematically analyze the fate of *Salmonella* in different cell types *in vivo* was lacking. We developed a method, which allows distinguishing different *Salmonella* populations *in vivo* (live, low ROS/RNS-stressed; live, ROS-stressed; live RNS-stressed; live ROS/RNS-stressed; live, fast growing; live, slow growing; and killed) using high-resolution microscopy and flow cytometry.

We applied fluorescent *Salmonella* reporters to determine in which host environments *Salmonella* experience oxidative or nitrosative stress. To monitor oxidative stress we used *Salmonella* carrying an episomal *katGp-gfpOVA* fusion, which is controlled by the transcription factor OxyR. In comparison to previously used *ahpCp* [120] this promoter has low baseline activity and a large dynamic range. In addition, the unstable GFP variant GFP_*OVA* [152] reports only current promoter activities. To monitor nitrosative stress, we used *Salmonella* carrying an episomal *hmpAp-gfpOVA* fusion, which is repressed by NsrR. In the presence of nitric oxide (NO) NsrR is inactivated and *hmpA* is expressed.

To assess *Salmonella* growth heterogeneity, we constructed a *Salmonella* growth reporter, called TIMER^{bac}. The branched maturation of TIMER protein results in different green/orange fluorescence ratios depending on division rate.

To distinguish live and dead bacteria, we infected mice with *Salmonella* strains which constitutively express fluorescent proteins and counterstained spleen sections with an antibody against *Salmonella* LPS (lipopolysaccharide) or CSA (common *Salmonella* antigen). Viable *Salmonella* are positive for both the fluorescent protein and LPS/CSA, while dead bacteria lose fluorescence and remain only LPS/CSA positive. To our knowledge, our data showed for the first time the spatial distribution of live and dead *Salmonella* in diverse host microenvironments in infected spleen. Nonetheless, there are some methodological limitations, which include lack of temporal resolution and substantial work load. In comparison to flow cytometry, where millions of bacteria can be analyzed in one day, microscopy analysis includes tedious counting of individual bacteria, with a limitation of a few hundred bacteria per microscopy section. So far, we also do not know how long bacterial envelopes are preserved and remain stainable by an anti-LPS antibody. However, the method enables localization of at least recent killing.

Our single cell analysis revealed that a large fraction of *Salmonella* is killed in inflammatory lesions (neutrophils surrounded by monocytes). It was initially quite surprising, that *Salmonella* were killed even at later stages of infection, although *Salmonella* replicate in spleen with a net growth of around one log per day. Mastroeni and colleagues suggested that *Salmonella* killing only happens during an early time point of infection [35]. They concluded that the lack of disappearing tagged *Salmonella* strains (WITS) suggests very low bacterial killing at later stages. However, their method can only estimate bacterial killing if one strain disappears, and not if individual bacteria are killed and thus provides reliable data only for early stages of infection where *Salmonella* loads are still low. In comparison to their approach, we can distinguish individual bacterial killing using our method. Our data showed that the majority of live *Salmonella* resides in resident macrophages, whereas neutrophils and monocytes efficiently kill *Salmonella*. In conclusion, our single-cell analyses revealed detailed information on location and dissemination of live and dead *Salmonella* in spleen, which could not be revealed with earlier methods. The following section will discuss in more detail the diverse *Salmonella*-host cell encounters.

1.) Neutrophil/*Salmonella* encounters

Neutrophils are potent antimicrobial phagocytic cells, which use oxidative and non-oxidative mechanisms to kill pathogens. The oxidative arm uses NADPH oxidase and myeloperoxidase (MPO) to produce large amounts of ROS, which are lethal for a majority of pathogens (see section 1.2.3). NADPH oxidase is important for *Salmonella* control *in vitro* and *in vivo* [106, 108]. We confirmed that $Cybb^{-/-}$ mice, deficient in an essential subunit of NADPH oxidase, are highly susceptible to salmonellosis. However, it remained unclear if this was due to a direct bactericidal effect of ROS [39, 78]. One report even suggested that ROS levels *in vivo* are too low to have a direct impact on wild-type *Salmonella* [120]. In addition, ROS can act as signaling molecules that regulate innate immune functions [108].

Our single-cell analysis revealed that neutrophil NADPH oxidase kills *Salmonella* efficiently with bactericidal ROS. Neutrophils deficient in NAPDH oxidase were significantly impaired in *Salmonella* clearance *in vivo* compared to WT neutrophils. Nonetheless, our data indicated that a certain subpopulation was killed independently of NADPH oxidase. Non-oxidative mechanisms might play a role [238], but were not investigated here. Although neutrophils were very effective in *Salmonella* killing, some *Salmonella* survived inside neutrophils. Overall, our data is consistent with a strong but incomplete control of salmonellosis by neutrophils [7, 183, 239].

The second key enzyme in the neutrophil oxidative burst is myeloperoxidase (MPO). However, the role of MPO in a typhoid fever model has not been studied before. MPO converts diffusible ROS, such as hydrogen peroxide to highly bactericidal hypohalides [45]. These hypohalides, specifically hypochlorite, efficiently kill various microbes in cell culture. Nonetheless, the role of MPO for host defense is controversial, because humans deficient in MPO have mostly minor phenotypes [45]. We combined computational modeling with *in vitro* and *in vivo* data to elucidate the role of MPO in *Salmonella* infection.

Our data revealed that MPO colocalized mainly to surfaces of dead *Salmonella in vivo*, suggesting a contribution of hypochlorite in *Salmonella* killing. However, MPO deficient mice had only slightly elevated *Salmonella* loads compared to congenic WT mice, indicating alternative killing mechanisms. Winterbourn and coworkers predicted that hydrogen peroxide increases to about 30 µM in neutrophil phagosomes in absence of MPO, which they considered inadequate for killing [44]. We combined their computational model with expression data of *Salmonella* ROS defense enzymes [146]. Our model predicted cytosolic H_2O_2 levels of around 15 µM in *Salmonella,* far above the lethality threshold of 2 µM [240]. These data are similar to lethality of moderate continuous H_2O_2 levels in *E.coli* [149]. In conclusion, our model predicted that *Salmonella* are either killed with MPO derived hypochloride or with high concentrations of H_2O_2 in absence of MPO. However, we asked why MPO is produced in daily amounts of hundreds of milligrams [45], if it is mainly unnecessary for killing.

To answer this question, we extended our computational model with the complex redox chemistry of MPO. This model predicted a constant decline of HOCl yield and an increase of H_2O_2 leakage with decreasing MPO content. The concentrations of H_2O_2 in absence of MPO were predicted to be too high for the buffering capacity of the cell, resulting in extracellular H_2O_2 leakage. In comparison to our model, Winterbourn and coworkers suggested that H_2O_2 leakage would be scavenged by neutrophil redox protection mechanisms such as glutathione peroxidase [44], because earlier studies using MPO deficient neutrophils did not reveal increased accumulation of hydrogen peroxide compared to WT neutrophils [217]. However, these data only recorded early time points, where oxidative bursts were just starting.

We confirmed our modeling predictions with *in vitro* experiments of human neutrophils and *in vivo* experiments of infected mice. Finally, we showed that MPO deficient mice infected with *Salmonella* had elevated hydrogen peroxide tissue levels, which ultimately induced oxidative damage of host lipids and DNA. Overall, we showed that the MPO catalyzed reaction of diffusible hydrogen peroxide to highly reactive HOCl potentiates antimicrobial attack to pathogens, while minimizing ROS reach

and collateral tissue damage. In conclusion, we discovered a previously unrecognized self-protective role of MPO in *Salmonella* infection.

2.) Inflammatory monocyte/*Salmonella* encounters

The role of inflammatory monocytes in infection is less well studied than the role of neutrophils. Inflammatory monocytes are recruited to *Salmonella* infectious foci and form a ring structure around neutrophils. Monocytes and neutrophils cooperate and stimulate each other, enhancing their antimicrobial activity [29]. Stimulated inflammatory monocytes express high amounts of iNOS, which produce high amounts of reactive nitrogen species and could potentially control *Salmonella* replication. Yet, the role of iNOS in *Salmonella* infection has remained unclear. In cell culture iNOS inhibits growth of surviving *Salmonella* 5 h after infection [106]. However, mice deficient in iNOS can handle *Salmonella* infection equally well to WT mice until day 5 of infection [108], in spite of bacteriostatic effects in cell culture.

Our single cell analysis revealed that iNOS is expressed in specific infected tissue regions, which expose *Salmonella* to various amounts of RNS. Interestingly, live *Salmonella* resided both inside and outside of iNOS-expressing regions, suggesting efficient RNS detoxification mechanisms. However, the majority of *Salmonella* within inflammatory monocytes were dead. Inflammatory monocytes also produce substantial amounts of NADPH oxidase and intermediate amounts of MPO, which killed *Salmonella* mainly with ROS, similar to neutrophils. These data suggested that *Salmonella* exposure to RNS in monocytes played negligible roles in killing.

3.) Macrophage/*Salmonella* encounters

Resident red pulp macrophages are a primary niche for *Salmonella* replication, as previously reported [97, 102]. However, there is contradictory evidence regarding whether macrophages play a role in *Salmonella* killing. Specifically the role of NADPH oxidase in macrophages has remained controversial. On the one hand, cell culture studies showed that macrophages kill *Salmonella* efficiently with NADPH oxidase [106]. On the other hand, *Salmonella* can inhibit assembly of NADPH oxidase using its SPI-2 T3SS [117, 118]. One critical aspect to examine is the cell types used for cell culture infections. Peritoneal elicited macrophages, which produce high amounts of ROS [106] do not resemble resident red pulp macrophages with moderate oxidative bursts. Moreover, data obtained from cell culture studies lack important features of the immune system *in vivo*. Our data showed that resident red pulp macrophages impose only sub-lethal transient oxidative bursts on *Salmonella*, but killed *Salmonella* through NADPH oxidase independent mechanism (discussed below).

To determine the location and amount of *Salmonella* that experience ROS, we used a *Salmonella* biosensor, which indicates ROS (specifically H_2O_2) exposure by GFP expression (see above). Our data revealed that *Salmonella* experienced heterogeneous ROS exposure, with a small subpopulation of GFP^{bright} *Salmonella* (high H_2O_2 exposure). GFP^{bright} *Salmonella* resided in all host cell types, but were absent in $Cybb^{-/-}$ (NADPH oxidase deficient) mice indicating a specific response to ROS generated by NADPH oxidase. In comparison to WT mice, $MPO^{-/-}$ mice contained a larger proportion of GFP^{bright} *Salmonella* suggesting increased exposure to H_2O_2. It was initially surprising to observe these additional GFP^{bright} *Salmonella* in $MPO^{-/-}$ mice predominantly in resident macrophages, although MPO is only expressed in neutrophils and monocytes. However, neutrophils and monocytes efficiently kill most intracellular *Salmonella* and destroy their fluorescent proteins (GFP and mCherry), making biosensor activities undetectable. Our data suggested that H_2O_2 from neutrophils and monocytes diffused to neighboring macrophages, where *Salmonella* were exposed to increased H_2O_2 levels. These results in combination with the computational model suggested that *Salmonella* can efficiently detoxify sublethal concentrations of ROS in resident macrophages both in WT and MPO deficient mice. The *in silico* model predicted that periplasmic SodCI was the only *Salmonella* defense enzyme that had an impact on ROS defense, which is in full agreement with previously published experimental data [110, 112]. Two recent studies suggested additional ROS defense enzymes, which helped *Salmonella* to partially survive in neutrophils. *Salmonella* expressing an ABC importer specific for D-alanine limit exposure to oxidative damage elicited by D-amino acid oxidase (DAO). DAO apparently generates H_2O_2 independent of NADPH oxidase [241]. However, our data showed that in absence of NADPH oxidase *Salmonella* do not experience any detectable H_2O_2 stress. The second study reports that *Salmonella* express a methionine sulfoxide reductase which repairs HOCl mediated damage, but phenotypes are only observed if additional factors are missing [242]. In addition, *in vivo* data for the second study are lacking. Further studies might clarify if these defense enzymes play a role *in vivo*.

In addition to ROS exposure, *Salmonella* were exposed to various amounts of RNS, including nitric oxide, which are primarily produced by inflammatory monocytes. Nitric oxide can diffuse freely through cellular membranes [164] and reach *Salmonella* in neighboring macrophages. A nitric oxide specific *Salmonella* biosensor revealed that *Salmonella* indeed experienced heterogeneous amounts of nitric oxide. However, *Salmonella* can detoxify even high levels of RNS. A mutant lacking 22 genes involved in RNS repair/defense had only a slight virulence effect, suggesting that toxic effects occur only when several RNS defense systems are dysfunctional. These data are in agreement with a minor role for RNS in early *Salmonella* infection [108]. Nevertheless, it is still unclear how RNS can control *Salmonella* at later stages of infection. To test if RNS may have more profound effects in resistant

mice, as previously suggested [243], we infected genetically resistant 129/SV mice with *Salmonella*. However, our data suggested similar heterogeneous and sublethal RNS stress for *Salmonella* during early infection in both susceptible and resistant mice. Future studies need to investigate the role of RNS at later stages of *Salmonella* infection.

Moreover, we constructed a dual ROS/RNS biosensor to monitor if *Salmonella* experienced synergistic or separate ROS and RNS stresses. Our data showed that the majority of *Salmonella* experienced either ROS or RNS stresses. However, highly toxic ROS/RNS reaction products, such as peroxynitrite could have killed *Salmonella,* preventing their detection with FACS. But such synergistic ROS and RNS likely played a minor role, because iNOS has little impact on early *Salmonella* infection.

In addition to expression of detoxification or virulence proteins to survive inside host cells, some bacteria can slow down their metabolic activity and escape transient stress. To address this issue in our *in vivo* model, we measured *Salmonella* growth heterogeneity using TIMER^{bac} *Salmonella* (see above). This biosensor allows distinguishing fast vs. slow growing bacteria. Our data revealed extensive growth heterogeneity in infected spleen. *Salmonella* within the same infected cell had similar colors, whereas neighboring cells often contained *Salmonella* with different colors. Interestingly, *Salmonella* growth rate did not correlate with *Salmonella* load or host cell type. These data suggest a potential impact of the individual host cell, rather than cell specific features or regional factors.

Although *Salmonella* is quite efficient to detoxify major stresses in macrophages, we showed that a certain subpopulation of bacteria is killed with non-oxidative mechanisms. Interestingly, *Salmonella* killing in macrophages was almost abolished in mice treated with a neutralizing antibody to interferon gamma (IFNγ). IFNγ is a cytokine which plays a crucial role in early *Salmonella* growth control [244, 245]. Moreover, treatment of chronically-infected mice with neutralizing anti-IFNγ antibodies causes relapse into acute infection [246]. IFNγ strongly induces several antimicrobial defenses, particularly autophagy, RNS and antimicrobial GTPases such as guanylate binding protein (GBP) family members [86]. Meunier and coworkers showed that GBPs have an essential role in cell autonomous immunity, and are required for the activation of the non-canonical inflammasome pathway [247]. As a part of their study, we investigated the role of GBPs in infected mouse spleen. We showed that GBP2 specifically colocalized to dead *Salmonella* and that the absolute amount of GBPs colocalizing to *Salmonella* was lower in mice, which were treated with an IFNγ neutralizing antibody. In addition, we showed that GBPs are mainly expressed in resident red pulp macrophages. Overall, our data indicated that GBPs correlated with non-oxidative killing in macrophages. However, whether GBPs themselves are responsible for killing needs to be elucidated. In addition to GBPs

several other non-oxidative killing mechanisms may play a role. Recently, the specific pore-forming protein Perforin-2 was shown to control systemic dissemination of *Salmonella* Typhimurium in mice [67]. Except for the case of Perforin-2, *in vivo* evidence has been scarce (see section 1.2.3). Non-oxidative killing mechanisms may act synergistically or redundantly, impairing analysis with single knock-out mice. Future studies using advanced techniques like CRISPR-Cas9 may elucidate the concerted action of non-oxidative killing mechanisms.

Overall, we showed that *Salmonella* is exposed to different stresses in macrophages (ROS, RNS, GBPs). Although a certain subpopulation is killed with non-oxidative IFNγ dependent mechanisms, a large amount of *Salmonella* can survive inside macrophages and detoxify moderate amounts of ROS and high amounts of RNS. In addition, we showed that *Salmonella* grow heterogeneously in macrophages; however, the underlying factors still need to be elucidated.

3.4 Effects of *Salmonella*-host encounters on disease progression

Salmonella proliferate primarily by escaping from lesions and spreading to form new infection foci [7]. We demonstrated that *Salmonella* is effectively cleared in most lesions in neutrophils and inflammatory monocytes, although *Salmonella* possess elaborate defense mechanisms against host attacks. However, some *Salmonella* disseminate and replicate in resident red pulp macrophages, which can only partially control *Salmonella*. The race between *Salmonella* dissemination and counteraction of the immune system thus determines the overall course of disease [6]. More specifically, disease progression does not depend on a general incapability of host control, but on individual local failures. This becomes specifically important in antimicrobial treatment. Antibiotic therapy often fails to eliminate a certain subpopulation of bacteria, which causes relapses and chronic infections [248]. Heterogeneous host microenvironments could lead to inhomogeneous drug distribution because of variable penetration of antibiotic into infection foci and local differences in pH and protein binding [249]. In addition, heterogeneous pathogen growth rates can have a major impact on drug sensitivity. Nonetheless, the extent of pathogen variation on treatment efficacy was still unclear [248]. We showed that during antibiotic therapy *Salmonella* with moderate growth rates survived best. In contrast to our work, Helaine and coworkers reported that mainly non-growing *Salmonella* in mouse organs persisted over several days of infection [250]. However, they used different experimental conditions, such as early onset and high doses of antibiotics and stationary phase *Salmonella* to inoculate, which may explain the different outcomes. Nonetheless, both studies showed a major impact of pathogen heterogeneity on antibiotic treatment success. Specific targeting of antimicrobial survivors could accelerate therapy and help to avoid relapses.

3.5 Conclusion & Outlook

Together, our results revealed remarkable diverse *Salmonella*-host encounters with implications for disease progression. We showed that *Salmonella* is heterogeneously distributed in spleen. It is exposed to diverse host microenvironments, such as inflammatory lesions, which produce large amounts of ROS, RNS, and lipids; and non-inflammatory tissue regions with low amounts of these species. Depending on the respective host environment *Salmonella* replicates, survives or is killed. Neutrophils and inflammatory monocytes kill *Salmonella* mainly with NADPH oxidase and MPO dependent mechanisms. To confine the oxidative attack to *Salmonella* and to protect host environments, MPO converts diffusible hydrogen peroxide to ROS within short reach. Inflammatory monocytes express high amounts of iNOS to produce RNS. However, RNS play a negligible role for *Salmonella* killing in early *Salmonella* infection.

In resident red pulp macrophages *Salmonella* is able to survive and replicate. The moderate oxidative burst of resident macrophages does not kill *Salmonella*, because *Salmonella* efficiently detoxifies ROS and RNS. However, a certain subpopulation of *Salmonella* dies even in red pulp macrophages. We showed that resident red pulp macrophages kill mainly through IFNγ-dependent mechanisms associated with GBPs.

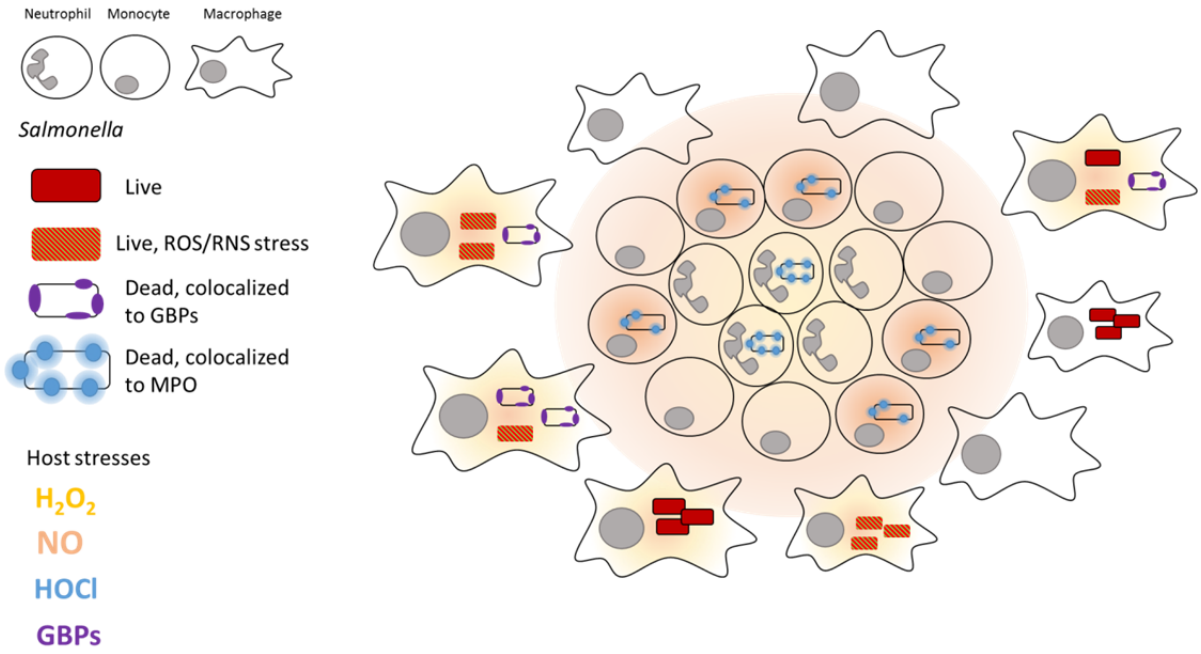

Figure 5 Diverse *Salmonella*-host cell encounters in WT mice

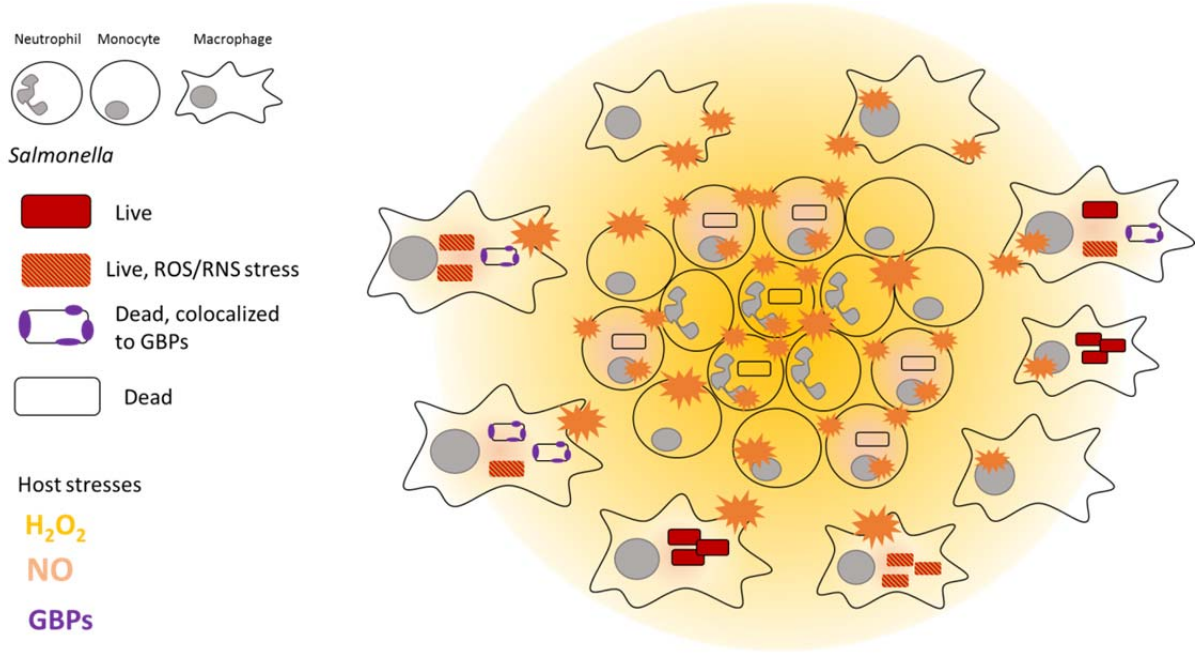

Figure 6 Diverse *Salmonella*-host cell encounters in MPO deficient mice

In conclusion, we demonstrated that individual *Salmonella*-host encounters have divergent outcomes (see Figure 5 and Figure 6). As a result, disease progression is not the consequence of a weak immune system as such, but rather the failure to control individual local encounters. Moreover, pre-existing *Salmonella* subsets impede antibiotic therapy. Thus, specific encounters make the difference between disease progression and disease control.

Additional studies may reveal how some *Salmonella* can survive in neutrophils and monocytes, and how resident macrophages kill *Salmonella* through additional NADPH oxidase independent mechanisms. Moreover, additional host factors such as pH, low oxygen, nutrient access and adaptive immune cells may also have an impact on the fate of *Salmonella*.

To identify infected host environments we have used immunohistochemistry and confocal microscopy on tissue cryosections. However, this yields only limited 3D data, based on restricted z-range. In addition, fluorescence bleaching becomes problematic with oversampling and high resolution confocal microscopy. Further methods, which are currently established in our lab, enable multi-scale 3D analysis of host microenvironments. Serial 2-photon tomography provides 3D fluorescence images of spleen at sub-micron resolution. The second method is serial block-face scanning electron microscopy to obtain ultrastructural data of tissue volumes of up to 1 mm^3. However, these techniques generate large amounts of data, which are challenging to analyze. In the future, automatic imaging analyses of these advanced techniques will help to capture the multi-scale complexity of heterogeneous host-pathogen interactions.

4 References

1. **Lozano, R., et al., *Global and regional mortality from 235 causes of death for 20 age groups in 1990 and 2010: a systematic analysis for the Global Burden of Disease Study 2010.* Lancet, 2012. 380(9859): p. 2095-128.**
2. **Spellberg, B., et al., *Trends in antimicrobial drug development: implications for the future.* Clinical infectious diseases : an official publication of the Infectious Diseases Society of America, 2004. 38(9): p. 1279-86.**
3. **Norrby, S.R., C.E. Nord, and R. Finch, *Lack of development of new antimicrobial drugs: a potential serious threat to public health.* The Lancet. Infectious diseases, 2005. 5(2): p. 115-9.**
4. **Zinkernagel, R.M. and H. Hengartner, *On immunity against infections and vaccines: credo 2004.* Scandinavian journal of immunology, 2004. 60(1-2): p. 9-13.**
5. **Kaufmann, S.H., *The contribution of immunology to the rational design of novel antibacterial vaccines.* Nature reviews. Microbiology, 2007. 5(7): p. 491-504.**
6. **Bumann, D., *Heterogeneous host-pathogen encounters: act locally, think globally.* Cell host & microbe, 2015. 17(1): p. 13-9.**
7. **Sheppard, M., et al., *Dynamics of bacterial growth and distribution within the liver during Salmonella infection.* Cellular microbiology, 2003. 5(9): p. 593-600.**
8. **Barry, C.E., 3rd, et al., *The spectrum of latent tuberculosis: rethinking the biology and intervention strategies.* Nature reviews. Microbiology, 2009. 7(12): p. 845-55.**
9. **Tan, S., et al., *Mycobacterium tuberculosis responds to chloride and pH as synergistic cues to the immune status of its host cell.* PLoS pathogens, 2013. 9(4): p. e1003282.**
10. **Muller, A.J., et al., *Photoconvertible pathogen labeling reveals nitric oxide control of Leishmania major infection in vivo via dampening of parasite metabolism.* Cell host & microbe, 2013. 14(4): p. 460-7.**
11. **Fenhalls, G., et al., *In situ detection of Mycobacterium tuberculosis transcripts in human lung granulomas reveals differential gene expression in necrotic lesions.* Infection and immunity, 2002. 70(11): p. 6330-8.**
12. **Ryan, G.J., et al., *Multiple M. tuberculosis phenotypes in mouse and guinea pig lung tissue revealed by a dual-staining approach.* PloS one, 2010. 5(6): p. e11108.**
13. **Crump, J.A. and E.D. Mintz, *Global trends in typhoid and paratyphoid Fever.* Clinical infectious diseases : an official publication of the Infectious Diseases Society of America, 2010. 50(2): p. 241-6.**
14. **Vidal, S., P. Gros, and E. Skamene, *Natural resistance to infection with intracellular parasites: molecular genetics identifies Nramp1 as the Bcg/Ity/Lsh locus.* Journal of leukocyte biology, 1995. 58(4): p. 382-90.**
15. **Santos, R.L., et al., *Animal models of Salmonella infections: enteritis versus typhoid fever.* Microbes and infection / Institut Pasteur, 2001. 3(14-15): p. 1335-44.**
16. **Vazquez-Torres, A., et al., *Extraintestinal dissemination of Salmonella by CD18-expressing phagocytes.* Nature, 1999. 401(6755): p. 804-8.**
17. **Lim, C.H., et al., *Independent bottlenecks characterize colonization of systemic compartments and gut lymphoid tissue by salmonella.* PLoS pathogens, 2014. 10(7): p. e1004270.**
18. **Coburn, B., G.A. Grassl, and B.B. Finlay, *Salmonella, the host and disease: a brief review.* Immunology and cell biology, 2007. 85(2): p. 112-8.**
19. **Haraga, A., M.B. Ohlson, and S.I. Miller, *Salmonellae interplay with host cells.* Nature reviews. Microbiology, 2008. 6(1): p. 53-66.**

20. **Watson, K.G. and D.W. Holden, *Dynamics of growth and dissemination of Salmonella in vivo.* Cellular microbiology, 2010. 12(10): p. 1389-97.**
21. **Hormaeche, C.E., *The in vivo division and death rates of Salmonella typhimurium in the spleens of naturally resistant and susceptible mice measured by the superinfecting phage technique of Meynell.* Immunology, 1980. 41(4): p. 973-9.**
22. **Mebius, R.E. and G. Kraal, *Structure and function of the spleen.* Nature reviews. Immunology, 2005. 5(8): p. 606-16.**
23. **Cesta, M.F., *Normal structure, function, and histology of the spleen.* Toxicologic pathology, 2006. 34(5): p. 455-65.**
24. **Geijtenbeek, T.B., et al., *Marginal zone macrophages express a murine homologue of DC-SIGN that captures blood-borne antigens in vivo.* Blood, 2002. 100(8): p. 2908-16.**
25. **Oehen, S., et al., *Marginal zone macrophages and immune responses against viruses.* Journal of immunology, 2002. 169(3): p. 1453-8.**
26. **Swirski, F.K., et al., *Identification of splenic reservoir monocytes and their deployment to inflammatory sites.* Science, 2009. 325(5940): p. 612-6.**
27. **Hormaeche, C.E., et al., *T cells do not mediate the initial suppression of a Salmonella infection in the RES.* Immunology, 1990. 70(2): p. 247-50.**
28. **Richter-Dahlfors, A., A.M. Buchan, and B.B. Finlay, *Murine salmonellosis studied by confocal microscopy: Salmonella typhimurium resides intracellularly inside macrophages and exerts a cytotoxic effect on phagocytes in vivo.* The Journal of Experimental Medicine, 1997. 186(4): p. 569-80.**
29. **Silva, M.T., *Macrophage phagocytosis of neutrophils at inflammatory/infectious foci: a cooperative mechanism in the control of infection and infectious inflammation.* Journal of leukocyte biology, 2011. 89(5): p. 675-83.**
30. **Mastroeni, P., et al., *A dynamic view of the spread and intracellular distribution of Salmonella enterica.* Nature reviews. Microbiology, 2009. 7(1): p. 73-80.**
31. **Grant, A.J., et al., *Bacterial growth rate and host factors as determinants of intracellular bacterial distributions in systemic Salmonella enterica infections.* Infection and immunity, 2009. 77(12): p. 5608-11.**
32. **Maw, J. and G.G. Meynell, *The true division and death rates of Salmonella typhimurium in the mouse spleen determined with superinfecting phage P22.* British journal of experimental pathology, 1968. 49(6): p. 597-613.**
33. **Hormaeche, C.E., R.A. Pettifor, and J. Brock, *The fate of temperature-sensitive salmonella mutants in vivo in naturally resistant and susceptible mice.* Immunology, 1981. 42(4): p. 569-76.**
34. **Benjamin, W.H., Jr., et al., *The primary effect of the Ity locus is on the rate of growth of Salmonella typhimurium that are relatively protected from killing.* Journal of immunology, 1990. 144(8): p. 3143-51.**
35. **Grant, A.J., et al., *Modelling within-host spatiotemporal dynamics of invasive bacterial disease.* PLoS Biol, 2008. 6(4): p. e74.**
36. **Helaine, S., et al., *Dynamics of intracellular bacterial replication at the single cell level.* Proc Natl Acad Sci U S A, 2010. 107(8): p. 3746-51.**
37. **Munday, M.C., *Absence of Neutrophils.* British medical journal, 1964. 2(5414): p. 892.**
38. **Hurst, J.K., *What really happens in the neutrophil phagosome?* Free radical biology & medicine, 2012. 53(3): p. 508-20.**
39. **Slauch, J.M., *How does the oxidative burst of macrophages kill bacteria? Still an open question.* Molecular microbiology, 2011. 80(3): p. 580-3.**
40. **Nauseef, W.M., *Assembly of the phagocyte NADPH oxidase.* Histochemistry and cell biology, 2004. 122(4): p. 277-91.**
41. **Cech, P. and R.I. Lehrer, *Phagolysosomal pH of human neutrophils.* Blood, 1984. 63(1): p. 88-95.**

42. **van Dalen, C.J., et al., *Thiocyanate and chloride as competing substrates for myeloperoxidase.* The Biochemical journal, 1997. 327 (Pt 2): p. 487-92.**

43. **Harrison, J.E. and J. Schultz, *Studies on the chlorinating activity of myeloperoxidase.* The Journal of biological chemistry, 1976. 251(5): p. 1371-4.**

44. **Winterbourn, C.C., et al., *Modeling the reactions of superoxide and myeloperoxidase in the neutrophil phagosome: implications for microbial killing.* The Journal of biological chemistry, 2006. 281(52): p. 39860-9.**

45. **Klebanoff, S.J., et al., *Myeloperoxidase: a front-line defender against phagocytosed microorganisms.* Journal of leukocyte biology, 2013. 93(2): p. 185-98.**

46. **Green, J.N., A.J. Kettle, and C.C. Winterbourn, *Protein chlorination in neutrophil phagosomes and correlation with bacterial killing.* Free radical biology & medicine, 2014. 77: p. 49-56.**

47. **Rosen, H., et al., *Methionine oxidation contributes to bacterial killing by the myeloperoxidase system of neutrophils.* Proceedings of the National Academy of Sciences of the United States of America, 2009. 106(44): p. 18686-91.**

48. **Wang, J. and A. Slungaard, *Role of eosinophil peroxidase in host defense and disease pathology.* Archives of biochemistry and biophysics, 2006. 445(2): p. 256-60.**

49. **Nauseef, W.M., *Myeloperoxidase in human neutrophil host defence.* Cellular microbiology, 2014. 16(8): p. 1146-55.**

50. **Goldblatt, D. and A.J. Thrasher, *Chronic granulomatous disease.* Clinical and experimental immunology, 2000. 122(1): p. 1-9.**

51. **Assari, T., *Chronic Granulomatous Disease; fundamental stages in our understanding of CGD.* Medical immunology, 2006. 5: p. 4.**

52. **Johnston, R.B., Jr. and R.L. Baehner, *Improvement of leukocyte bactericidal activity in chronic granulomatous disease.* Blood, 1970. 35(3): p. 350-5.**

53. **Kutter, D., *Prevalence of myeloperoxidase deficiency: population studies using Bayer-Technicon automated hematology.* Journal of molecular medicine, 1998. 76(10): p. 669-75.**

54. **Kitahara, M., et al., *Hereditary myeloperoxidase deficiency.* Blood, 1981. 57(5): p. 888-93.**

55. **Marchetti, C., et al., *Genetic studies on myeloperoxidase deficiency in Italy.* Japanese journal of infectious diseases, 2004. 57(5): p. S10-2.**

56. **Cech, P., et al., *Hereditary myeloperoxidase deficiency.* Blood, 1979. 53(3): p. 403-11.**

57. **Lehrer, R.I. and M.J. Cline, *Leukocyte myeloperoxidase deficiency and disseminated candidiasis: the role of myeloperoxidase in resistance to Candida infection.* The Journal of clinical investigation, 1969. 48(8): p. 1478-88.**

58. **Keyer, K., A.S. Gort, and J.A. Imlay, *Superoxide and the production of oxidative DNA damage.* Journal of bacteriology, 1995. 177(23): p. 6782-90.**

59. **Hogg, N., et al., *Production of hydroxyl radicals from the simultaneous generation of superoxide and nitric oxide.* The Biochemical journal, 1992. 281 (Pt 2): p. 419-24.**

60. **Pham, C.T., *Neutrophil serine proteases: specific regulators of inflammation.* Nature reviews. Immunology, 2006. 6(7): p. 541-50.**

61. **Flannagan, R.S., G. Cosio, and S. Grinstein, *Antimicrobial mechanisms of phagocytes and bacterial evasion strategies.* Nature reviews. Microbiology, 2009. 7(5): p. 355-66.**

62. **Flannagan, R.S., V. Jaumouille, and S. Grinstein, *The cell biology of phagocytosis.* Annual review of pathology, 2012. 7: p. 61-98.**

63. **Elsbach, P., et al., *The bactericidal/permeability increasing protein of neutrophils is a potent antibacterial and anti-endotoxin agent in vitro and in vivo.* Progress in clinical and biological research, 1994. 388: p. 41-51.**

64. **Lennartsson, A., et al., *A murine antibacterial ortholog to human bactericidal/permeability-increasing protein (BPI) is expressed in testis, epididymis, and bone marrow.* Journal of leukocyte biology, 2005. 77(3): p. 369-77.**

65. **Wittmann, I., et al., *Murine bactericidal/permeability-increasing protein inhibits the endotoxic activity of lipopolysaccharide and gram-negative bacteria.* Journal of immunology, 2008. 180(11): p. 7546-52.**
66. **McCormack, R., et al., *Inhibition of intracellular bacterial replication in fibroblasts is dependent on the perforin-like protein (perforin-2) encoded by macrophage-expressed gene 1.* Journal of innate immunity, 2013. 5(2): p. 185-94.**
67. **McCormack, R.M., et al., *Perforin-2 is essential for intracellular defense of parenchymal cells and phagocytes against pathogenic bacteria.* eLife, 2015. 4.**
68. **Weinrauch, Y., et al., *Neutrophil elastase targets virulence factors of enterobacteria.* Nature, 2002. 417(6884): p. 91-4.**
69. **Mallen-St Clair, J., et al., *Mast cell dipeptidyl peptidase I mediates survival from sepsis.* The Journal of clinical investigation, 2004. 113(4): p. 628-34.**
70. **Sutherland, R.E., et al., *Dipeptidyl peptidase I controls survival from Klebsiella pneumoniae lung infection by processing surfactant protein D.* Biochemical and biophysical research communications, 2014. 450(1): p. 818-23.**
71. **Liu, W., et al., *Olfactomedin 4 inhibits cathepsin C-mediated protease activities, thereby modulating neutrophil killing of Staphylococcus aureus and Escherichia coli in mice.* Journal of immunology, 2012. 189(5): p. 2460-7.**
72. **Pham, C.T., et al., *Papillon-Lefevre syndrome: correlating the molecular, cellular, and clinical consequences of cathepsin C/dipeptidyl peptidase I deficiency in humans.* Journal of immunology, 2004. 173(12): p. 7277-81.**
73. **Hirche, T.O., et al., *Myeloperoxidase plays critical roles in killing Klebsiella pneumoniae and inactivating neutrophil elastase: effects on host defense.* Journal of immunology, 2005. 174(3): p. 1557-65.**
74. **Vethanayagam, R.R., et al., *Role of NADPH oxidase versus neutrophil proteases in antimicrobial host defense.* PloS one, 2011. 6(12): p. e28149.**
75. **Vissers, M.C. and C.C. Winterbourn, *Oxidative damage to fibronectin. I. The effects of the neutrophil myeloperoxidase system and HOCl.* Archives of biochemistry and biophysics, 1991. 285(1): p. 53-9.**
76. **Femling, J.K., W.M. Nauseef, and J.P. Weiss, *Synergy between extracellular group IIA phospholipase A2 and phagocyte NADPH oxidase in digestion of phospholipids of Staphylococcus aureus ingested by human neutrophils.* Journal of immunology, 2005. 175(7): p. 4653-61.**
77. **Reeves, E.P., et al., *Killing activity of neutrophils is mediated through activation of proteases by K+ flux.* Nature, 2002. 416(6878): p. 291-7.**
78. **Fang, F.C., *Antimicrobial actions of reactive oxygen species.* mBio, 2011. 2(5).**
79. **Amulic, B., et al., *Neutrophil function: from mechanisms to disease.* Annual review of immunology, 2012. 30: p. 459-89.**
80. **Murray, P.J. and T.A. Wynn, *Protective and pathogenic functions of macrophage subsets.* Nature reviews. Immunology, 2011. 11(11): p. 723-37.**
81. **Price, J.V. and R.E. Vance, *The macrophage paradox.* Immunity, 2014. 41(5): p. 685-93.**
82. **Davies, L.C., et al., *Tissue-resident macrophages.* Nature immunology, 2013. 14(10): p. 986-95.**
83. **den Haan, J.M. and G. Kraal, *Innate Immune Functions of Macrophage Subpopulations in the Spleen.* Journal of innate immunity, 2012.**
84. **Hashimoto, D., et al., *Tissue-resident macrophages self-maintain locally throughout adult life with minimal contribution from circulating monocytes.* Immunity, 2013. 38(4): p. 792-804.**
85. **Volkman, A. and J.L. Gowans, *The Origin of Macrophages from Bone Marrow in the Rat.* British journal of experimental pathology, 1965. 46: p. 62-70.**

86. **Kim, B.H., et al., *IFN-inducible GTPases in host cell defense.* Cell host & microbe, 2012. 12(4): p. 432-44.**
87. **Nordenfelt, P. and H. Tapper, *Phagosome dynamics during phagocytosis by neutrophils.* Journal of leukocyte biology, 2011. 90(2): p. 271-84.**
88. **Reeves, E.P., et al., *Reassessment of the microbicidal activity of reactive oxygen species and hypochlorous acid with reference to the phagocytic vacuole of the neutrophil granulocyte.* Journal of medical microbiology, 2003. 52(Pt 8): p. 643-51.**
89. **Schneider, B., R. Gross, and A. Haas, *Phagosome acidification has opposite effects on intracellular survival of Bordetella pertussis and B. bronchiseptica.* Infection and immunity, 2000. 68(12): p. 7039-48.**
90. **Rathman, M., M.D. Sjaastad, and S. Falkow, *Acidification of phagosomes containing Salmonella typhimurium in murine macrophages.* Infection and immunity, 1996. 64(7): p. 2765-73.**
91. **Randow, F. and R.J. Youle, *Self and nonself: how autophagy targets mitochondria and bacteria.* Cell host & microbe, 2014. 15(4): p. 403-11.**
92. **Chow, A., B.D. Brown, and M. Merad, *Studying the mononuclear phagocyte system in the molecular age.* Nature reviews. Immunology, 2011. 11(11): p. 788-98.**
93. **Banchereau, J. and R.M. Steinman, *Dendritic cells and the control of immunity.* Nature, 1998. 392(6673): p. 245-52.**
94. **Epelman, S., K.J. Lavine, and G.J. Randolph, *Origin and functions of tissue macrophages.* Immunity, 2014. 41(1): p. 21-35.**
95. **Mosser, D.M. and J.P. Edwards, *Exploring the full spectrum of macrophage activation.* Nature reviews. Immunology, 2008. 8(12): p. 958-69.**
96. **Xue, J., et al., *Transcriptome-based network analysis reveals a spectrum model of human macrophage activation.* Immunity, 2014. 40(2): p. 274-88.**
97. **Nix, R.N., et al., *Hemophagocytic macrophages harbor Salmonella enterica during persistent infection.* PLoS Pathogens, 2007. 3(12): p. e193.**
98. **Yrlid, U., et al., *In vivo activation of dendritic cells and T cells during Salmonella enterica serovar Typhimurium infection.* Infection and immunity, 2001. 69(9): p. 5726-35.**
99. **Tam, M.A., et al., *Early cellular responses to Salmonella infection: dendritic cells, monocytes, and more.* Immunological reviews, 2008. 225: p. 140-62.**
100. **Rosales-Reyes, R., et al., *Survival of Salmonella enterica serovar Typhimurium within late endosomal-lysosomal compartments of B lymphocytes is associated with the inability to use the vacuolar alternative major histocompatibility complex class I antigen-processing pathway.* Infection and immunity, 2005. 73(7): p. 3937-44.**
101. **Rosche, K.L., et al., *Infection with Salmonella enterica Serovar Typhimurium Leads to Increased Proportions of F4/80+ Red Pulp Macrophages and Decreased Proportions of B and T Lymphocytes in the Spleen.* PloS one, 2015. 10(6): p. e0130092.**
102. **Salcedo, S.P., et al., *Intracellular replication of Salmonella typhimurium strains in specific subsets of splenic macrophages in vivo.* Cellular microbiology, 2001. 3(9): p. 587-97.**
103. **Eisele, N.A., et al., *Salmonella require the fatty acid regulator PPARdelta for the establishment of a metabolic environment essential for long-term persistence.* Cell host & microbe, 2013. 14(2): p. 171-82.**
104. **Geddes, K., F. Cruz, and F. Heffron, *Analysis of cells targeted by Salmonella type III secretion in vivo.* PLoS pathogens, 2007. 3(12): p. e196.**
105. **Kirby, A.C., et al., *Differential involvement of dendritic cell subsets during acute Salmonella infection.* Journal of immunology, 2001. 166(11): p. 6802-11.**
106. **Vazquez-Torres, A., et al., *Antimicrobial Actions of the Nadph Phagocyte Oxidase and Inducible Nitric Oxide Synthase in Experimental Salmonellosis. I. Effects on Microbial Killing by Activated Peritoneal Macrophages in Vitro.* The Journal of Experimental Medicine, 2000. 192(2): p. 227-236.**

107. **Rydstrom, A. and M.J. Wick, *Monocyte and neutrophil recruitment during oral Salmonella infection is driven by MyD88-derived chemokines.* Eur J Immunol, 2009. 39(11): p. 3019-30.**

108. **Mastroeni, P., et al., *Antimicrobial actions of the NADPH phagocyte oxidase and inducible nitric oxide synthase in experimental salmonellosis. II. Effects on microbial proliferation and host survival in vivo.* The Journal of Experimental Medicine, 2000. 192(2): p. 237-48.**

109. **Fang, F.C., et al., *Virulent Salmonella typhimurium has two periplasmic Cu, Zn-superoxide dismutases.* Proceedings of the National Academy of Sciences of the United States of America, 1999. 96(13): p. 7502-7.**

110. **De Groote, M.A., et al., *Periplasmic superoxide dismutase protects Salmonella from products of phagocyte NADPH-oxidase and nitric oxide synthase.* Proc.Natl.Acad.Sci.U.S.A, 1997. 94(25): p. 13997-14001.**

111. **Hebrard, M., et al., *Redundant hydrogen peroxide scavengers contribute to Salmonella virulence and oxidative stress resistance.* Journal of bacteriology, 2009. 191(14): p. 4605-14.**

112. **Craig, M. and J.M. Slauch, *Phagocytic superoxide specifically damages an extracytoplasmic target to inhibit or kill Salmonella.* PLoS One, 2009. 4(3): p. e4975.**

113. **Suvarnapunya, A.E., H.A. Lagasse, and M.A. Stein, *The role of DNA base excision repair in the pathogenesis of Salmonella enterica serovar Typhimurium.* Molecular microbiology, 2003. 48(2): p. 549-59.**

114. **Pacello, F., et al., *Periplasmic Cu,Zn superoxide dismutase and cytoplasmic Dps concur in protecting Salmonella enterica serovar Typhimurium from extracellular reactive oxygen species.* Biochimica et biophysica acta, 2008. 1780(2): p. 226-32.**

115. **Velayudhan, J., et al., *The role of ferritins in the physiology of Salmonella enterica sv. Typhimurium: a unique role for ferritin B in iron-sulphur cluster repair and virulence.* Molecular microbiology, 2007. 63(5): p. 1495-507.**

116. **Gallois, A., et al., *Salmonella pathogenicity island 2-encoded type III secretion system mediates exclusion of NADPH oxidase assembly from the phagosomal membrane.* Journal of immunology, 2001. 166(9): p. 5741-8.**

117. **Vazquez-Torres, A., et al., *Salmonella pathogenicity island 2-dependent evasion of the phagocyte NADPH oxidase.* Science, 2000. 287(5458): p. 1655-8.**

118. **Chakravortty, D., I. Hansen-Wester, and M. Hensel, *Salmonella pathogenicity island 2 mediates protection of intracellular Salmonella from reactive nitrogen intermediates.* The Journal of Experimental Medicine, 2002. 195(9): p. 1155-66.**

119. **van der Heijden, J., et al., *Direct measurement of oxidative and nitrosative stress dynamics in Salmonella inside macrophages.* Proceedings of the National Academy of Sciences of the United States of America, 2015. 112(2): p. 560-5.**

120. **Aussel, L., et al., *Salmonella detoxifying enzymes are sufficient to cope with the host oxidative burst.* Molecular microbiology, 2011. 80(3): p. 628-40.**

121. **Suvarnapunya, A.E. and M.A. Stein, *DNA base excision repair potentiates the protective effect of Salmonella Pathogenicity Island 2 within macrophages.* Microbiology, 2005. 151(Pt 2): p. 557-67.**

122. **Grant, A.J., et al., *Attenuated Salmonella Typhimurium lacking the pathogenicity island-2 type 3 secretion system grow to high bacterial numbers inside phagocytes in mice.* PLoS pathogens, 2012. 8(12): p. e1003070.**

123. **Alpuche Aranda, C.M., et al., *Salmonella typhimurium activates virulence gene transcription within acidified macrophage phagosomes.* Proceedings of the National Academy of Sciences of the United States of America, 1992. 89(21): p. 10079-83.**

124. **Miller, S.I., A.M. Kukral, and J.J. Mekalanos, *A two-component regulatory system (phoP phoQ) controls Salmonella typhimurium virulence.* Proceedings of the National Academy of Sciences of the United States of America, 1989. 86(13): p. 5054-8.**

125. **Bader, M.W., et al., *Regulation of Salmonella typhimurium virulence gene expression by cationic antimicrobial peptides.* Molecular microbiology, 2003. 50(1): p. 219-30.**
126. **LaRock, D.L., A. Chaudhary, and S.I. Miller, *Salmonellae interactions with host processes.* Nature reviews. Microbiology, 2015. 13(4): p. 191-205.**
127. **Avraham, R., et al., *Pathogen Cell-to-Cell Variability Drives Heterogeneity in Host Immune Responses.* Cell, 2015. 162(6): p. 1309-21.**
128. **Nathan, C. and M.U. Shiloh, *Reactive oxygen and nitrogen intermediates in the relationship between mammalian hosts and microbial pathogens.* Proc Natl Acad Sci U S A, 2000. 97(16): p. 8841-8.**
129. **Fang, F.C., *Antimicrobial reactive oxygen and nitrogen species: concepts and controversies.* Nat Rev Microbiol, 2004. 2(10): p. 820-32.**
130. **Hurst, J.K., *What really happens in the neutrophil phagosome?* Free Radic Biol Med, 2012. 53(3): p. 508-20.**
131. **Fang, F.C., *Antimicrobial actions of reactive oxygen species.* MBio, 2011. 2(5): p. 00141-11.**
132. **Slauch, J.M., *How does the oxidative burst of macrophages kill bacteria? Still an open question.* Mol Microbiol, 2011. 80(3): p. 580-3.**
133. **Liu, P.T. and R.L. Modlin, *Human macrophage host defense against Mycobacterium tuberculosis.* Curr Opin Immunol, 2008. 20(4): p. 371-6.**
134. **Horta, M.F., et al., *Reactive oxygen species and nitric oxide in cutaneous leishmaniasis.* J Parasitol Res, 2012. 2012: p. 203818.**
135. **Richter-Dahlfors, A., A.M. Buchan, and B.B. Finlay, *Murine salmonellosis studied by confocal microscopy: Salmonella typhimurium resides intracellularly inside macrophages and exerts a cytotoxic effect on phagocytes in vivo.* J.Exp.Med., 1997. 186(4): p. 569-580.**
136. **Rydstrom, A. and M.J. Wick, *Monocyte recruitment, activation, and function in the gut-associated lymphoid tissue during oral Salmonella infection.* J.Immunol., 2007. 178(9): p. 5789-5801.**
137. **Barat, S., et al., *Immunity to Intracellular Salmonella Depends on Surface-associated Antigens.* PLoS Pathog, 2012. 8(10): p. e1002966.**
138. **Muotiala, A., *Anti-IFN-gamma-treated mice--a model for testing safety of live Salmonella vaccines.* Vaccine, 1992. 10(4): p. 243-6.**
139. **Vancott, J.L., et al., *Regulation of host immune responses by modification of Salmonella virulence genes.* Nat.Med, 1998. 4(11): p. 1247-1252.**
140. **Gulig, P.A., et al., *Systemic infection of mice by wild-type but not Spv- Salmonella typhimurium is enhanced by neutralization of gamma interferon and tumor necrosis factor alpha.* Infect Immun, 1997. 65(12): p. 5191-7.**
141. **Vazquez-Torres, A., et al., *Antimicrobial actions of the NADPH phagocyte oxidase and inducible nitric oxide synthase in experimental salmonellosis. I. Effects on microbial killing by activated peritoneal macrophages in vitro.* J Exp Med, 2000. 192(2): p. 227-36.**
142. **Mastroeni, P., et al., *Antimicrobial actions of the NADPH phagocyte oxidase and inducible nitric oxide synthase in experimental salmonellosis. II. Effects on microbial proliferation and host survival in vivo.* J.Exp.Med., 2000. 192(2): p. 237-248.**
143. **Swirski, F.K., et al., *Myeloperoxidase-rich Ly-6C+ myeloid cells infiltrate allografts and contribute to an imaging signature of organ rejection in mice.* J Clin Invest, 2010. 120(7): p. 2627-34.**
144. **Klebanoff, S.J., et al., *Myeloperoxidase: a front-line defender against phagocytosed microorganisms.* J Leukoc Biol, 2013. 93(2): p. 185-98.**
145. **Winterbourn, C.C., et al., *Modeling the reactions of superoxide and myeloperoxidase in the neutrophil phagosome: implications for microbial killing.* J Biol Chem, 2006. 281(52): p. 39860-9.**
146. **Steeb, B., et al., *Parallel exploitation of diverse host nutrients enhances salmonella virulence.* PLoS Pathog, 2013. 9(4): p. e1003301.**

147. **Korshunov, S.S. and J.A. Imlay, *A potential role for periplasmic superoxide dismutase in blocking the penetration of external superoxide into the cytosol of Gram-negative bacteria.* Mol Microbiol, 2002. 43(1): p. 95-106.**
148. **Seaver, L.C. and J.A. Imlay, *Hydrogen peroxide fluxes and compartmentalization inside growing Escherichia coli.* J Bacteriol, 2001. 183(24): p. 7182-9.**
149. **Park, S., X. You, and J.A. Imlay, *Substantial DNA damage from submicromolar intracellular hydrogen peroxide detected in Hpx- mutants of Escherichia coli.* Proc Natl Acad Sci U S A, 2005. 102(26): p. 9317-22.**
150. **Dubbs, J.M. and S. Mongkolsuk, *Peroxide-sensing transcriptional regulators in bacteria.* J Bacteriol, 2012. 194(20): p. 5495-503.**
151. **Aussel, L., et al., *Salmonella detoxifying enzymes are sufficient to cope with the host oxidative burst.* Mol Microbiol, 2011. 2011(1): p. 1365-2958.**
152. **Rollenhagen, C., et al., *Antigen selection based on expression levels during infection facilitates vaccine development for an intracellular pathogen.* Proc Natl Acad Sci U S A, 2004. 101(23): p. 8739-8744.**
153. **VanderVen, B.C., R.M. Yates, and D.G. Russell, *Intraphagosomal measurement of the magnitude and duration of the oxidative burst.* Traffic, 2009. 10(4): p. 372-8.**
154. **Imlay, J.A., *Oxidative Stress*, in *EcoSal*, R.I.K. Curtiss, J.B.; Squires, C.L.; Karp, P.D.; Neidhardt, F.C.; Slauch, J.M., Editor 2009, ASM Press: Washington, DC.**
155. **Nusrat, A.R., et al., *Properties of isolated red pulp macrophages from mouse spleen.* J Exp Med, 1988. 168(4): p. 1505-10.**
156. **Gort, A.S. and J.A. Imlay, *Balance between endogenous superoxide stress and antioxidant defenses.* J Bacteriol, 1998. 180(6): p. 1402-10.**
157. **Uzzau, S., L. Bossi, and N. Figueroa-Bossi, *Differential accumulation of Salmonella[Cu, Zn] superoxide dismutases SodCI and SodCII in intracellular bacteria: correlation with their relative contribution to pathogenicity.* Mol.Microbiol., 2002. 46(1): p. 147-156.**
158. **Pacelli, R., et al., *Nitric oxide potentiates hydrogen peroxide-induced killing of Escherichia coli.* The Journal of experimental medicine, 1995. 182(5): p. 1469-1479.**
159. **Khan, S.A., et al., *Early responses to Salmonella typhimurium infection in mice occur at focal lesions in infected organs.* Microbial pathogenesis, 2001. 30(1): p. 29-38.**
160. **Umezawa, K., et al., *Induction of nitric oxide synthesis and xanthine oxidase and their roles in the antimicrobial mechanism against Salmonella typhimurium infection in mice.* Infection and immunity, 1997. 65(7): p. 2932-40.**
161. **Tucker, N.P., et al., *The transcriptional repressor protein NsrR senses nitric oxide directly via a [2Fe-2S] cluster.* PloS one, 2008. 3(11): p. e3623.**
162. **Bang, I.S., et al., *Maintenance of nitric oxide and redox homeostasis by the salmonella flavohemoglobin hmp.* The Journal of biological chemistry, 2006. 281(38): p. 28039-47.**
163. **Gilberthorpe, N.J. and R.K. Poole, *Nitric oxide homeostasis in Salmonella typhimurium: roles of respiratory nitrate reductase and flavohemoglobin.* The Journal of biological chemistry, 2008. 283(17): p. 11146-54.**
164. **Pacher, P., J.S. Beckman, and L. Liaudet, *Nitric oxide and peroxynitrite in health and disease.* Physiological reviews, 2007. 87(1): p. 315-424.**
165. **Leone, A.M., et al., *Visualisation of nitric oxide generated by activated murine macrophages.* Biochemical and biophysical research communications, 1996. 221(1): p. 37-41.**
166. **Hausladen, A., A. Gow, and J.S. Stamler, *Flavohemoglobin denitrosylase catalyzes the reaction of a nitroxyl equivalent with molecular oxygen.* Proc Natl Acad Sci U S A, 2001. 98(18): p. 10108-12.**
167. **Justino, M.C., et al., *Escherichia coli di-iron YtfE protein is necessary for the repair of stress-damaged iron-sulfur clusters.* The Journal of biological chemistry, 2007. 282(14): p. 10352-9.**

168. **Wolfe, M.T., et al., *Hydroxylamine reductase activity of the hybrid cluster protein from Escherichia coli.* Journal of bacteriology, 2002. 184(21): p. 5898-902.**
169. **Kim, C.C., D. Monack, and S. Falkow, *Modulation of virulence by two acidified nitrite-responsive loci of Salmonella enterica serovar Typhimurium.* Infect.Immun., 2003. 71(6): p. 3196-3205.**
170. **Gilberthorpe, N.J., et al., *NsrR: a key regulator circumventing Salmonella enterica serovar Typhimurium oxidative and nitrosative stress in vitro and in IFN-gamma-stimulated J774.2 macrophages.* Microbiology, 2007. 153(Pt 6): p. 1756-71.**
171. **Richardson, A.R., et al., *Multiple targets of nitric oxide in the tricarboxylic acid cycle of Salmonella enterica serovar typhimurium.* Cell host & microbe, 2011. 10(1): p. 33-43.**
172. **Tan, S., et al., *Mycobacterium tuberculosis Responds to Chloride and pH as Synergistic Cues to the Immune Status of its Host Cell.* PLoS Pathog, 2013. 9(4): p. e1003282.**
173. **Gardner, A.M., R.A. Helmick, and P.R. Gardner, *Flavorubredoxin, an inducible catalyst for nitric oxide reduction and detoxification in Escherichia coli.* The Journal of biological chemistry, 2002. 277(10): p. 8172-7.**
174. **Mills, P.C., et al., *A combination of cytochrome c nitrite reductase (NrfA) and flavorubredoxin (NorV) protects Salmonella enterica serovar Typhimurium against killing by NO in anoxic environments.* Microbiology, 2008. 154(Pt 4): p. 1218-28.**
175. **Spiro, S., *Nitric oxide-sensing mechanisms in Escherichia coli.* Biochemical Society transactions, 2006. 34(Pt 1): p. 200-2.**
176. **Bower, J.M. and M.A. Mulvey, *Polyamine-mediated resistance of uropathogenic Escherichia coli to nitrosative stress.* Journal of bacteriology, 2006. 188(3): p. 928-33.**
177. **Henard, C.A. and A. Vazquez-Torres, *Nitric oxide and salmonella pathogenesis.* Front Microbiol, 2011. 2(84): p. 84.**
178. **White, J.K., et al., *Slc11a1-mediated resistance to Salmonella enterica serovar Typhimurium and Leishmania donovani infections does not require functional inducible nitric oxide synthase or phagocyte oxidase activity.* J Leukoc Biol, 2005. 77(3): p. 311-20.**
179. **Lin, F.R., et al., *Electron microscopic studies on the location of bacterial proliferation in the liver in murine salmonellosis.* Br J Exp Pathol, 1987. 68(4): p. 539-50.**
180. **Benjamin, W.H., Jr., et al., *The primary effect of the Ity locus is on the rate of growth of Salmonella typhimurium that are relatively protected from killing.* J Immunol., 1990. 144(8): p. 3143-3151.**
181. **Miao, E.A., et al., *Caspase-1-induced pyroptosis is an innate immune effector mechanism against intracellular bacteria.* Nat Immunol, 2010. 11(12): p. 1136-42.**
182. **Broz, P., et al., *Caspase-11 increases susceptibility to Salmonella infection in the absence of caspase-1.* Nature, 2012. 490(7419): p. 288-91.**
183. **Daley, J.M., et al., *Use of Ly6G-specific monoclonal antibody to deplete neutrophils in mice.* J Leukoc Biol, 2008. 83(1): p. 64-70.**
184. **Vassiloyanakopoulos, A.P., S. Okamoto, and J. Fierer, *The crucial role of polymorphonuclear leukocytes in resistance to Salmonella dublin infections in genetically susceptible and resistant mice.* Proc Natl Acad Sci U S A, 1998. 95(13): p. 7676-81.**
185. **Conlan, J.W., *Critical roles of neutrophils in host defense against experimental systemic infections of mice by Listeria monocytogenes, Salmonella typhimurium, and Yersinia enterocolitica.* Infect Immun, 1997. 65(2): p. 630-5.**
186. **Sheppard, M., et al., *Dynamics of bacterial growth and distribution within the liver during Salmonella infection.* Cell Microbiol., 2003. 5(9): p. 593-600.**
187. **Ramakrishnan, L., *Revisiting the role of the granuloma in tuberculosis.* Nat Rev Immunol, 2012. 12(5): p. 352-66.**
188. **Dickinson, B.C., C. Huynh, and C.J. Chang, *A palette of fluorescent probes with varying emission colors for imaging hydrogen peroxide signaling in living cells.* J Am Chem Soc, 2010. 132(16): p. 5906-15.**

189. **Li, X.J., et al., *A fluorescently tagged C-terminal fragment of p47phox detects NADPH oxidase dynamics during phagocytosis.* Mol Biol Cell, 2009. 20(5): p. 1520-32.**
190. **Diard, M., et al., *Stabilization of cooperative virulence by the expression of an avirulent phenotype.* Nature, 2013. 494(7437): p. 353-6.**
191. **Cummings, L.A., et al., *In vivo, fliC expression by Salmonella enterica serovar Typhimurium is heterogeneous, regulated by ClpX, and anatomically restricted.* Mol.Microbiol., 2006. 61(3): p. 795-809.**
192. **Ackermann, M., et al., *Self-destructive cooperation mediated by phenotypic noise.* Nature, 2008. 454(7207): p. 987-90.**
193. **Yang, C.T., et al., *Neutrophils exert protection in the early tuberculous granuloma by oxidative killing of mycobacteria phagocytosed from infected macrophages.* Cell Host Microbe, 2012. 12(3): p. 301-12.**
194. **Ugel, S., et al., *Immune tolerance to tumor antigens occurs in a specialized environment of the spleen.* Cell Rep, 2012. 2(3): p. 628-39.**
195. **Becker, D., et al., *Robust Salmonella metabolism limits possibilities for new antimicrobials.* Nature., 2006. 440(7082): p. 303-307.**
196. **Hoiseth, S.K. and B.A. Stocker, *Aromatic-dependent Salmonella typhimurium are non-virulent and effective as live vaccines.* Nature, 1981. 291(5812): p. 238-9.**
197. **Kroger, C., et al., *The transcriptional landscape and small RNAs of Salmonella enterica serovar Typhimurium.* Proc Natl Acad Sci U S A, 2012. 109(20): p. E1277-86.**
198. **Bumann, D. and R.H. Valdivia, *Identification of host-induced pathogen genes by differential fluorescence induction reporter systems.* Nature protocols, 2007. 2(4): p. 770-7.**
199. **Zaslaver, A., et al., *A comprehensive library of fluorescent transcriptional reporters for Escherichia coli.* Nature methods, 2006. 3(8): p. 623-8.**
200. **Datsenko, K.A. and B.L. Wanner, *One-step inactivation of chromosomal genes in Escherichia coli K-12 using PCR products.* Proceedings of the National Academy of Sciences of the United States of America, 2000. 97(12): p. 6640-5.**
201. **Rollenhagen, C., et al., *Antigen selection based on expression levels during infection facilitates vaccine development for an intracellular pathogen.* Proceedings of the National Academy of Sciences of the United States of America, 2004. 101(23): p. 8739-44.**
202. **Neidhardt, F.C., P.L. Bloch, and D.F. Smith, *Culture medium for enterobacteria.* Journal of bacteriology, 1974. 119(3): p. 736-47.**
203. **Beuzon, C.R. and D.W. Holden, *Use of mixed infections with Salmonella strains to study virulence genes and their interactions in vivo.* Microbes and infection / Institut Pasteur, 2001. 3(14-15): p. 1345-52.**
204. **Stroppolo, M.E., et al., *Single mutation at the intersubunit interface confers extra efficiency to Cu,Zn superoxide dismutase.* FEBS Lett, 2000. 483(1): p. 17-20.**
205. **Bull, C. and J.A. Fee, *Steady-state kinetic studies of superoxide dismutases: properties of the iron containing protein from Escherichia coli.* Journal of the American Chemical Society, 1985. 107(11): p. 3295-3304.**
206. **Meir, E. and E. Yagil, *Further characterization of the two catalases inEscherichia coli.* Current Microbiology, 1985. 12(6): p. 315-319.**
207. **Baker, L.M. and L.B. Poole, *Catalytic mechanism of thiol peroxidase from Escherichia coli. Sulfenic acid formation and overoxidation of essential CYS61.* J Biol Chem, 2003. 278(11): p. 9203-11.**
208. **Poole, L.B., *Bacterial defenses against oxidants: mechanistic features of cysteine-based peroxidases and their flavoprotein reductases.* Arch Biochem Biophys, 2005. 433(1): p. 240-54.**
209. **Behar, D., et al., *Acid dissociation constant and decay kinetics of the perhydroxyl radical.* The Journal of Physical Chemistry, 1970. 74(17): p. 3209-3213.**

210. **Aurudi, R.L.R., A.B., *Reactivity of HO_2/O^{-2} radicals in aqueous solution.* J Phys Chem Ref Data, 1985. 14: p. 1041–1100.**

211. **Seaver, L.C. and J.A. Imlay, *Are respiratory enzymes the primary sources of intracellular hydrogen peroxide?* J Biol Chem, 2004. 279(47): p. 48742-50.**

212. **Bradley, P.P., et al., *Measurement of cutaneous inflammation: estimation of neutrophil content with an enzyme marker.* The Journal of investigative dermatology, 1982. 78(3): p. 206-9.**

213. **Storkey, C., M.J. Davies, and D.I. Pattison, *Reevaluation of the rate constants for the reaction of hypochlorous acid (HOCl) with cysteine, methionine, and peptide derivatives using a new competition kinetic approach.* Free radical biology & medicine, 2014. 73: p. 60-6.**

214. **Podrez, E.A., H.M. Abu-Soud, and S.L. Hazen, *Myeloperoxidase-generated oxidants and atherosclerosis.* Free radical biology & medicine, 2000. 28(12): p. 1717-25.**

215. **Imlay, J.A., *The molecular mechanisms and physiological consequences of oxidative stress: lessons from a model bacterium.* Nature reviews. Microbiology, 2013. 11(7): p. 443-54.**

216. **Burton, N.A., et al., *Disparate impact of oxidative host defenses determines the fate of Salmonella during systemic infection in mice.* Cell host & microbe, 2014. 15(1): p. 72-83.**

217. **Nauseef, W.M., J.A. Metcalf, and R.K. Root, *Role of myeloperoxidase in the respiratory burst of human neutrophils.* Blood, 1983. 61(3): p. 483-92.**

218. **Gerber, C.E., et al., *Phagocytic activity and oxidative burst of granulocytes in persons with myeloperoxidase deficiency.* European journal of clinical chemistry and clinical biochemistry : journal of the Forum of European Clinical Chemistry Societies, 1996. 34(11): p. 901-8.**

219. **Gross, S., et al., *Bioluminescence imaging of myeloperoxidase activity in vivo.* Nature medicine, 2009. 15(4): p. 455-61.**

220. **Kettle, A.J., et al., *Inhibition of myeloperoxidase by benzoic acid hydrazides.* The Biochemical journal, 1995. 308 (Pt 2): p. 559-63.**

221. **Tsolis, R.M., et al., *How to become a top model: The impact of animal experimentation on human Salmonella disease research.* Infect Immun, 2011. 79: p. 1806-1814.**

222. **Lee, C., et al., *Redox regulation of OxyR requires specific disulfide bond formation involving a rapid kinetic reaction path.* Nature structural & molecular biology, 2004. 11(12): p. 1179-85.**

223. **Swirski, F.K., et al., *Myeloperoxidase-rich Ly-6C+ myeloid cells infiltrate allografts and contribute to an imaging signature of organ rejection in mice.* The Journal of clinical investigation, 2010. 120(7): p. 2627-34.**

224. **Liou, G.Y. and P. Storz, *Detecting reactive oxygen species by immunohistochemistry.* Methods in molecular biology, 2015. 1292: p. 97-104.**

225. **Seki, S., et al., *In situ detection of lipid peroxidation and oxidative DNA damage in non-alcoholic fatty liver diseases.* Journal of hepatology, 2002. 37(1): p. 56-62.**

226. **Loft, S. and H.E. Poulsen, *Cancer risk and oxidative DNA damage in man.* Journal of molecular medicine, 1996. 74(6): p. 297-312.**

227. **Finkel, T. and N.J. Holbrook, *Oxidants, oxidative stress and the biology of ageing.* Nature, 2000. 408(6809): p. 239-47.**

228. **Crimmins, E.M. and C.E. Finch, *Infection, inflammation, height, and longevity.* Proceedings of the National Academy of Sciences of the United States of America, 2006. 103(2): p. 498-503.**

229. **Hoiseth, S.K. and B.A. Stocker, *Aromatic-dependent Salmonella typhimurium are non-virulent and effective as live vaccines.* Nature, 1981. 291(5812): p. 238-239.**

230. **Hjorth, R., A.K. Jonsson, and P. Vretblad, *A rapid method for purification of human granulocytes using percoll. A comparison with dextran sedimentation.* Journal of Immunological Methods, 1981. 43(1): p. 95-101.**

231. **Kutter, D., et al., *Consequences of total and subtotal myeloperoxidase deficiency: risk or benefit ?* Acta haematologica, 2000. 104(1): p. 10-5.**

232. **de Chaumont, F., et al., *Icy: an open bioimage informatics platform for extended reproducible research.* Nature methods, 2012. 9(7): p. 690-6.**

233. **Huang, L.-K. and M.-J.J. Wang, *Image thresholding by minimizing the measures of fuzziness.* Pattern recognition, 1995. 28(1): p. 41-51.**

234. **Kayagaki, N., et al., *Non-canonical inflammasome activation targets caspase-11.* Nature, 2011. 479(7371): p. 117-21.**

235. **Kayagaki, N., et al., *Noncanonical Inflammasome Activation by Intracellular LPS Independent of TLR4.* Science, 2013.**

236. **Hagar, J.A., et al., *Cytoplasmic LPS activates caspase-11: implications in TLR4-independent endotoxic shock.* Science, 2013. 341(6151): p. 1250-3.**

237. **Rathinam, V.A., et al., *TRIF Licenses Caspase-11-Dependent NLRP3 Inflammasome Activation by Gram-Negative Bacteria.* Cell, 2012. 150(3): p. 606-19.**

238. **Levine, A.P., et al., *Alkalinity of neutrophil phagocytic vacuoles is modulated by HVCN1 and has consequences for myeloperoxidase activity.* PloS one, 2015. 10(4): p. e0125906.**

239. **Conlan, J.W., *Neutrophils and tumour necrosis factor-alpha are important for controlling early gastrointestinal stages of experimental murine listeriosis.* Journal of medical microbiology, 1997. 46(3): p. 239-50.**

240. **Seaver, L.C. and J.A. Imlay, *Hydrogen peroxide fluxes and compartmentalization inside growing Escherichia coli.* Journal of bacteriology, 2001. 183(24): p. 7182-9.**

241. **Tuinema, B.R., S.A. Reid-Yu, and B.K. Coombes, *Salmonella evades D-amino acid oxidase to promote infection in neutrophils.* mBio, 2014. 5(6): p. e01886.**

242. **Trivedi, R.N., et al., *Methionine sulfoxide reductase A (MsrA) contributes to Salmonella Typhimurium survival against oxidative attack of neutrophils.* Immunobiology, 2015. 220(12): p. 1322-7.**

243. **Henard, C.A. and A. Vazquez-Torres, *Nitric oxide and salmonella pathogenesis.* Frontiers in microbiology, 2011. 2: p. 84.**

244. **Gulig, P.A., et al., *Systemic infection of mice by wild-type but not Spv- Salmonella typhimurium is enhanced by neutralization of gamma interferon and tumor necrosis factor alpha.* Infection and immunity, 1997. 65(12): p. 5191-7.**

245. **Bao, S., et al., *Interferon-gamma plays a critical role in intestinal immunity against Salmonella typhimurium infection.* Immunology, 2000. 99(3): p. 464-72.**

246. **Monack, D.M., A. Mueller, and S. Falkow, *Persistent bacterial infections: the interface of the pathogen and the host immune system.* Nature reviews. Microbiology, 2004. 2(9): p. 747-65.**

247. **Meunier, E., et al., *Caspase-11 activation requires lysis of pathogen-containing vacuoles by IFN-induced GTPases.* Nature, 2014. 509(7500): p. 366-70.**

248. **Balaban, N.Q., et al., *A problem of persistence: still more questions than answers?* Nature reviews. Microbiology, 2013. 11(8): p. 587-91.**

249. **Wagner, C., R. Sauermann, and C. Joukhadar, *Principles of antibiotic penetration into abscess fluid.* Pharmacology, 2006. 78(1): p. 1-10.**

250. **Helaine, S., et al., *Internalization of Salmonella by macrophages induces formation of nonreplicating persisters.* Science, 2014. 343(6167): p. 204-8.**

5 Acknowledgement

First of all I would like to thank Dirk to be an awesome PhD supervisor. He always motivated me with his enthusiasm about my projects and supported me during the whole time. Thanks for all the time you invested in my PhD project.

Thanks to my PhD committee members Petr Broz and Markus Heim for their valuable time and suggestions on my project.

Many thanks to the Imaging Core Facility (Alexia, Niko and Oliver). You helped me a lot in learning microscopy techniques and always helped out, if something didn't work.

Thanks to current and previous members of the Bumann lab, the Broz lab, the Khanna lab and the Hardt lab. In the last 3 ½ years I worked in 4 different labs, and people always welcomed me and were very friendly.

Special thanks to Mauricio for always helping out, discussions, suggestions and jokes. Thanks to Bea for helping me a lot with mice work and for being such a funny and cheerful labmate. Thanks a lot to Pascal, not only for the help on the MPO project, but also for a very pleasant working atmosphere and funny lunch breaks. Thanks to Nina, Boas and Wolf for their help and suggestions on the MPO project. Thanks to all the people who voluntarily donated blood for the MPO project. Thanks to Mauricio, Olivier, Dave and Julian for proof-reading parts of my Thesis.

Thanks to all the PhD-Reps who worked together with me and made PhD student life better, by providing PhD talks, career lecture series, conferences and social activities.

Thanks to Julie Beaudoin, who was a mentor for me during the last year and discussed with me career options outside of academic research. Thanks also to the whole antelope team and antelopes, for funny and serious meetings and discussions.

Thanks to Julia, Lisa, Alain, Ricardo, Max and Roland for pleasant lunch breaks, specifically for those in the summer at and in the Rhine.

Thanks to Michaela for providing her home to the yearly Christmas dinner and for organizing nice hikes during the summer.

Last but not least I want to thank my husband Julian, my family and my friends who are always there for me and supported me during the whole time.